Aus der Klinik für Innere Medizin, Schwerpunkt für Hämatologie, Onkologie und Immunologie
Geschäftsführender Direktor: Prof. Dr. med. Andreas Neubauer
des Fachbereichs Medizin der Philipps-Universität Marburg

In Kooperation mit
Cluster für Frauen- und Kindermedizin
Clusterleiter: PD Dr. med. habil. Claudius Werner
des Universitären Campus an den Helios Kliniken Schwerin
der Medical School Hamburg (MSH)

Präklinische Evaluation von Organogold-Verbindungen zur Therapie maligner Erkrankungen

Kumulative Dissertation zur Erlangung des Doktorgrades
der Humanmedizin
(Dr. med.)

dem Fachbereich der Medizin
der Philips-Universität Marburg

vorgelegt von

Marie-Christin Ahrweiler-Sawaryn, geb. Ahrweiler aus Münster
Marburg, 2024

Angenommen vom Fachbereich Medizin der Philipps-Universität Marburg am: 22.02.2024
Gedruckt mit Genehmigung des Fachbereichs Medizin

Dekanin: Frau Prof. Dr. D. Hilfiker-Kleiner
Referent: Herr Prof. Dr. A. Neubauer/ Herr Prof. Dr. Dr. A. Prokop
1. Korreferent: Herr Prof. Dr. T. Worzfeld

Inhaltsverzeichnis

Zusammenfassung i

Summary iii

Tabellenverzeichnis v

Abkürzungen vi

1. Einleitung 1

1.1. Hintergrund und Forschungsstand 1

1.1.1. Tumortherapie und Resistenzen 1

1.1.2. Mitochondriale Apoptose als Form des Zelltodes 1

1.1.3. Platinderivate als metallbasierte Zytostatika 3

1.1.4. NHC-Gold (I)-Verbindungen als potentielle Antitumormittel 4

1.2. Fragestellung 5

2. Publikationen 6

2.1. Novel gold(I) complexes induce apoptosis in leukemia cells via the ROS-induced mitochondrial pathway with an upregulation of Harakiri and overcome multi drug resistances in leukemia and lymphoma cells and sensitize drug resistant tumor cells to apoptosis in vitro. 6

2.2. Gold(I) Bis(1,2,3-triazol-5-ylidene) Complexes as Promising Selective Anticancer Compounds 9

3. Diskussion 12

4. Literaturverzeichnis 18

5. Anhang viii

5.1. Verzeichnis der akademischen Lehrer/-innen viii

5.2. Danksagung ix

5.3. Publikationen x

Zusammenfassung

Krebserkrankungen nehmen weltweit zu und stellen weiterhin eine enorme Belastung für die Gesellschaft und das Gesundheitssystem dar. Kaum ein Feld hat sich dabei in den letzten Jahrzehnten auf Forschungsebene als auch klinisch so entwickelt wie das der Tumortherapie. Und obwohl so die Letalität vieler maligner Erkrankungen deutlich gesenkt werden konnte, spielt Therapieversagen immer noch eine gewichtige Rolle. Zytostatikaresistenzen, ob intrinsisch oder erworben, können hier ursächlich sein. Vor Jahrzehnten wurde das zytotoxische Potenzial von Platin entdeckt und somit das Interesse an Metallverbindungen für die Behandlung maligner Erkrankungen geweckt. Platinhaltige Derivate werden noch immer in einem Großteil der heutigen Therapieregime eingesetzt. Trotz dessen limitieren eine Vielzahl an Nebenwirkungen und Resistenzen die Therapieoptionen und es besteht ein stetiges Interesse an der Erforschung neuartiger Substanzen, darunter neuer Metallverbindungen. Bisher sind jedoch nur wenige im klinischen Gebrauch. In den letzten Jahrzehnten stieg das Interesse an Metallorganischen Verbindungen wie etwa NHC-Gold-Komplexen. Als zytotoxischer Wirkungsmechanismus wurde vielfach die Bindung der Thioredoxinreduktase, hiermit einhergehend die Entstehung von *Reactive Oxygen Species* (ROS) und die mitochondriale Apoptose beschrieben.

Diese kumulative Dissertation untersucht die Zytotoxizität verschiedener Organogoldkomplexe (NHC-Au(I)-Verbindungen) auf verschiedenen immortalisierten Krebszelllinien und somit die Frage, ob sie potenzielle Antitumormittel darstellen. Dabei umfasst die Arbeit zwei Publikationen in Form erster präklinischer Studien. Als untersuchter Wirkmechanismus steht die Apoptose im Zentrum. Die Hypothese, dass diese Verbindungen vornehmlich über den mitochondrialen Signalweg wirken, war zu evaluieren. Der Fokus liegt hierbei auf der Interaktion mit verschiedenen Proteinen der Bcl-2-Familie. Die Analyse hierfür verantwortlicher Stressoren wie die Bildung von *Reactive Oxygen Species* und der Inhibition der Oxidoreduktase Thioredoxinreduktase stellt einen Unterpunkt dar. Ein Großteil der Arbeit umfasst den Vergleich der Substanzen auf nativen Ausgangszellen sowie kultivierten Ablegerzellen mit induzierter Zytostatikaresistenz. Dies erlaubt Rückschlüsse über das Potenzial der Resistenzüberwindung sowie über die Wirkweise bei bekanntem Resistenzmechanismus.

Die Ergebnisse beider Publikationen zeigen, dass die besten untersuchten Verbindungen im nanomolaren Bereich auf Leukämie- und Lymphomzellen *in vitro* zytotoxisch und zytostatisch wirksam sind. Apoptose wurde dabei auf verschiedenen immortalisierten Krebszelllinien nachgewiesen, nicht jedoch auf kultivierten, gesunden Leukozyten. Somit ist von einem

Wirkmechanismus auszugehen, der von der Zellteilung abhängig ist. Die erste Publikation „Novel gold(I) complexes induce apoptosis in leukemia cells via the ROS-induced mitochondrial pathway with an upregulation of Harakiri and overcome multi drug resistances in leukemia and lymphoma cells and sensitize drug resistant tumor cells to apoptosis in vitro“ arbeitet zudem die Involvierung der mitochondrialen Apoptose heraus. Charakteristika sind die Beteiligung verschiedener Bcl-2-Proteine, der Zusammenbruch des mitochondrialen Transmembranpotenzials sowie der Efflux mitochondrialer Proteine wie Cytochrome C und Smac. Die Beteiligung von ROS konnte hier indirekt nachgewiesen werden. Für die Substanzen der Publikation „Gold(I) Bis(1,2,3-triazol-5-ylidene) Complexes as Promising Selective Anticancer Compounds“ konnte die Inhibition der Thioredoxinreduktase nur in moderatem Ausmaß bestimmt werden. Auf einer Vielzahl an Zytostatika-resistenten Krebszellen wurden in beiden Publikationen Resistenzüberwindungen beobachtet. Spannende Ergebnisse liefert der Vergleich einer Substanz der erstgenannten Publikation auf einigen Ausgangszellen und hiervon abgeleiteten Zytostatika-resistenten Tochterzellen, die im Zuge ihrer Resistenzbildung Über- oder Unterexpressionen verschiedener Bcl-2-Proteine entwickelt haben. Der untersuchte Organogoldkomplex zeigte auf diesen nicht nur Resistenzüberwindungen. Drei resistente Zelllinien waren signifikant sensibler gegenüber der Substanz. Dies unterstützt die Annahme, dass Proteine der Bcl-2-Familie als Indikatoren des mitochondrialen Apoptosewegs wichtige Akteure im Wirkungsmechanismus dieses Goldkomplexes sind und lässt vermuten, dass dieser den Resistenzmechanismus unterwandert und kollabieren lässt.

Zusammenfassend zeigen die hier untersuchten Organogoldverbindungen in den ersten präklinischen Studien spannendes Potenzial für die weitere Erforschung zur Therapie maligner Erkrankungen.

Summary

Cancer is on the rise worldwide and continues to represent an enormous burden for society as well as the healthcare system. Hardly any other field has developed as much in recent decades, both clinically and in terms of research, as tumor therapy. And although the lethality of many malignant diseases has been significantly reduced, therapy failure still plays an important role. Cytostatic resistance, whether intrinsic or acquired, may be causative in this regard. Decades ago, the cytotoxic potential of platinum was discovered, sparking interest in metal compounds for the treatment of malignant diseases. Platinum-containing derivatives are still used in the majority of current therapeutic regimens. Despite this, a variety of side effects and resistance limit therapeutic options and there is a constant interest in exploring novel compounds, including new metal compounds. To date, however, few are in clinical use. In recent decades, there has been increasing interest in organometallic compounds such as NHC-gold complexes. The cytotoxic mechanism of action has been widely described as binding of thioredoxin reductase, concomitant generation of Reactive Oxygen Species and mitochondrial apoptosis. This cumulative dissertation investigates the cytotoxicity of various organogold complexes (NHC-Au(I) compounds) on different immortalized cancer cell lines and thus whether they represent potential antitumor agents. In this regard, the work includes two publications in the form of initial preclinical studies. The mechanism of action under investigation is apoptosis. The hypothesis that the substances act primarily via the mitochondrial signaling pathway was to be evaluated. The focus here is on the interaction with various proteins of the Bcl-2 family. The analysis of stressors responsible for this, such as the formation of Reactive Oxygen Species and the inhibition of the oxidoreductase thioredoxin reductase, represents a sub-point. A large part of the work involves the comparison of the substances on native starting cells as well as cultured offshoot cells with induced cytostatic resistance. This allows conclusions to be drawn about the potential for overcoming resistance as well as the mode of action when the mechanism of resistance is known.

The results of both publications show that the best investigated compounds in the nanomolar range have cytotoxic and cytostatic activity on leukemia and lymphoma cells in vitro. Apoptosis was thereby detected on various immortalized cancer cell lines, but not on cultured healthy human leukemia cells. Thus, a mechanism of action that is dependent on cell division can be assumed. The first publication "Novel gold(I) complexes induce apoptosis in leukemia cells via the ROS-induced mitochondrial pathway with an upregulation of hara-kiri and overcome multi-drug resistances in leukemia and lymphoma cells and sensitize drug-resistant tumor cells to apoptosis in vitro" also elaborates on the involvement of mitochondrial apoptosis.

Characteristics are the involvement of different Bcl-2 proteins, the breakdown of the mitochondrial transmembrane potential and the efflux of mitochondrial proteins such as cytochromes C and Smac. The involvement of ROS could be indirectly demonstrated here. For the compounds in the publication "Gold(I) Bis(1,2,3-triazol-5-ylidene) Complexes as Promising Selective Anticancer Compounds", inhibition of thioredoxin reductase could only be determined to a moderate extent. Resistance overcomes were observed on a variety of cytostatic-resistant cancer cells in both publications. Exciting results were obtained by comparing a substance of the former publication on some initial cells and cytostatic drug-resistant daughter cells derived therefrom, which developed over- or underexpression of various Bcl-2 proteins in the course of their resistance formation. The organogold complex studied not only showed resistance overcomes on these, but three resistant cell lines were significantly more sensitive to the compound. This supports the notion that Bcl-2 family proteins, as indicators of the mitochondrial apoptosis pathway, are important players in the mechanism of action of this gold complex and suggests that it subverts and collapses the resistance mechanism.

In summary, the organogold compounds investigated here show exciting potential for further exploration in the therapy of malignant diseases in the initial preclinical studies.

Tabellenverzeichnis

Tabelle 1: Übersicht über die Wirkung von ANB4014 auf sechs Zytostatika-resistenten Zelllinien. 8
Tabelle 2: Übersicht über die Wirkung von Komplex 2 auf vier Zytostatika-resistenten Zelllinien. 11

Abkürzungen

µM	Mikromolar
AC_{50}	Konzentration bei der 50 % der Zellen apoptotisch sind
ALL	Akute lymphatische Leukämie
ATO	Arsentrioxid
Au	Elementsymbol für Gold
Bak	Bcl-2 Homologous Antagonist Killer
Bax	Bcl-2-associated X protein
Bcl-2	B-cell lymphoma 2
Bcl-xL	B-cell lymphoma-extra large
BIM	Bcl-2-like protein 11
BJAB	Menschliche Burkitt-like Lymphomzellen
Cisp	Cisplatin
Cisplatin-res. SK-N-AS	SK-N-AS-Zellen mit induzierter Cisplatin-Resistenz
CLL	Chronische lymphatische Leukämie
CML	Chronische myeloische Leukämie
Cytarabin-res. Nalm-6	Nalm-6-Zellen mit induzierter Cytarabin-Resistenz
Dauno	Daunorubicin
Dauno-res. K562	K562-Zellen mit induzierter Daunorubicin-Resistenz
Dauno-res. Nalm-6	Nalm-6-Zellen mit induzierter Daunorubicin-Resistenz
Doxo	Doxorubicin
Doxo-res. BJAB	BJAB-Zellen mit induzierter Doxorubicin-Resistenz
Etoposid-res. Nalm-6	Nalm-6-Zellen mit induzierter Etoposid-Resistenz
FDA	Food and Drug Administration
GADD45A	Growth arrest and DNA-damage-inducible protein
GSH	Glutathion
Hrk	Harakiri

IC_{50}	Konzentration bei der 50 % der Zellen inhibiert werden
K562	Menschliche chronische myeloische Leukämiezellen in Blastenkrise
Mcl-1	Myeloid cell leukemia 1
MDR	Multidrug Resistenz
Nalm-6	Menschliche B-Zell-Vorläufer-Leukämiezellen
NHC	N-Heterozyklische Carbene
nm	nanomolar
(RT q)PCR	(Quantitative reverse Transkriptions) Polymerase Kettenreaktion
P-gp	P-Glykoprotein
PI	Propidiumiodid
Pt	Elementsymbol für Platin
RA	Rheumatoide Arthritis
ROS	*Reactive oxygen species*
SK-N-AS	Menschliche Neuroblastomzellen
Trx	Thioredoxin
TrxR	Thioredoxinreduktase
VCR	Vincristin
VCR-res. BJAB	BJAB-Zellen mit induzierter Vincristin-Resistenz
VCR-res. Nalm-6	Nalm-6-Zellen mit induzierter Vincristin-Resistenz

1. Einleitung

1.1. Hintergrund und Forschungsstand

1.1.1. Tumortherapie und Resistenzen

Im Jahr 2020 wurde weltweit eine steigende Tumorinzidenz (19,3 Millionen) dokumentiert und es wurden 10 Millionen Tode durch maligne Erkrankungen festgestellt. Diese Zahlen veröffentlichten die Global Cancer Studies und machten deutlich, dass maligne Erkrankungen durch eine hohe Morbidität und Mortalität weiterhin eine enorme Belastung für die Gesellschaft und das Gesundheitssystem darstellen (Sung et al. 2021; Bray et al. 2018). Kaum ein Feld hat sich dabei in den letzten Jahrzehnten auf Forschungsebene als auch klinisch so entwickelt wie das der Tumortherapie. Heute verfolgt man, neben den drei klassischen Therapiesäulen aus Operation, Chemotherapie und Strahlentherapie, individualisierte Ansätze. Lassen sich molekulare oder zelluläre Marker als treibende Kräfte des Tumorwachstums identifizieren, besteht die Möglichkeit, an diesem Punkt im Sinne einer *Targeted Therapy* anzusetzen (Friedman et al. 2015). Eine Vielzahl an Meilensteinen, wie die Identifizierung des BCR-ABL Gens und Entwicklung des Tyrosinkinaseinhibitors Imatinib oder die Entdeckung des CD20-Antigens und die Entwicklung des monoklonalen Antikörpers Rituximab, um nur zwei zu nennen, haben die Heilungschancen einiger Tumore erst revolutioniert und gehören heute zum Standardrepertoire (Goetz und Schork 2018; Smith 2003). Und obwohl so die Letalität vieler maligner Erkrankungen deutlich gesenkt werden konnte, spielt Therapieversagen immer noch eine gewichtige Rolle. Zytostatikaresistenzen, ob intrinsisch oder erworben, können hier ursächlich sein. Beschriebene Resistenzmechanismen sind etwa Efflux oder Inaktivierung von Arzneimitteln, Reparaturprozesse von DNA-Schäden, aber auch Hemmung der Apoptose (Holohan et al. 2013).

1.1.2. Mitochondriale Apoptose als Form des Zelltodes

Ein Großteil der gegenwärtigen Tumortherapieoptionen induzieren Apoptose, auch programmierter Zelltod genannt (Fulda und Debatin 2006). Unter physiologischen Bedingungen fungiert die Apoptose als wichtiges Mittel, um Zellzahl und Zellfunktion im Organismus im Optimum zu halten und ist daher fein reguliert (Hengartner 2000). Über zwei Wege können Stressoren wahrgenommen und umgesetzt werden: Zum einen findet über den extrinsischen Weg die rezeptorvermittelte Signalkaskade statt. Liganden sind beispielsweise FasL, TRAIL und TNFα (Taylor et al. 2008; Fulda und Debatin 2006). Zum anderen können Störungen auf Zellebene wie DNA-Schäden und oxidativer Stress als Auslöser des intrinsischen Weges

fungieren (Redza-Dutordoir und Averill-Bates 2016). Die anti- und proapoptotischen Proteine der Bcl-2-Familie sind die Schlüsselenzyme dieses Weges, die sich gegenseitig hemmen und aktivieren und so einen balancierten Zustand aufrechterhalten. Hierzu gehören die antiapoptotischen Proteine Bcl-2, Mcl-1 oder Bcl-xL, die proapoptotischen Proteine BAX und BAK und die proapoptotischen BH-3-only Proteine, die sich weiter in *sensitizer*- und *activator*-Proteine unterteilen lassen und die zuvor genannten beeinflussen. Überwiegen Stressoren, werden *sensitizer*-BH-3-only Proteine aktiviert, binden antiapoptotische Bcl-2-Proteine und setzen so *activator*-BH3-only-Proteine oder direkt Bax oder Bak frei (Kale et al. 2018). Dies initiiert schließlich die Oligomerisierung von Bax und Bak, was zur Permeabilisierung der äußeren Mitochondrienmembran und zum Efflux mitochondrialer Proteine wie Cytochrome C und Smac führt, die weitere Schritte dieses Apoptosewegs anstoßen (Kroemer et al. 2007). Beide Wege münden vereinfacht dargestellt, in der kaskadenförmigen Aktivierung von einer Gruppe von Cysteinproteasen, den Caspasen. Diese spalten funktionelle und strukturelle Zellproteine proteolytisch und dies resultiert in den morphologischen Charakteristika der Apoptose wie Kernkondensation und DNA-Fragmentierung (Alnemri et al. 1996; Earnshaw et al. 1999; Taylor et al. 2008). In Tumorzellen ist die Apoptose jedoch häufig entkoppelt: Zeigen viele Tumore Unter- bzw. Überexpressionen Apoptose-induzierender oder -hemmender Enzyme, kann zusammen mit konstanten Wachstumsimpulsen eine ungehemmte Proliferation entdifferenzierter Zellen die Folge sein (Hanahan und Weinberg 2000a). Dies kann nicht nur bei der Tumorgenese eine Rolle spielen, sondern, wie schon angedeutet, auch bei der Bildung relevanter Zytostatikaresistenzen (Holohan et al. 2013). Jedoch könnten diese fehlfunktionierenden Signalstellen auch entsprechend einer Achillesferse für Tumorzellen vulnerabel sein. Certo und Kollegen beschreiben einen Zustand, bei dem Tumorzellen durch *activator*-BH-3-only Proteine auf den Tod „geprimed“ sind und entsprechend von antiapoptotischen Bcl-2 Proteinen abhängig sind, die *activator*-BH-3-only Proteine zu binden und davon abzuhalten Bax/Bak zu aktivieren. Kommt es nun beispielsweise durch einen Stressor zu einer Zunahme von *sensitizer*-BH3-only Proteinen, die die *activator*-BH-3-only Proteine von den antiapoptotischen Bcl-2-Proteinen freisetzen, wird Apoptose ausgelöst (Certo et al. 2006). Die Zunahme von *sensitizier*-BH-3-only-Proteinen lässt sich unspezifisch durch gängige Zytostatika auslösen, aber auch gezielt durch sogenannte BH3-Mimetika „vortäuschen“. Das BH3-Mimetikum Venetoclax, das Bcl-2 blockiert, ist 2016 erstmalig von der U.S. Food and Drug Administration (FDA) zugelassen worden und inzwischen für die Chronische lymphatische Leukämie und die Akute myeloische Leukämie in klinischem Gebrauch (Deeks 2016; European Medicines Agency 2021).

1.1.3. Platinderivate als metallbasierte Zytostatika

Mit Rosenberg et al.'s Entdeckung im Jahr 1965, dass Cisplatin die Zellteilung in E. coli. hemmt, wurde das Interesse an Metallkomplexen als neue Klasse von Antitumormitteln geweckt und hiermit einhergehend das Potenzial von Metallkoordinationsverbindungen erkannt (Rosenberg et al. 1965; Rosenberg 1980). Innerhalb der folgenden Dekade zeigte Cisplatin sukzessiv in den präklinischen und klinischen Studien Potenz gegenüber einer Vielzahl von Tumorentitäten und wurde schließlich 1979 von der FDA als Zytostatikum für Hoden- und Ovarialtumore zugelassen (Wiltshaw 1979). Cisplatin findet inzwischen vielfältige Anwendung in der Behandlung von soliden Tumoren wie etwa Hoden-, Brust-, Blasen-, Eierstock-, Darm-, Lungen- und Kopf-Hals-Krebs (Ghosh 2019; Rabik und Dolan 2007). Hierbei stellen jedoch starke Nebenwirkungen wie etwa Nephro-, Neuro-, Hepato- oder Ototoxizität immer wieder eine Therapielimitation dar, die bereits bei den ersten klinischen Studien mit Cisplatin in den siebziger Jahren ausdrücklich Erwähnung fanden (Rabik und Dolan 2007; Manohar und Leung 2018; Santos et al. 2020). Darüber hinaus zeigen viele Tumore eine intrinsische oder erworbene Cisplatinresistenz, die so zu Therapieversagen oder Rezidiven führen kann (Galluzzi et al. 2012; Rottenberg et al. 2021). In den letzten sechzig Jahren wurden tausende von Platinanaloga synthetisiert und untersucht, um Cisplatin sowohl hinsichtlich der Toxizität als auch der Resistenzbildung überlegen zu sein, jedoch nur wenige wurden in klinische Studien aufgenommen oder fanden ihren Weg bis zur Zulassung (Ghosh 2019; Wheate et al. 2010). Trotz der vielen Nebenwirkungen als auch der Resistenzen und trotz einer enormen Weiterentwicklung der therapeutischen Möglichkeiten in den letzten Jahrzehnten spielen diese platinhaltigen Metallkoordinationsverbindungen immer noch eine Hauptrolle in der Behandlung maligner Erkrankungen. Sie werden in etwa 50-70 Prozent aller Therapieregime eingesetzt und sind zum jetzigen Zeitpunkt aus der Onkologie nicht wegzudenken (Dasari und Tchounwou 2014; Rottenberg et al. 2021; Simpson et al. 2019). Dies schürte das Interesse an der Erforschung weiterer Metallverbindungen, die im Rahmen der Tumortherapie erfolgsversprechend sein könnten. Eine Vielzahl von neu synthetisierten Verbindungen mit zytotoxischem Potenzial wurde publiziert und ihre biologische Aktivität näher untersucht. Darunter Ruthenium-, Iridium-, Rhodium-, Eisen- und auch Goldverbindungen (Simpson et al. 2019). Bis heute sind nur wenige weitere metallbasierte Zytostatika wie beispielsweise Arsentriooxid bei der Promyelozyten Leukämie zugelassen und im Gebrauch (Simpson et al. 2019).

1.1.4. NHC-Gold (I)-Verbindungen als potentielle Antitumormittel

Die therapeutischen Ursprünge von Gold lassen sich zurückdatieren auf das antike China 2500 v.Chr. (Huaizhi und Yuantao 2001). Das moderne Interesse an Gold entwickelte sich jedoch erst nach 1890, als Robert Koch entdeckte, dass Cyan-Goldverbindungen das Wachstum von Tuberkelbazillen hemmen. Zwar konnte dies weder in tuberkulösen Tieren noch in klinischer Anwendung bestätigt werden, doch legte diese Entdeckung den Grundstein für die Erforschung von Goldsalzen im medizinischen Kontext (Koch 2010; Benedek 2004). 1929 bewies der französische Mediziner Jacques Forestier erstmals in klinischen Studien einen heilsamen Effekt von Goldsalzen bei Rheumatoider Arthritis (RA) und im Laufe des Jahrhunderts wurden verschiedene goldbasierte RA-Therapeutika etabliert – mit heute eher untergeordneter Rolle. Darunter ist der Au(I)-Phosphine-Komplex Auranofin, welcher 1985 als orales Antirheumatikum zugelassen wurde (Forestier 1932; Berners-Price und Filipovska 2011). Um diese Zeit wurden auch die antiproliferativen Eigenschaften Auranofins erkannt und dies initiierte die Entwicklung weiterer Goldverbindungen in verschiedenen Oxidationsstufen und gebunden an verschiedene Liganden und der Erforschung ihres zytotoxischen Potenzials (Mirabelli et al. 1985; Simon et al. 1979; Berners-Price und Filipovska 2011). Organometallkomplexe zeichnen sich durch mindestens eine Metallkarbonbindung aus und unterscheiden sich hierdurch von den Koordinationskomplexen der Cisplatin-Familie, dem Antirheumatikum Auranofin oder dem Kontrastmittel Gadolinium (Ong und Gasser 2020). Galt früher allgemein, Organometalle seien instabil und somit für medizinische Zwecke nicht von Nutzen, konnte dies inzwischen nicht nur durch eine Vielzahl an synthetisierten Verbindungen und Studien widerlegt werden, auch fand man weitere vielversprechende Wirkungen antibakterieller oder antikanzeröser Art (Gasser et al. 2011). N-Heterocyclische Carbene (NHC) haben sich in den letzten Jahren als besonders geeignete Gerüste für Organometallverbindungen und im Speziellen für Goldkomplexverbindungen herausgestellt. Sie überzeugen durch eine einfache Ligandenmodifikation, eine gute Stabilität im physiologischen Milieu, eine hohe Aktivität in Tumoren und sie sind relativ untoxisch (Mora et al. 2019; Zou et al. 2015). Als Zielstruktur wurden vielfach Enzyme beschrieben, die eine Thiolgruppe im aktiven Zentrum aufweisen wie beispielsweise Thioredoxinreduktase oder Glutathionperoxidase (Zou et al. 2015; Crooke und Snyder 1986). Hierbei zeigte sich, dass Goldverbindungen aufgrund des Selenocysteins im katalytischen Zentrum hoch selektiv die Thioredoxinreduktase (TrxR) binden, welche im Mitochondrium und Zytosol lokalisiert ist und von einigen Tumoren überexprimiert wird (Casini et al. 2018; Bindoli et al. 2009). Dies konnte sowohl für Goldverbindungen in verschiedenen Oxidationsstufen (+I mehr als +III) als auch gebunden an verschiedene Liganden beobachtet

werden (Rigobello et al. 2004; Bindoli et al. 2009). TrxR besitzt als Oxidoreduktase zentrale Funktionen beim Zellwachstum, der DNA-Synthese und der Transkription, aber auch im Rahmen der Resistenzbildung gegenüber Medikamenten und zur Abwehr oxidativen Stresses (Zou et al. 2015; Nguyen et al. 2006; Saccoccia et al. 2014). Wird das TrxR-System blockiert, wird im Mitochondrion weniger ROS abgebaut und eine Zunahme oxidativen Stresses resultiert. Dies kann zum Zusammenbruch des mitochondrialen Transmembranpotentials und somit zur intrinsischen Apoptose führen (McKeage et al. 2002; McKeage 2002; Rigobello et al. 2002; Bindoli et al. 2009). Auch für NHC-Au-Verbindungen bestätigten sich diese Annahmen vielfach (Barnard et al. 2004; Hickey et al. 2008; Schmidt et al. 2017; Rubbiani et al. 2010).

1.2. Fragestellung

Auf Ebene der präklinischen Forschung beschäftigt sich die Arbeitsgruppe *Experimentelle Onkologie* mit der Analyse neuartiger Substanzen, meist Metallkomplexe, die im Rahmen der Krebstherapie vielversprechend sein können. Diese Dissertation fokussiert sich auf das zytotoxische Potenzial verschiedener Organogold(I)-Komplexe (NHC-Au(I)-Verbindungen) und die Frage, ob sie potenzielle Antitumormittel darstellen. Es handelt sich um erste präklinische Studien auf immortalisierten Krebszelllinien. Zudem erfolgt ein Vergleich auf gesunden menschlichen Leukozyten *in vitro* (Aktenzeichen des Ethikvotums: EK_MR_150321_Neubauer). Als untersuchter Wirkmechanismus steht die Apoptose im Zentrum. Die Hypothese, dass diese vornehmlich über den mitochondrialen Signalweg und die hier beteiligten Enzymen, vor allem der Bcl-2-Familie, *Reactive oxygen Species* und der Thioredoxinreduktase induziert wird, ist zu evaluieren. Darüber hinaus soll der Vergleich auf Zellen mit induzierter Zytostatika-Resistenz und den Ausgangszellen nicht nur Aufschluss über das Potenzial der Resistenzüberwindung geben, auch gibt dies bei bekanntem Resistenzmechanismus weitere Rückschlüsse über die Wirkweise.

2. Publikationen

2.1. Novel gold(I) complexes induce apoptosis in leukemia cells via the ROS-induced mitochondrial pathway with an upregulation of Harakiri and overcome multi drug resistances in leukemia and lymphoma cells and sensitize drug resistant tumor cells to apoptosis in vitro.

Marie-C. Ahrweiler-Sawaryn, Animesh Biswas, Corazon Frias, Jerico Frias, Nicola L. Wilke, Nathalie Wilke, Albrecht Berkessel, Aram Prokop

Veröffentlicht in Biomed Pharmacother. 2023 Mar 21;161:114507. doi: 10.1016/j.biopha.2023.114507 (Ahrweiler-Sawaryn et al. 2023).

In diesem Paper konzentrierten wir uns auf die apoptotischen Wirkmechanismen von fünf neuartigen NHC-Au(I)-Verbindungen.

Um einen ersten Eindruck über die apoptotische Wirksamkeit zu erlangen, haben wir die fünf Komplexe in einem Konzentrationsbereich von 0,01 µM bis 100 µM auf immortalisierten Leukämiezellen gescreent. Die Apoptose wurde mittels stöchiometrischer Färbung apoptotischer DNA-Fragmente und zytometrischer Messung untersucht (Riccardi und Nicoletti 2006). Im Screening-Vergleich hoben sich die zwei Verbindungen ANB4014 und ANB4016 hervor, die bereits im nanomolaren Bereich antiproliferativ und zytotoxisch wirksam waren (ANB4014: AC_{50} 0,36 µM und IC_{50} 0,1 µM; ANB4016 AC_{50} 0,22 µM und IC_{50} 0,2 µM, s. Table 1, Figure 1; AC_{50}= Konzentration, bei der 50 % der Zellen apoptotisch sind, IC_{50} =Konzentration, bei der 50 % der Zellen inhibiert werden). Im Paper konzentrieren wir uns auf die Verbindung ANB4014, da diese sich in der Gesamtschau verschiedener Experimente als die potentere Verbindung herausstellte. Auch auf fünf weiteren Krebszelllinien (Leukämie-, Lymphom-, Mammakarzinom-, Neuroblastom- und Melanomzellen) war ANB4014 im nano- bis mikromolaren Bereich wirksam (s. Table 2). Mittels LDH-Messung im Zytosol wurden unspezifische, toxische Effekte nach einer Stunde Inkubation auf Nalm-6- und BJAB-Zellen ausgeschlossen (s. Figure 2). Die Annexin V/PI Doppelfärbung erlaubt darüber hinaus Rückschlüsse über die apoptotischen Stadien: Nach 48 Stunden Inkubation überwog die konzentrationsabhängige Zunahme frühapoptotischer Zellen bei gleichzeitiger Abnahme der vitalen Zellen (s. Supplement 4 und 5). Wir führten einen Selektivitätsversuch durch und verglichen die Verbindung ANB4014 auf Leukämiezellen und auf gesunden, menschlichen Leukozyten *in vitro*. Während auf den Leukämiezellen konzentrationsabhängig eine Zunahme der apoptotischen Zellen zu beobachten war und bereits in einer Konzentration von 0,75 µM die

meisten Zellen apoptotisch waren, war bis zu einer Konzentration von 1,5 µM kein relevanter Zelltod der gesunden Leukozyten zu beobachten (s. Figure 3).

In weiteren Analysen fokussierten wir uns auf die Erforschung des Wirkmechanismus mit Schwerpunkt auf der mitochondrialen Apoptose. Diese bestätigte sich für ANB4014 durch den konzentrationsabhängigen Zusammenbruch des mitochondrialen Transmembranpotentials als auch der Freigabe von Cytochrome C und Smac aus dem Mitochondrium ins Zytosol (s. Figure 4 und Figure 5). Die Beteiligung von *Reactive Oxygen species* (ROS) wiesen wir indirekt nach: Die apoptotische Wirkung von ANB4014 ließ sich durch die beiden antioxidativ wirkenden Substanzen N-Acetylcystein (vollständig) und Taurin (teilweise) aufheben (s. Figure 6). Ebenso war eine deutliche Überexpression des Stress-Proteins GADD45A in der PCR-Analyse zu beobachten (+25,8-fach Fold regulation, s. Table 3). Mediatoren des intrinsischen Apoptosewegs sind die Proteine der Bcl-2-Familie. So zeigte sich durch ANB4014 eine Zunahme der proapoptotischen BH-3-only Proteine Harakiri (HRK) im Western Blot nach 24 Stunden Inkubation (s. Figure 8) und BIM in der PCR nach 14-stündiger Inkubation (+4,2-fach Fold Regulation s. Table 3) sowie eine Abnahme des antiapoptotischen Bcl-2 in der PCR (-4,7-fach Fold regulation, s. Table 3). In unserem Labor gibt es drei Zytostatika-resistente Zelllinien, die sich durch eine Zu- oder Abnahme relevanter anti- oder proapoptotischer Proteine der Bcl-2-Familie auszeichnen: Daunorubicin-resistente K562 (CML-Zellen mit HRK-Unterexpression), Vincristin-resistente BJAB (Burkitt-like Lymphoma-Zellen mit Bcl-2-Überexpression) und Methotrexat-resistente Nalm-6 (B-ALL-Zellen mit Mcl-1-Überexpression sowie zusätzlich p53-Unterexpression). Für alle drei resistente Zellreihen beobachteten wir einen gleichen Effekt durch ANB4014: Diese Zellen waren deutlich sensibler als die Ausgangszellen ohne die genannten molekularen Veränderungen. Während auf den Ausgangszellen BJAB keinerlei oder kaum Apoptose beobachtet werden konnte, war die gleiche Konzentration von ANB4014 für nahezu alle VCR-resistente BJAB-Zellen letal (s. Figure 7, B). Auf den CML-Zellen K562 war ANB4014 bis zu einer Konzentration von 2 µM sogar nahezu wirkungslos, während die Verbindung in den Daunorubicin-resistenten K562 in einer Konzentration von 0,5 µM bereits fast 100 % Apoptose auslöste (s. Figure 7, A). Auch die MTX-resistenten Nalm-6 Zellen waren für ANB4014 deutlich sensibler als die Wildtyp-Zellen (s. Figure 7, C). Da für die VCR-resistenten BJAB bisher eine Bcl-2-Überexpression detektiert wurde, untersuchten wir auf diesen Zellen die Wirkung des BH-3-Mimetikums Venetoclax, um zu überprüfen, ob eine Blockade von Bcl-2 den Resistenzmechanismus unterwandert und Apoptose auslöst. Doch zeigten die VCR-resistenten BJAB eine Resistenz gegenüber dem Medikament (s. Figure 9). Die Resistenz der VCR-res. BJAB gegenüber Vincristin oder aber gegenüber Venetoclax ließ sich jedoch durch die Kombination

der beiden Wirkstoffe durchbrechen (s. Figure 10). Wichtige Enzyme der Apoptose und downstream des intrinsischen sowie extrinsischen Apoptosewegs zu finden, sind die Caspasen. Eine Caspase 3-Aktivierung ließ sich im Western Blot nach 24 Stunden Inkubation zeigen (s. Figure 8). Eine Caspase 3-Abhängigkeit verdeutlichte auch der Vergleich auf Wildtyp-BJAB und Doxorubicin-resistenten BJAB-Zellen mit Caspase 3-Unterexpression, die im untersuchten Konzentrationsbereich gegenüber ANB4014 vollständig resistent waren (s. Figure 11). In der PCR wurde nach 14 Stunden Inkubation eine Caspase 7-Überexpression (+7,8-fach Fold regulation, s. Table 3) nachgewiesen.

Ein Schwerpunkt der Arbeit war der Vergleich auf verschiedenen Zytostatika-resistenten Zellen und den Wildtyp-Zellen. Die Resistenzen sind von uns induziert und daher erworben. Darüber hinaus zeichnen sich nahezu alle resistenten Zelllinien durch eine Vielzahl an Ko-Resistenzen gegenüber gängigen Zytostatika aus. Insgesamt testeten wir ANB4014 auf sechs unterschiedlichen resistenten Zelllinien, fünf von sechs Resistenzen wurden hierbei überwunden. Darunter sind auch zwei Zelllinien, die sich durch eine Überexpression des *Multidrug resistence*-Rezeptors P-Glykoprotein auszeichnen und auf denen ANB4014 die gleiche Wirksamkeit zeigte wie auf den Ausgangszellen (s. Figure 12). Eine Übersicht über die entsprechenden Zellen, die Resistenzmechanismen, Ko-Resistenzen und den Effekt von ANB4014 gibt die hier dargestellte Tabelle 1.

Tabelle 1: Übersicht über die Wirkung von ANB4014 auf sechs Zytostatika-resistenten Zelllinien. Fünf Zelllinien sind gegenüber ANB4014 sensibel (S), nur die Doxo-resistenten BJAB-Zellen sind resistent (R). Die Ko-Resistenzen sowie die Resistenzmechanismen, die wir bisher ermittelt konnten, sind in der Tabelle mit angegeben. Die Tabelle wurde bereits teilweise im Originalpaper veröffentlicht (Ahrweiler-Sawaryn et al. 2023) und hier um die Ko-Resistenzen ergänzt.

Ausgangszelllinie	**Resistente Zelllinie**	**Resistenzmechanismus**	**Ko-Resistenzen**	**Effekt**
Nalm-6 (B-ALL)	VCR-res. Nalm-6	P-gp-Überexpression	Anthrazykline, Vincaalkaloide Epipodophyllotoxine, Paclitaxel und Colchicin	S
	Dauno-res. Nalm-6	P-gp-Überexpression	Anthrazykline, Vincaalkaloide Epipodophyllotoxine, Paclitaxel und Colchicin	S
	MTX-res. Nalm-6	p53-Unterexpression, Mcl-1-Überexpression	Cytarabin	S
BJAB (Burkitt-like Lymphoma)	VCR-res. BJAB	Bcl-2-Überexpression	Cytarabin, Vincaalkaloide	S

	Doxo-res. BJAB	Caspase 3-Unterexpression	u.a. Anthrazykline, einige Antimetabolite, Vincaalkaloide, Oxaliplatin	R
K562 (CML)	Dauno-res. K562	Harakiri-Unterexpression	Anthrazykline, Vincaalkaloide, Mitoxantron, Prednisolon	S

Mein Anteil an dem Paper umfasst alle im Paper dargestellten und den in 2.1 beschriebenen biologischen Versuche, mit Ausnahme des Screenings der fünf Goldverbindungen (Table 1 im Paper) und des Versuchs auf den MTX-resistenten Nalm-6 Zellen (Figure 7, C im Paper). Außerdem ist das Paper zum Großteil und mit Ausnahme des chemischen Anteils von mir verfasst.

2.2. Gold(I) Bis(1,2,3-triazol-5-ylidene) Complexes as Promising Selective Anticancer Compounds

Jonas F. Schlagintweit, Christian H. G. Jakob, Nicola L. Wilke, **Marie Ahrweiler**, Corazon Frias, Jerico Frias, Marcel König, Eva-Maria H. J. Esslinger, Fernanda Marques, João F. Machado, Robert M. Reich, Tânia S. Morais, João D. G. Correia, Aram Prokop, and Fritz E. Kühn

Veröffentlicht in J Med Chem. 2021 Nov 11;64(21):15747-15757. doi: 10.1021/acs.jmedchem.1c01021 (Schlagintweit et al. 2021).

In diesem Paper werden zwei neuartige NHC-Gold(I)-Komplexe vorgestellt und ihre antitumoralen Eigenschaften herausgearbeitet. Hierfür wurden diese bezüglich ihrer Stabilität und Selektivität sowie hinsichtlich ihrer antiproliferativen, zytotoxischen und synergistischen Eigenschaften untersucht und verglichen.

Die Synthese der Verbindungen kann dem vorliegenden Paper entnommen werden, es wird hier jedoch aufgrund des chemischen Hintergrunds nicht auf diese eingegangen. Stabilitätsuntersuchungen mittels ^{1}H NMR-Kinetik zeigten eine gute Stabilität der beiden Komplexe gegenüber L-Cystein und Glutathion (s. Figure S9-S18). Aufgrund der umfangreichen Datenlage, dass Goldkomplexe die Thioredoxinreduktase hemmen (Zou et al. 2015; Crooke und Snyder 1986; Casini et al. 2018; Bindoli et al. 2009; Rigobello et al. 2002), wurde die inhibitorische Wirkung für die zwei Komplexe untersucht. Beide Komplexe hemmten die Thioredoxinreduktase in moderater Weise, jedoch deutlich schwächer als das Antirheumatikum Auranofin (IC_{50}- Werte: Komplex 1 1,0 µM; Komplex 2 1,6 µM; Auranofin 17 nM; s. Figure S29 und S31). In MTT Assays wurden erste antiproliferative Eigenschaften auf Tumorzellen

bestimmt. Hier konnten für beide Komplexe auf vier verschiedenen Krebszelllinien (Ovarialkarzinom-, zwei Mammakarzinom- und Prostatakarzinomzellen) IC_{50}-Werte im mikromolaren und nanomolaren Bereich ermittelt werden, wobei sich Komplex 2 in allen vier Zelllinien als die potentere Verbindung erwies und deutlich besser wirkte als Cisplatin oder Auranofin (IC_{50}–Werte auf den Brustkrebszellen MDAMB231: Komplex 1 3,65 µM ± 0,75; Komplex 2 0,063 µM ± 0,02; Cisplatin 13,8 µM ± 4,5 µM; Auranofin 1,9 µM ± 0,7; s. Table 1).

Diese Ergebnisse konnten wir mit den Analysen unserer Arbeitsgruppe, die die folgenden Untersuchungen der Apoptose umfassen, bestärken. Wir screenten die zwei dargestellten Komplexe hinsichtlich ihrer apoptotischen Wirkung auf Leukämiezellen (Nalm-6) im Konzentrationsbereich 0,05 µM bis 50 µM. Aufgrund der größeren Wirksamkeit konzentrierten wir uns auf den Komplex 2. Dieser zeigt einen konzentrationsabhängigen Anstieg der Apoptose im Bereich 0,05 µM bis 10 µM und eine Plateauwirkung ab 10 µM. Die ungefähre AC_{50} liegt bei 0,5 µM (s. Figure 3). Die Apoptose als Zelltod als auch die Differenzierung apoptotischer Stadien bestätigten sich mittels Annexin V/Propidiumiodid (PI)-Doppelfärbung. Nach 48 Stunden Inkubation präsentierte sich eine konzentrationsabhängige Zunahme vornehmlich frühapoptotischer und auch spätapoptotischer Stadien (s. Figure 2). Während Komplex 2 auf Leukämiezellen als auch Lymphomzellen bereits im nanomolaren Bereich Apoptose induziert, war diese in einem direkten Vergleich auf gesunden, menschlichen Leukozyten bis zu einer Konzentration von 5 µM nicht nachweisbar (s. Figure 6).

Eine Säule der Arbeit stellt das Thema Resistenzüberwindungen dar. Wir untersuchten Komplex 2 auf verschiedenen Krebszelllinien, die wir gegenüber gängigen Zytostatika resistent gemacht haben. Diese Resistenzen basieren auf verschiedenen Resistenzmechanismen und zeichnen sich durch Ko-Resistenzen gegenüber weiteren Zytostatika aus. Komplex 2 überwand alle hier untersuchten Resistenzen in einer Konzentration von 0,5 µM. Dabei wurden folgende Zytostatikaresistenzen überwunden: Cytarabin, Etoposid, Daunorubicin und Cisplatin (s. Figure 4, 5 und S28). Interessanterweise war die Wirkung auf allen resistenten Zellen besser als auf den Ausgangszellen, insbesondere auch auf den Cisplatin-resistenten Neuroblastomzellen, die sich durch eine Caspase 8 -Unterexpression auszeichnen (für 0,5 µM: 38,19 ±SD Apoptose auf SK-N-AS vs. 75,17 ±SD auf Cisp.-res. SK-N-AS). Eine Übersicht über die entsprechenden Zellen, die Resistenzmechanismen, Ko-Resistenzen und den Effekt von Komplex 2 gibt die hier dargestellte Tabelle 2.

Tabelle 2: Übersicht über die Wirkung von Komplex 2 auf vier Zytostatika-resistenten Zelllinien. Alle Zelllinien sind gegenüber der Verbindung sensibel. Die Ko-Resistenzen sowie die Resistenzmechanismen, die wir bisher ermittelt konnten, sind in der Tabelle mit angegeben. S= Sensibel, R=Resistent.

Ausgangszelllinie	Resistente Zelllinie	Resistenzmechanismus	Ko-Resistenzen	Effekt
Nalm-6 (B-ALL)	Etoposid-res. Nalm-6	GADD45A-Unterexpression	Anthrazykline und Mitoxantron	S
	Cytarabin-res. Nalm-6	FOXI1 (Forkhead box I1)-Unterexpression	Antimetabolite wie Cladribin, Clofarabin; Vincristin	S
SK-N-AS (Neuroblastom)	Cisplatin-res. SK-N-AS	Caspase 8-Unterexpression	Platinderivate, Cytarabin, Ifosfamid und Cyclophosphamid	S
K562 (CML)	Dauno-res. K562	Harakiri-Unterexpression	Anthrazykline, Vincaalkaloide, Mitoxantron und Prednisolon	S

In vielen Therapieregimen werden Zytostatika kombiniert, um die Wirksamkeit und die therapeutischen Effekte zu erhöhen und die Resistenzbildung zu minimieren (Bayat Mokhtari et al. 2017). In einem Synergieversuch auf Leukämiezellen mit dem Anthrazyklin Daunorubicin ließ sich eine Synergie mit Komplex 2 von 182 % im Vergleich zum summarischen Effekt nachweisen (s. Figure 7).

Mein Teil an diesem Paper entspricht den ersten Screening-Untersuchungen bezüglich der Apoptoseinduktion, die sowohl die zwei hier aufgeführten Komplexe umfasst als auch zwei weitere Komplexe, die nicht mit in den Artikel mit aufgenommen wurden. Eine Graphik ist als *Figure 3* im Paper enthalten.

3. Diskussion

In dieser Dissertation wurden zwei Paper vorgestellt, die die antitumorale Wirkung neuartiger NHC-Au(I)-Komplexe untersuchen. NHC-Komplexe haben in den letzten zwei Jahrzehnten als mögliche Antitumormittel vermehrte Aufmerksamkeit erhalten, da die Liganden die Goldkomplexe gut stabilisieren und eine antiproliferative Wirkung vielfach beobachtet werden konnte (Mora et al. 2019; Casini et al. 2018). Dies bestätigt sich hier. Alle hier untersuchten Komplexe zeigten auf verschiedenen immortalisierten Krebszellen (Leukämie-, Lymphom- und soliden Tumorzellen) ein Wirkungsspektrum im nanomolaren bis niedrigen mikromolaren Bereich. Die besten Verbindungen beider Publikationen zeigten auf Leukämie- und Lymphomzellen eine IC_{50} von 0,1 µM und weniger und auch die AC_{50} lag bei den untersuchten Verbindungen im nanomolaren Bereich. Eine Annexin V/Propidiumiodid-Doppelfärbung eignet sich gut, um den Zelltod näher zu beschreiben. Dabei ließ sich für die besten Verbindungen der beiden Publikationen im untersuchten Konzentrationsbereich vor allem ein Anstieg frühapoptotischer Stadien nach 48 Stunden Inkubation nachweisen und bestätigte die Apoptose als Ursache des Zelltods. Unspezifische, toxische Effekte wurden zudem für die ANB-Verbindung mittels Messung des zytosolischen LDH-Gehalts ausgeschlossen. Genauso wurden in beiden Publikationen Versuche zur Selektivität durchgeführt. Hierfür wurden die Au(I)-Komplexe auf Leukämiezellen und auf gesunden, menschlichen Leukozyten, die isoliert und kultiviert worden sind, verglichen und zeigten auf letztgenannten keine oder kaum zytotoxische Wirkung bis in einen Konzentrationsbereich, der einem Vielfachen der AC_{50} entspricht. Neben der Malignität unterscheiden sich die Leukozyten von den Leukämiezellen dadurch, dass sie sich nicht mehr teilen. Dies deutet darauf hin, dass, wie auch bei den meisten gängigen Zytostatika, die Zellteilung relevant für die apoptotische Wirkung ist.

Goldkomplexe eignen sich etwa hervorragend, das Flavoenzym Thioredoxinreduktase gezielt und irreversibel zu binden und zu blockieren (Saccoccia et al. 2014). Die Thioredoxinreduktase gilt neben der Glutathionperoxidase als wichtigstes Redoxsystem der Zelle und ist an einer Reihe antioxidativer Prozesse beteiligt: NADPH-abhängig reduziert es Thioredoxin und andere endogene und exogene Substrate. Eine Blockade führt zu einer Anreicherung von ROS bis zu oxidativen Stress und zur Apoptose (Mustacich und Powis 2000; Tonissen und Di Trapani 2009). In der Publikation 2.2 wurde die Inhibition der TrxR für die beiden genannten Komplexe untersucht. Interessanterweise lag die IC_{50} für Komplex 1 und 2 im direkten Vergleich deutlich über der des Phosphin-Au(I)-Komplexes Auranofin. In der erst aufgeführten Publikation (s. 2.1) wurde die Wirkung des Komplexes ANB4014 mit und ohne antioxidativ wirkenden Substanzen (N-Acetylcystein (NAC) und Taurin) als indirekter ROS-Nachweis analysiert. NAC hob die Wirkung

von ANB4014 vollständig auf, wohingegen Taurin dieses nur teilweise vermochte. Eine direkte ROS-Produktion durch Goldkomplexe, die sich mit einer Inhibition der TrxR deckt, wurde bereits beschrieben (Rubbiani et al. 2010). Auch konnte gezeigt werden, dass N-Acetylcystein die zytotoxische Wirkung von Gold aufhebt, vermutlich durch die Aufrechterhaltung der Thioredoxinreduktion (Saggioro et al. 2007). Weinberg und Kollegen postulierten in ihrem berühmten Artikel *The Hallmarks of cancer* sechs Kennzeichen der Tumorgenese und die Bildung von *Reactive oxygen species* (ROS) spielt bei jeder dieser *Hallmarks* eine Rolle (Hanahan und Weinberg 2000b; Hornsveld und Dansen 2016). Viele Tumorzellen bilden im Vergleich zu ihren gesunden Ausgangszellen einen erhöhten Gehalt an ROS und um dies auszugleichen, werden gleichzeitig antioxidative Systeme hochreguliert, darunter auch das Thioredoxinsystem (Trachootham et al. 2009; Zhang et al. 2017; Toyokuni et al. 1995). Hier anzusetzen, stellt eine legitime Strategie dar. Zou et al. zeigten beispielsweise, dass frisch isolierte CLL-Zellen, die ein erhöhtes ROS-Level zeigten, auch anfälliger für 2-Methoxyestradiol (2-ME) oder Arsentrioxid (ATO) waren, die beide die Bildung von ROS provozieren, 2-ME, indem es die Superoxiddismutase (SOD) hemmt (Zhou et al. 2003). Für ATO konnte gezeigt werden, dass es auch die TrxR inhibiert (Lu et al. 2007). Genotoxischer Stress kann das Signalmolekül GADD45A aktivieren, das in vielen Signalwegen des Zellzyklus oder der Apoptose beteiligt ist. GADD45A wurde durch ANB4014 auf Leukämiezellen hochreguliert (PCR: 25,8-fach). Eine Aktivierung kann schlussendlich zur Aktivierung des proapoptotischen BH3-only-Proteins BIM und so zur Aktivierung des intrinsischen Apoptosewegs führen (Salvador et al. 2013). Es ist vielfach beschrieben, dass Goldkomplexe und auch Organogoldverbindungen über den intrinsischen, also mitochondrialen Apoptoseweg, wirken (Barnard et al. 2004; Hickey et al. 2008). Dies konnten wir in der ersten Publikation für den dargestellten Komplex ANB4014 auf verschiedene Wege nachweisen. Der Zusammenbruch des mitochondrialen Transmembranpotentials als Indikator für die Permeabilisierung der äußeren Mitochondrienmembran (englisch: *mitochondrial outer membrane permeabilization* (MOMP)) und ein hieraus resultierender Cytochrom C- und Smac-Release ins Zytosol konnte beobachtet werden. MOMP und der Efflux der mitochondriale Proteine Cytochrom C und Smac ins Zytosol gilt als sogenannter „Point of no return“ in der Apoptose (Leber et al. 2007). Dabei sind die Proteine der Bcl-2-Familie die Torhüter dieses Mechanismus, bei dem sich das Verhältnis aus anti- und proapoptotischen Mitgliedern Richtung Apoptose verschieben muss (Kale et al. 2018). Diese Verschiebung konnten wir in verschiedenen Experimenten für ANB4014 belegen: Überexpression des proapoptotischen BH3-only-Proteins BIM und Unterexpression des antiapoptotischen Bcl-2 in der PCR sowie Hochregulierung des proapoptotischen BH3-only-Proteins Harakiri (Hrk) im

Western Blot. BIM gilt als das wichtigste proapoptotische Bcl-2-Protein und spielt eine entscheidende Rolle in der Wirkung vieler Zytostatika und auch gezielter Therapien, die häufig über das Mitochondrium agieren (Hata et al. 2015; Friedman et al. 2015). Die Zelllinien VCR-res. BJAB (Bcl-2-Überexpression), Dauno-res. K562 (Hrk-Unterexpression) und MTX-res. Nalm-6 (Mcl-1-Überexpression, p53-Unterexpression) haben im Zuge ihrer Resistenzbildung Über- oder Unterexpressionen anti- oder proapoptotischer Bcl-2-Proteine entwickelt. ANB4014 zeigte auf allen nicht nur Resistenzüberwindungen, sondern diese drei Zelllinien waren signifikant sensibler gegenüber der Substanz. Dies unterstützt die Annahme, dass Proteine der Bcl-2-Familie als Indikatoren des mitochondrialen Apoptosewegs wichtige Akteure im Wirkungsmechanismus dieses Goldkomplexes sind. Letai und Kollegen heben jedoch hervor, dass nicht unbedingt die Konzentration der antiapoptotischen Enzyme der entscheidende Faktor ist, sondern die Menge der an diese gebundenen Proapoptotika wie etwa das *activator*-BH-3-only-Protein BIM (Konopleva und Letai 2018). In 1.1.2 wurde bereits der Begriff „primed for death“ vorgestellt. Dieser erklärt die Abhängigkeit einiger Tumore von antiapoptotischen Bcl-2-Proteinen, da sie ein Überangebot an proapoptotischen Bcl-2-Proteinen binden und so eine Aktivierung von Bax/Bak verhindert wird (Certo et al. 2006). Die beiden Zelllinien MTX-res. Nalm-6 und VCR-res. BJAB zeichnen sich durch eine Überexpression der Antiapoptotika Mcl-1 und Bcl-2 aus. Dies ist ein häufig beobachteter Resistenzmechanismus bei hämatologischen Neoplasien (Singh et al. 2019). Es wäre vorstellbar, dass dieser Abhängigkeitsmechanismus von den antiapoptotischen Proteinen auch hier bestünde und bereits geringere Konzentrationen von ANB4014 dies unterwandert, der Resistenzmechanismus kollabiert und zur Apoptose der Zelle führt. In diesem Zusammenhang liefern die Versuche auf den Dauno.-resistenten K562 interessante Ergebnisse. Diese zeichnen sich im Vergleich zu ihren Ausgangszellen durch die Unterexpression des *sensitizer*-BH3-only-Proteins Harakiri (HRK) aus (Schlagintweit et al. 2021). Harakiri bindet die antiapoptotischen Proteine Bcl-2 und Bcl-xL (Inohara et al. 1997). Für ANB4014 konnte im Western Blot nach 24 Stunden eine Hochregulierung dieses Proteins beobachtet werden. Entsprechend interessant ist die Wirkung des Goldkomplexes auf diesen Zellen: Auf K562 zeigten sie im untersuchten Konzentrationsbereich keinerlei Wirkung, auf Dauno-res. K562 führte ANB4014 hingegen bereits in niedriger Konzentration zur Induktion der Apoptose in nahezu allen Zellen. Diese Ergebnisse könnten zu folgender Interpretation führen: Die Dauno-res. K562 scheinen von den niedrigen Hrk-Leveln abhängig zu sein. Führt ANB4014 zu einer Aktivierung proapoptotischer BH3-*sensitizer* wie Hrk, könnten diese über die Bindung an Bcl-2 oder Bcl-xL *activator*-BH3-only-Proteine freisetzen und so zur Apoptose führen. Interessant ist auch, dass sich dieser Effekt nicht für den Komplex 2 der zweiten Publikation

nachweisen lässt. Komplex 2 überwindet die Daunorubicin-Resistenz und ist auch wirksamer auf diesen Zellen, jedoch nicht in dem ausprägten Maß wie ANB4014. Die Neutralisierung antiapoptotischer Bcl-2-Proteine hat sich als wirksamer Mechanismus in der Tumortherapie herausgestellt. Medikamente, die bereits zugelassen sind, sind etwa BH-3-Mimetika wie Venetoclax, welches Bcl-2 selektiv bindet (Fulda 2011). Die Idee, Venetoclax auf den VCR-res. BJAB und den naiven BJAB zu vergleichen, bot sich daher an. Interessanterweise waren die Wildtyp-Zellen sensibler für Venetoclax. Eine Bcl-2-Überexpression allein muss jedoch noch nicht für Venetoclax sensibilisieren. So zeichnet sich das Follikuläre Lymphom durch hohe Bcl-2-Level aus, ist jedoch klinisch nicht sensibel für Venetoclax (Pham et al. 2018). Auch kann eine gleichzeitige Überexpression von Mcl-1 oder Bcl-xL neben Bcl-2 Zellen gegenüber Venetoclax resistent machen (Hormi et al. 2020; Choudhary et al. 2015). Interessanterweise zeigten Venetoclax und Vincristin zusammen einen synergistischen Effekt und Venetoclax scheint über die Bindung von Bcl-2 die VCR-res. BJAB-Zellen vollständig für Vincristin zu re-sensibilisieren. Dies legt die Vermutung nahe, dass die Bcl-2-Überexpression die resistenten Zellen vor Vincristin schützt, aber die Bcl-2-Bindung allein nicht Apoptose auslöst, sondern ein weiterer Stresstrigger notwendig ist.

Neben den Proteinen der Bcl-2-Familie sind die Caspasen die zweite große relevante Enzymgruppe der Apoptose. Caspasen können durch den intrinsischen oder extrinsischen Weg aktiviert werden und führen schlussendlich zur proteolytischen Spaltung funktioneller und morphologischer Proteine der Zelle (Taylor et al. 2008). Komplex 2 überwand die Cisplatin-Resistenz auf Neuroblastomzellen, die sich durch eine Caspase 8-Unterexpression auszeichnet. Caspase 8 ist ein wichtiges Enzym der extrinsischen Signalkaskade (van Cruchten und van den Broeck 2002). Eine starke Abhängigkeit der Wirkung dieses Goldkomplexes von Caspase 8 besteht in diesem Zusammenhang demnach nicht und unterstützt die Theorie, dass Goldkomplexe vornehmlich über den intrinsischen Apoptoseweg funktionieren. Caspase 3 und Caspase 7 sind wichtige Effektorcaspasen. Sie befinden sich downstream des intrinsischen und extrinsischen Apoptosewegs (Taylor et al. 2008). Für ANB4014 konnte eine Aktivierung von Caspase 3 im Western Blot und von Caspase 7 in der PCR gezeigt werden. Darüber hinaus spiegelt die Resistenz der Doxo-res. BJAB, die sich durch eine Caspase 3-Unterexpression auszeichnen, eine direkte Abhängigkeit der Wirkung von ANB4014 von Caspase 3 wider.

Der Vergleich der Gold(I)-Verbindungen auf Zytostatika-resistenten Tumorzellen und ihren naiven Ausgangszellen erlaubt nicht nur Rückschlüsse über den Wirkmechanismus, sondern spiegelt natürlich auch die Potenz der Substanzen wider, Resistenzen zu überwinden. Wie

bereits erwähnt, stellen Zytostatikaresistenzen einen erheblichen Teil der Therapielimitationen dar und können unterschiedlicher Genese sein (Longley und Johnston 2005). Die untersuchten Au(I)-Komplexe überwanden die meisten hier untersuchten Resistenzen, darunter auch eine Cisplatin-Resistenz. Nahezu alle Zytostatika-resistenten Subzelllinien, die wir in den beiden Papern präsentieren, zeichnen sich durch eine Vielzahl von Ko-Resistenzen gegenüber weiteren gängigen Chemotherapeutika aus. So eine genannte *Multidrug Resistance (MDR)* stellte eine enorme Herausforderung für die Onkologie dar (Szakács et al. 2006). Ein erhöhter, aktiver Efflux zytotoxischer Substanzen ist ein vielfach beobachteter Mechanismus und wird beispielsweise durch den MDR-Transporter P-Glykoprotein möglich, zu dessen Substraten hydrophobe, amphipathische Naturstoffe wie Anthrazykline, Vinca-Alkaloide, Epipodophyllotoxine, Paclitaxel und Colchicin gehören (Ambudkar et al. 1999; Holohan et al. 2013). Dies deckt sich mit unseren Beobachtungen zu den VCR-res.- und Dauno-res.-Leukämiezellen, die sich durch solch eine Überexpression des P-gp-Transporters auszeichnen (Simon et al. 1979). Beide Zelllinien zeigten keine Resistenz gegenüber dem Goldkomplex ANB4014 und dieser scheint hier somit kein Substrat zu sein. Dies deckt sich mit früheren Beobachtungen unserer Arbeitsgruppe zu NHC-Gold(I)-Verbindungen, bei denen sich auch der Gold-Uptake in die resistenten Zellen mit P-gp-Überexpression nicht von dem in den Ausgangszellen unterschied (Schmidt et al. 2017).

Schlussendlich lässt sich zusammenfassen, dass die NHC-Au(I)-Verbindungen, die hier vorgestellt wurden, potenzielle Antitumormittel darstellen. Sie sind im nanomolaren Bereich antiproliferativ und apoptotisch. Für die Komplexe 1 und 2 als auch für ANB4014 sind weitere Experimente wie beispielsweise ein direkter ROS-Nachweis und die Untersuchung der IC_{50} in Abhängigkeit von den ROS-Leveln verschiedener Tumorentitäten als auch die inhibitorische Aktivität für ANB4014 in Bezug auf die TrxR nötig. Die Diskonkordanz zwischen der Inhibition der TrxR und der Zellproliferation von Komplex 1 und 2 (Publikation 2.2) deuten darauf hin, dass dies nicht der Hauptwirkmechanismus ist. Ebenso lässt die unterschiedliche Wirksamkeit der Goldsubstanzen auf den K562-Zellen und ihren Dauno-res.-Abkömmling einen unterschiedlichen Wirkmechanismus vermuten. Ein hohes Potenzial wird durch die Überwindung vieler Zytostatikaresistenzen deutlich, da dies ein großes Problem in der Tumortherapie darstellt. Die Verbindung ANB4014 muss im Bezug auf Zytostatika-resistenten Zellen hervorgehoben werden, die durch molekulare Veränderungen der Bcl-2-Proteine charakterisiert sind und abhängig von diesen scheinen. Der Komplex unterwandert beeindruckend diese Resistenzmechanismen und macht die Zellen signifikant sensitiver gegenüber diesem. Hierbei konnte eine Vielzahl verschiedener Interaktionen mit verschiedenen Akteuren der Bcl-2-Familie beschrieben werden. Ein BH3-Profiling würde interessante

Aufschlüsse über noch offene Fragen hinsichtlich der Wirkweise geben und erste theoretische Ansätze konkretisieren.

4. Literaturverzeichnis

Ahrweiler-Sawaryn, Marie-C; Biswas, Animesh; Frias, Corazon; Frias, Jerico; Wilke, Nicola L.; Wilke, Nathalie et al. (2023): Novel gold(I) complexes induce apoptosis in leukemia cells via the ROS-induced mitochondrial pathway with an upregulation of Harakiri and overcome multi drug resistances in leukemia and lymphoma cells and sensitize drug resistant tumor cells to apoptosis in vitro. In: *Biomedicine & pharmacotherapy = Biomedecine & pharmacotherapie* 161, S. 114507. DOI: 10.1016/j.biopha.2023.114507.

Alnemri, Emad S.; Livingston, David J.; Nicholson, Donald W.; Salvesen, Guy; Thornberry, Nancy A.; Wong, Winnie W.; Yuan, Junying (1996): Human ICE/CED-3 Protease Nomenclature. In: *Cell* 87 (2), S. 171. DOI: 10.1016/S0092-8674(00)81334-3.

Ambudkar, S. V.; Dey, S.; Hrycyna, C. A.; Ramachandra, M.; Pastan, I.; Gottesman, M. M. (1999): Biochemical, cellular, and pharmacological aspects of the multidrug transporter. In: *Annual review of pharmacology and toxicology* 39, S. 361–398. DOI: 10.1146/annurev.pharmtox.39.1.361.

Barnard, Peter J.; Baker, Murray V.; Berners-Price, Susan J.; Day, David A. (2004): Mitochondrial permeability transition induced by dinuclear gold(I)-carbene complexes: potential new antimitochondrial antitumour agents. In: *Journal of inorganic biochemistry* 98 (10), S. 1642–1647. DOI: 10.1016/j.jinorgbio.2004.05.011.

Bayat Mokhtari, Reza; Homayouni, Tina S.; Baluch, Narges; Morgatskaya, Evgeniya; Kumar, Sushil; Das, Bikul; Yeger, Herman (2017): Combination therapy in combating cancer. In: *Oncotarget* 8 (23), S. 38022–38043. DOI: 10.18632/oncotarget.16723.

Benedek, Thomas G. (2004): The history of gold therapy for tuberculosis. In: *Journal of the history of medicine and allied sciences* 59 (1), S. 50–89. DOI: 10.1093/jhmas/jrg042.

Berners-Price, Susan J.; Filipovska, Aleksandra (2011): Gold compounds as therapeutic agents for human diseases. In: *Metallomics : integrated biometal science* 3 (9), S. 863–873. DOI: 10.1039/C1MT00062D.

Bindoli, Alberto; Rigobello, Maria Pia; Scutari, Guido; Gabbiani, Chiara; Casini, Angela; Messori, Luigi (2009): Thioredoxin reductase: A target for gold compounds acting as potential anticancer drugs. In: *Coordination Chemistry Reviews* 253 (11-12), S. 1692–1707. DOI: 10.1016/j.ccr.2009.02.026.

Bray, Freddie; Ferlay, Jacques; Soerjomataram, Isabelle; Siegel, Rebecca L.; Torre, Lindsey A.; Jemal, Ahmedin (2018): Global cancer statistics 2018: GLOBOCAN estimates of incidence and mortality worldwide for 36 cancers in 185 countries. In: *CA: a cancer journal for clinicians* 68 (6), S. 394–424. DOI: 10.3322/caac.21492.

Casini, Angela; Sun, Raymond Wai-Yin; Ott, Ingo (2018): Medicinal Chemistry of Gold Anticancer Metallodrugs. In: *Metal ions in life sciences* 18. DOI: 10.1515/9783110470734-013.

Certo, Michael; Del Gaizo Moore, Victoria; Nishino, Mari; Wei, Guo; Korsmeyer, Stanley; Armstrong, Scott A.; Letai, Anthony (2006): Mitochondria primed by death signals determine cellular addiction to antiapoptotic BCL-2 family members. In: *Cancer cell* 9 (5), S. 351–365. DOI: 10.1016/j.ccr.2006.03.027.

Choudhary, G. S.; Al-Harbi, S.; Mazumder, S.; Hill, B. T.; Smith, M. R.; Bodo, J. et al. (2015): MCL-1 and BCL-xL-dependent resistance to the BCL-2 inhibitor ABT-199 can be overcome by preventing PI3K/AKT/mTOR activation in lymphoid malignancies. In: *Cell death & disease* 6, e1593. DOI: 10.1038/cddis.2014.525.

Crooke, S. T.; Snyder, R. M. (1986): The cellular and molecular pharmacology of auranofin and related gold complexes. In: *Scandinavian journal of rheumatology. Supplement* 63, S. 1–18.

Dasari, Shaloam; Tchounwou, Paul Bernard (2014): Cisplatin in cancer therapy: molecular mechanisms of action. In: *European journal of pharmacology* 740, S. 364–378. DOI: 10.1016/j.ejphar.2014.07.025.

Deeks, Emma D. (2016): Venetoclax: First Global Approval. In: *Drugs* 76 (9), S. 979–987. DOI: 10.1007/s40265-016-0596-x.

Earnshaw, W. C.; Martins, L. M.; Kaufmann, S. H. (1999): Mammalian caspases: structure, activation, substrates, and functions during apoptosis. In: *Annual review of biochemistry* 68, S. 383–424. DOI: 10.1146/annurev.biochem.68.1.383.

European Medicines Agency (2021): Venclyxto (venetoclax). An overview of Venclyxto and why it is authorised in the EU (EMA/256462/2021). Online verfügbar unter https://www.ema.europa.eu/en/documents/overview/venclyxto-epar-medicine-overview_en.pdf.

Forestier, J. (1932): THE TREATMENT OF RHEUMATOID ARTHRITIS WITH GOLD SALTS INJECTIONS. In: *The Lancet* 219 (5661), S. 441–444. DOI: 10.1016/S0140-6736(01)24417-1.

Friedman, Adam A.; Letai, Anthony; Fisher, David E.; Flaherty, Keith T. (2015): Precision medicine for cancer with next-generation functional diagnostics. In: *Nature reviews. Cancer* 15 (12), S. 747–756. DOI: 10.1038/nrc4015.

Fulda, S.; Debatin, K-M (2006): Extrinsic versus intrinsic apoptosis pathways in anticancer chemotherapy. In: *Oncogene* 25 (34), S. 4798–4811. DOI: 10.1038/sj.onc.1209608.

Fulda, Simone (2011): Targeting apoptosis signaling pathways for anticancer therapy. In: *Frontiers in oncology* 1, S. 23. DOI: 10.3389/fonc.2011.00023.

Galluzzi, L.; Senovilla, L.; Vitale, I.; Michels, J.; Martins, I.; Kepp, O. et al. (2012): Molecular mechanisms of cisplatin resistance. In: *Oncogene* 31 (15), S. 1869–1883. DOI: 10.1038/onc.2011.384.

Gasser, Gilles; Ott, Ingo; Metzler-Nolte, Nils (2011): Organometallic anticancer compounds. In: *Journal of medicinal chemistry* 54 (1), S. 3–25. DOI: 10.1021/jm100020w.

Ghosh, Sumit (2019): Cisplatin: The first metal based anticancer drug. In: *Bioorganic chemistry* 88, S. 102925. DOI: 10.1016/j.bioorg.2019.102925.

Goetz, Laura H.; Schork, Nicholas J. (2018): Personalized medicine: motivation, challenges, and progress. In: *Fertility and sterility* 109 (6), S. 952–963. DOI: 10.1016/j.fertnstert.2018.05.006.

Hanahan, D.; Weinberg, R. A. (2000a): The hallmarks of cancer. In: *Cell* 100 (1), S. 57–70. DOI: 10.1016/s0092-8674(00)81683-9.

Hanahan, Douglas; Weinberg, Robert A. (2000b): The Hallmarks of Cancer. In: *Cell* 100 (1), S. 57–70. DOI: 10.1016/S0092-8674(00)81683-9.

Hata, Aaron N.; Engelman, Jeffrey A.; Faber, Anthony C. (2015): The BCL2 Family: Key Mediators of the Apoptotic Response to Targeted Anticancer Therapeutics. In: *Cancer discovery* 5 (5), S. 475–487. DOI: 10.1158/2159-8290.CD-15-0011.

Hengartner, M. O. (2000): The biochemistry of apoptosis. In: *Nature* 407 (6805), S. 770–776. DOI: 10.1038/35037710.

Hickey, James L.; Ruhayel, Rasha A.; Barnard, Peter J.; Baker, Murray V.; Berners-Price, Susan J.; Filipovska, Aleksandra (2008): Mitochondria-targeted chemotherapeutics: the rational design of gold(I) N-heterocyclic carbene complexes that are selectively toxic to cancer cells and target protein selenols in preference to thiols. In: *Journal of the American Chemical Society* 130 (38), S. 12570–12571. DOI: 10.1021/ja804027j.

Holohan, Caitriona; van Schaeybroeck, Sandra; Longley, Daniel B.; Johnston, Patrick G. (2013): Cancer drug resistance: an evolving paradigm. In: *Nature reviews. Cancer* 13 (10), S. 714–726. DOI: 10.1038/nrc3599.

Hormi, Myriam; Birsen, Rudy; Belhadj, Maya; Huynh, Tony; Cantero Aguilar, Lilia; Grignano, Eric et al. (2020): Pairing MCL-1 inhibition with venetoclax improves therapeutic efficiency of BH3-mimetics in AML. In: *European journal of haematology* 105 (5), S. 588–596. DOI: 10.1111/ejh.13492.

Hornsveld, Marten; Dansen, Tobias B. (2016): The Hallmarks of Cancer from a Redox Perspective. In: *Antioxidants & redox signaling* 25 (6), S. 300–325. DOI: 10.1089/ars.2015.6580.

Huaizhi, Zhao; Yuantao, Ning (2001): China's ancient gold drugs. In: *Gold Bull* 34 (1), S. 24–29. DOI: 10.1007/BF03214805.

Inohara, N.; Ding, L.; Chen, S.; Núñez, G. (1997): harakiri, a novel regulator of cell death, encodes a protein that activates apoptosis and interacts selectively with survival-promoting proteins Bcl-2 and Bcl-X(L). In: *The EMBO journal* 16 (7), S. 1686–1694. DOI: 10.1093/emboj/16.7.1686.

Kale, Justin; Osterlund, Elizabeth J.; Andrews, David W. (2018): BCL-2 family proteins: changing partners in the dance towards death. In: *Cell death and differentiation* 25 (1), S. 65–80. DOI: 10.1038/cdd.2017.186.

Koch, Robert (2010): Über bakteriologische Forschung. Unter Mitarbeit von Robert Koch-Institut und J. Schwalbe: Robert Koch-Institut.

Konopleva, Marina; Letai, Anthony (2018): BCL-2 inhibition in AML: an unexpected bonus? In: *Blood* 132 (10), S. 1007–1012. DOI: 10.1182/blood-2018-03-828269.

Kroemer, Guido; Galluzzi, Lorenzo; Brenner, Catherine (2007): Mitochondrial membrane permeabilization in cell death. In: *Physiological reviews* 87 (1), S. 99–163. DOI: 10.1152/physrev.00013.2006.

Leber, Brian; Lin, Jialing; Andrews, David W. (2007): Embedded together: the life and death consequences of interaction of the Bcl-2 family with membranes. In: *Apoptosis : an*

international journal on programmed cell death 12 (5), S. 897–911. DOI: 10.1007/s10495-007-0746-4.

Longley, D. B.; Johnston, P. G. (2005): Molecular mechanisms of drug resistance. In: *The Journal of pathology* 205 (2), S. 275–292. DOI: 10.1002/path.1706.

Lu, Jun; Chew, Eng-Hui; Holmgren, Arne (2007): Targeting thioredoxin reductase is a basis for cancer therapy by arsenic trioxide. In: *Proceedings of the National Academy of Sciences of the United States of America* 104 (30), S. 12288–12293. DOI: 10.1073/pnas.0701549104.

Manohar, Sandhya; Leung, Nelson (2018): Cisplatin nephrotoxicity: a review of the literature. In: *Journal of nephrology* 31 (1), S. 15–25. DOI: 10.1007/s40620-017-0392-z.

McKeage, Mark J. (2002): Gold opens mitochondrial pathways to apoptosis. In: *British journal of pharmacology* 136 (8), S. 1081–1082. DOI: 10.1038/sj.bjp.0704822.

McKeage, Mark J.; Maharaj, Lenushka; Berners-Price, Susan J. (2002): Mechanisms of cytotoxicity and antitumor activity of gold(I) phosphine complexes: the possible role of mitochondria. In: *Coordination Chemistry Reviews* 232 (1-2), S. 127–135. DOI: 10.1016/S0010-8545(02)00048-6.

Mirabelli, C. K.; Johnson, R. K.; Sung, C. M.; Faucette, L.; Muirhead, K.; Crooke, S. T. (1985): Evaluation of the in vivo antitumor activity and in vitro cytotoxic properties of auranofin, a coordinated gold compound, in murine tumor models. In: *Cancer research* 45 (1), S. 32–39.

Mora, Malka; Gimeno, M. Concepción; Visbal, Renso (2019): Recent advances in gold-NHC complexes with biological properties. In: *Chemical Society reviews* 48 (2), S. 447–462. DOI: 10.1039/c8cs00570b.

Mustacich, D.; Powis, G. (2000): Thioredoxin reductase. In: *The Biochemical journal* 346 (Pt 1), S. 1–8.

Nguyen, Phuongmai; Awwad, Rania T.; Smart, Dee Dee K.; Spitz, Douglas R.; Gius, David (2006): Thioredoxin reductase as a novel molecular target for cancer therapy. In: *Cancer letters* 236 (2), S. 164–174. DOI: 10.1016/j.canlet.2005.04.028.

Ong, Yih Ching; Gasser, Gilles (2020): Organometallic compounds in drug discovery: Past, present and future. In: *Drug discovery today. Technologies* 37, S. 117–124. DOI: 10.1016/j.ddtec.2019.06.001.

Pham, Lan V.; Huang, Shengjian; Zhang, Hui; Zhang, Jun; Bell, Taylor; Zhou, Shouhao et al. (2018): Strategic Therapeutic Targeting to Overcome Venetoclax Resistance in Aggressive B-cell Lymphomas. In: *Clinical cancer research : an official journal of the American Association for Cancer Research* 24 (16), S. 3967–3980. DOI: 10.1158/1078-0432.CCR-17-3004.

Rabik, Cara A.; Dolan, M. Eileen (2007): Molecular mechanisms of resistance and toxicity associated with platinating agents. In: *Cancer treatment reviews* 33 (1), S. 9–23. DOI: 10.1016/j.ctrv.2006.09.006.

Redza-Dutordoir, Maureen; Averill-Bates, Diana A. (2016): Activation of apoptosis signalling pathways by reactive oxygen species. In: *Biochimica et biophysica acta* 1863 (12), S. 2977–2992. DOI: 10.1016/j.bbamcr.2016.09.012.

Riccardi, Carlo; Nicoletti, Ildo (2006): Analysis of apoptosis by propidium iodide staining and flow cytometry. In: *Nature protocols* 1 (3), S. 1458–1461. DOI: 10.1038/nprot.2006.238.

Rigobello, Maria Pia; Scutari, Guido; Boscolo, Rita; Bindoli, Alberto (2002): Induction of mitochondrial permeability transition by auranofin, a gold(I)-phosphine derivative. In: *British journal of pharmacology* 136 (8), S. 1162–1168. DOI: 10.1038/sj.bjp.0704823.

Rigobello, Maria Pia; Scutari, Guido; Folda, Alessandra; Bindoli, Alberto (2004): Mitochondrial thioredoxin reductase inhibition by gold(I) compounds and concurrent stimulation of permeability transition and release of cytochrome c. In: *Biochemical pharmacology* 67 (4), S. 689–696. DOI: 10.1016/j.bcp.2003.09.038.

Rosenberg, B.; Vancamp, L.; Krigas, T. (1965): Inhibition of cell division in Escherichia coli by electrolysis products from a platinum electrode. In: *Nature* 205, S. 698–699. DOI: 10.1038/205698a0.

Rosenberg, Barnett (1980): Cisplatin: Its history and possible mechanisms of action. In: Cisplatin: Elsevier, S. 9–20.

Rottenberg, Sven; Disler, Carmen; Perego, Paola (2021): The rediscovery of platinum-based cancer therapy. In: *Nature reviews. Cancer* 21 (1), S. 37–50. DOI: 10.1038/s41568-020-00308-y.

Rubbiani, Riccardo; Kitanovic, Igor; Alborzinia, Hamed; Can, Suzan; Kitanovic, Ana; Onambele, Liliane A. et al. (2010): Benzimidazol-2-ylidene gold(I) complexes are thioredoxin reductase inhibitors with multiple antitumor properties. In: *Journal of medicinal chemistry* 53 (24), S. 8608–8618. DOI: 10.1021/jm100801e.

Saccoccia, Fulvio; Angelucci, Francesco; Boumis, Giovanna; Carotti, Daniela; Desiato, Gianni; Miele, Adriana E.; Bellelli, Andrea (2014): Thioredoxin reductase and its inhibitors. In: *Current protein & peptide science* 15 (6), S. 621–646. DOI: 10.2174/1389203715666140530091910.

Saggioro, Daniela; Rigobello, Maria Pia; Paloschi, Lucia; Folda, Alessandra; Moggach, Stephen A.; Parsons, Simon et al. (2007): Gold(III)-dithiocarbamato complexes induce cancer cell death triggered by thioredoxin redox system inhibition and activation of ERK pathway. In: *Chemistry & biology* 14 (10), S. 1128–1139. DOI: 10.1016/j.chembiol.2007.08.016.

Salvador, Jesús M.; Brown-Clay, Joshua D.; Fornace, Albert J. (2013): Gadd45 in stress signaling, cell cycle control, and apoptosis. In: *Advances in experimental medicine and biology* 793, S. 1–19. DOI: 10.1007/978-1-4614-8289-5_1.

Santos, Neife Aparecida Guinaim Dos; Ferreira, Rafaela Scalco; Santos, Antonio Cardozo Dos (2020): Overview of cisplatin-induced neurotoxicity and ototoxicity, and the protective agents. In: *Food and chemical toxicology : an international journal published for the British Industrial Biological Research Association* 136, S. 111079. DOI: 10.1016/j.fct.2019.111079.

Schlagintweit, Jonas F.; Jakob, Christian H. G.; Wilke, Nicola L.; Ahrweiler, Marie; Frias, Corazon; Frias, Jerico et al. (2021): Gold(I) Bis(1,2,3-triazol-5-ylidene) Complexes as Promising Selective Anticancer Compounds. In: *Journal of medicinal chemistry* 64 (21), S. 15747–15757. DOI: 10.1021/acs.jmedchem.1c01021.

Schmidt, Claudia; Karge, Bianka; Misgeld, Rainer; Prokop, Aram; Franke, Raimo; Brönstrup, Mark; Ott, Ingo (2017): Gold(I) NHC Complexes: Antiproliferative Activity, Cellular Uptake,

Inhibition of Mammalian and Bacterial Thioredoxin Reductases, and Gram-Positive Directed Antibacterial Effects. In: *Chemistry (Weinheim an der Bergstrasse, Germany)* 23 (8), S. 1869–1880. DOI: 10.1002/chem.201604512.

Simon, Timothy M.; Kunishima, Dennis H.; Vibert, Garry J.; Lorber, Arthur (1979): Inhibitory effects of a new oral gold compound on hela cells. In: *Cancer* 44 (6), S. 1965–1975. DOI: 10.1002/1097-0142(197912)44:6<1965::aid-cncr2820440602>3.0.co;2-6.

Simpson, Peter V.; Desai, Nima Maheshkumar; Casari, Ilaria; Massi, Massimiliano; Falasca, Marco (2019): Metal-based antitumor compounds: beyond cisplatin. In: *Future medicinal chemistry* 11 (2), S. 119–135. DOI: 10.4155/fmc-2018-0248.

Singh, Rumani; Letai, Anthony; Sarosiek, Kristopher (2019): Regulation of apoptosis in health and disease: the balancing act of BCL-2 family proteins. In: *Nature reviews. Molecular cell biology* 20 (3), S. 175–193. DOI: 10.1038/ s41580-018-0089-8.

Smith, Mitchell R. (2003): Rituximab (monoclonal anti-CD20 antibody): mechanisms of action and resistance. In: *Oncogene* 22 (47), S. 7359–7368. DOI: 10.1038/sj.onc.1206939.

Sung, Hyuna; Ferlay, Jacques; Siegel, Rebecca L.; Laversanne, Mathieu; Soerjomataram, Isabelle; Jemal, Ahmedin; Bray, Freddie (2021): Global Cancer Statistics 2020: GLOBOCAN Estimates of Incidence and Mortality Worldwide for 36 Cancers in 185 Countries. In: *CA: a cancer journal for clinicians* 71 (3), S. 209–249. DOI: 10.3322/caac.21660.

Szakács, Gergely; Paterson, Jill K.; Ludwig, Joseph A.; Booth-Genthe, Catherine; Gottesman, Michael M. (2006): Targeting multidrug resistance in cancer. In: *Nature reviews. Drug discovery* 5 (3), S. 219–234. DOI: 10.1038/nrd1984.

Taylor, Rebecca C.; Cullen, Sean P.; Martin, Seamus J. (2008): Apoptosis: controlled demolition at the cellular level. In: *Nature reviews. Molecular cell biology* 9 (3), S. 231–241. DOI: 10.1038/nrm2312.

Tonissen, Kathryn F.; Di Trapani, Giovanna (2009): Thioredoxin system inhibitors as mediators of apoptosis for cancer therapy. In: *Molecular nutrition & food research* 53 (1), S. 87–103. DOI: 10.1002/mnfr.200700492.

Toyokuni, Shinya; Okamoto, Keisei; Yodoi, Junji; Hiai, Hiroshi (1995): Persistent oxidative stress in cancer. In: *FEBS letters* 358 (1), S. 1–3. DOI: 10.1016/0014-5793(94)01368-b.

Trachootham, Dunyaporn; Alexandre, Jerome; Huang, Peng (2009): Targeting cancer cells by ROS-mediated mechanisms: a radical therapeutic approach? In: *Nature reviews. Drug discovery* 8 (7), S. 579–591. DOI: 10.1038/nrd2803.

van Cruchten, S.; van den Broeck, W. (2002): Morphological and biochemical aspects of apoptosis, oncosis and necrosis. In: *Anatomia, histologia, embryologia* 31 (4), S. 214–223. DOI: 10.1046/j.1439-0264.2002.00398.x.

Wheate, Nial J.; Walker, Shonagh; Craig, Gemma E.; Oun, Rabbab (2010): The status of platinum anticancer drugs in the clinic and in clinical trials. In: *Dalton transactions (Cambridge, England : 2003)* 39 (35), S. 8113–8127. DOI: 10.1039/c0dt00292e.

Wiltshaw, E.: Cisplatin in the treatment of cancer. In: *Platinum Metals Review* 1979 (23), S. 90–98.

Zhang, Junmin; Li, Xinming; Han, Xiao; Liu, Ruijuan; Fang, Jianguo (2017): Targeting the Thioredoxin System for Cancer Therapy. In: *Trends in pharmacological sciences* 38 (9), S. 794–808. DOI: 10.1016/j.tips.2017.06.001.

Zhou, Yan; Hileman, Elizabeth O.; Plunkett, William; Keating, Michael J.; Huang, Peng (2003): Free radical stress in chronic lymphocytic leukemia cells and its role in cellular sensitivity to ROS-generating anticancer agents. In: *Blood* 101 (10), S. 4098–4104. DOI: 10.1182/blood-2002-08-2512.

Zou, Taotao; Lum, Ching Tung; Lok, Chun-Nam; Zhang, Jing-Jing; Che, Chi-Ming (2015): Chemical biology of anticancer gold(III) and gold(I) complexes. In: *Chemical Society reviews* 44 (24), S. 8786–8801. DOI: 10.1039/c5cs00132c.

5. Anhang

5.1. Verzeichnis der akademischen Lehrer/-innen

„Meine akademischen Lehrenden im Fachbereich Medizin waren in Magdeburg: Fischer, Gottfried, Hofmann, Leßmann, Rothkötter, Sabel, Schlüter. “

„Meine akademischen Lehrenden im Fachbereich Medizin waren in Marburg: Bartsch, Becker, Birk, Bliemel, Bösner, Brendel, Burchert, Denkert, Donner-Banzhoff, Eberhart, Eschbach, Falkenberg, Geisthoff, Geks, Geraedts, Görg, Greulich, Hegele, Jansen, Kanngießer, Kalder, Köhler, Lüsebrink, Moll, Müller, Neubauer, Nimsky, Oberkircher, Pagenstecher, Pfützner, Plant, Renz, Ruchholtz, Schäfer, Schmeck, Sekundo, Sevinc, Stuck, Thieme, Timmermann, Vogt, Wagner, Wiesmann, Wollmer, Wulf.

Hiervon in Fulda:

Dörge, Hellinger, Hessmann, Hofmann, Kälbe, Kellersmann, Repp, Sasaki, Weber.“

5.2. Danksagung

An erster Stelle danke ich Aram Prokop, der sich vom ersten Bewerbungsgespräch bis hin zur Abgabe immer viel Zeit genommen hat. Dabei sind besonders die wöchentlichen Gespräche während der experimentellen Phase hervorzuheben, in denen er motivierende, lobende oder auch kritische Worte hatte, wenn die Versuche frustrierend, die Stunden lang, die Nerven dünn waren und am Ende doch das Meiste gelang. Für diese Zeit danke ich auch Corazon für ihre Hilfe, dafür, dass sie mir alles gezeigt hat, immer geduldig war und mir geholfen hat, wenn ich nicht weiterwusste. Ebenso danke ich Nicola und Jenny für die gegenseitige Unterstützung im Labor und den Austausch außerhalb des Labors. Vielen Dank darüber hinaus an Animesh Biswas und Professor Dr. Berkessel sowie Jonas F. Schlagintweit, Christian H. G. Jakob und Professor Dr. Kühn für die zur Verfügung gestellten Substanzen, die Zusammenarbeit und den Austausch. Ich danke zudem Herrn Professor Dr. Neubauer für die Annahme als Doktorandin, für das Vertrauen, für das Interesse an meiner Arbeit und den Input für weitere Versuche.

Fernab vom Labor danke ich meinen Eltern, die mich trotz des ein oder anderen Schlenkers im Werdegang immer unterstützt haben. Soweit ich mich erinnern kann, waren sie immer gelassen und haben unbeirrt an mich geglaubt. Meinem Mann danke ich für die Unterstützung während des Verfassens der Doktorarbeit, für seine fortwährende Geduld und seine Freude über jeden Meilenstein. Vielen Dank an Dan für das offene Ohr eines Gleichgesinnten, an Cecile für das Mitfiebern und an all die lieben Leute, die diese Zeit begleitet haben.

5.3. Publikationen

Publikation 1

Die nachfolgende Publikation “Novel gold(I) complexes induce apoptosis in leukemia cells via the ROS-induced mitochondrial pathway with an upregulation of Harakiri and overcome multi drug resistances in leukemia and lymphoma cells and sensitize drug resistant tumor cells to apoptosis in vitro”, veröffentlicht in Biomed Pharmacother. 2023 May;161:114507. https://doi.org/10.1016/j.biopha.2023.114507. Epub 2023 Mar 21. PMID: 36958194, ist lizensiert unter CC BY-NC-ND 4.0 DEED (https://creativecommons.org/licenses/by-nc-nd/4.0/) und nachgedruckt mit der Genehmigung durch Elsevier.

Biomedicine & Pharmacotherapy 161 (2023) 114507

Contents lists available at ScienceDirect

Biomedicine & Pharmacotherapy

journal homepage: www.elsevier.com/locate/biopha

Novel gold(I) complexes induce apoptosis in leukemia cells via the ROS-induced mitochondrial pathway with an upregulation of Harakiri and overcome multi drug resistances in leukemia and lymphoma cells and sensitize drug resistant tumor cells to apoptosis in vitro

Marie-C. Ahrweiler-Sawaryn [a,c,*], Animesh Biswas [b], Corazon Frias [a,c], Jerico Frias [a,c], Nicola L. Wilke [a,c], Nathalie Wilke [a,c], Albrecht Berkessel [b], Aram Prokop [a,c,d]

[a] Department of Pediatric Hematology/Oncology, Helios Clinic Schwerin, Wismarsche Straße 393-397, 19055 Schwerin, Germany
[b] Department of Chemistry, Organic Chemistry, University of Cologne, Greinstrasse 4, 50939 Cologne, Germany
[c] Department of Pediatric Hematology/Oncology, Children's Hospital Cologne, Amsterdamer Straße 59, 50735 Cologne, Germany
[d] Department of Research, Medical School Hamburg (MSH), University of Applied Sciences and Medical University, Am Kaiserkai 1, 20457, Germany

ARTICLE INFO

Keywords:
NHC-Au(I) complexes
Mitochondrial pathway
Apoptosis
ROS
Bcl-2
Harakiri
Multidrug resistance

ABSTRACT

Gold complexes could be promising for tumor therapy because of their cytotoxic and cytostatic properties. We present novel gold(I) complexes and clarify whether they also show antitumor activity by studying apoptosis induction in different tumor cell lines in vitro, comparing the compounds on resistant cells and analyzing the mechanism of action. We particularly highlight one gold complex that shows cytostatic and cytotoxic effects on leukemia and lymphoma cells already in the nanomolar range, induces apoptosis via the intrinsic signaling pathway, and plays a role in the production of reactive oxygen species. Furthermore, not only did we demonstrate a large number of resistance overcomes on resistant cell lines, but some of these cell lines were significantly more sensitive to the new gold compound. Our results show promising properties for the gold compound as antitumor drug and suggest that it can subvert resistance mechanisms and thus targets resistant cells for killing.

1. Introduction

Since the discovery of the cytostatic nature of the metal-based cytostatic drug cisplatin in 1965, it has been used as a chemotherapeutic agent for a variety of tumor entities [1,2]. Despite the drug's good efficacy, therapeutic options find their limit in cytostatic resistance and severe side effects, and recurrences occur [3]. However, with the discovery of cisplatin, interest in metal-based compounds has been aroused and there is a continuing interest in new compounds that can circumvent the aforementioned therapeutic limitations that affect many cytostatic drugs and tumor entities [4].

As a mechanism of action, many chemotherapeutic agents directly or indirectly target the induction of apoptosis [5,6]. Apoptosis as programmed cell death is regulated in two ways: The cell can receive external signals via so-called death receptors or perceive intracellular stressors such as reactive oxygen species (ROS) or DNA strand breaks [7,8]. One speaks of the extrinsic and intrinsic apoptosis pathways, which end in the activation of final self-destruction cascades. Key enzymes in this process are the caspases, which proteolytically cleave functional and structural enzymes of the cell [7,9,10]. Central players of the intrinsic pathway are the pro- and anti-apoptotic proteins of the Bcl-2 family, which, if apoptotic influences predominate, lead to permeabilization of the mitochondrial membrane and pro-apoptotic mitochondrial proteins leak out [11]. Under physiological conditions, apoptosis is finely regulated to prevent erroneous cell death [5]. Tumor cells, if not to a higher degree, are also exposed to the above signals and stressors from extra- and intracellular. Still tumors find ways to evade apoptosis, despite sometimes massive perturbations at the functional

Abbreviation: VCR-res. Nalm-6, Nalm-6 cells with induced vincristine resistance; Dauno-res. Nalm-6, Nalm-6 cells with induced daunorubicin resistance; MTX-res. Nalm-6, Nalm-6 cells with induced methotrexate resistance; VCR-res. BJAB, BJAB cells with induced vincristine resistance; Doxo-res. BJAB, BJAB cells with induced doxorubicin resistance; Dauno-res. K562, K562 cells with induced daunorubicin resistance.

* Corresponding author at: Department of Pediatric Hematology/Oncology, Helios Clinic Schwerin, Wismarsche Straße 393-397, 19055 Schwerin, Germany.
E-mail address: Ahrweile@students.uni-marburg.de (M.-C. Ahrweiler-Sawaryn).

https://doi.org/10.1016/j.biopha.2023.114507
Received 6 February 2023; Received in revised form 2 March 2023; Accepted 7 March 2023
Available online 21 March 2023

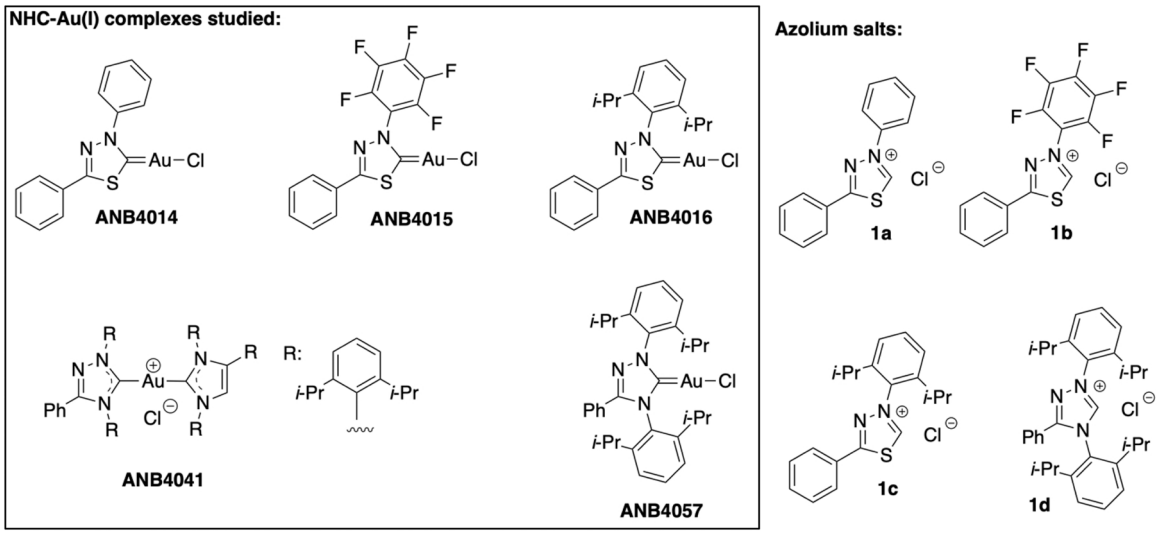

Scheme 1. NHC-Au(I) complexes (ANB4014, ANB4015, ANB4016, ANB4041, ANB4057) and corresponding Azolium salts (1a–d).

and structural levels [12,13]. The mechanisms that cells use for this are probably as diverse as the mechanisms of apoptosis that a cell encounters during tumorigenesis [14]. For example, a frequently described tool in malignant cells is the upregulation of the anti-apoptotic Bcl-2 and its close relatives such as Bcl-xL or Mcl-1 [13,15]. Impaired apoptosis is not only causal for the development of tumors, but cytostatic resistance, whether intrinsic or acquired, can also be the consequence [6].

In this article, we disclose our studies on the five novel Au(I) complexes ANB4014–4016, ANB4041 and ANB4057 summarized in Scheme 1. All of these complexes contain N-heterocyclic carbenes as a ligand(s), derived in the usual way from azolium salts by deprotonation in the presence of the Au(I)-source AuCl(SMe2) [16]. Specifically, ANB4014 is derived from the 3,5-diphenyl substituted1,3,4-thiadiazolium chloride 1a [16,17], ANB4015 from the 3-pentafluorophenyl-5-phenyl substituted 1,3,4-thiadiazolium chloride 1b [16], and ANB4016 from the 3-[2,6-di(2-propyl)phenyl]-5-phenyl substituted 1,3,4-thiadiazolium chloride 1c [16]. In the cases of ANB4041 and ANB4057, the 1,4-di[2,6-di(2-propyl)phenyl]-3-phenyl-1,2,4-triazolium chloride 1d served as the source of the corresponding 1,2,4-triazolin-5-ylidene [18].

In our research group, we investigate metal compounds for initial mechanistic effects. We investigated whether the new substances have cytotoxic and cytostatic properties as antitumor agents by analyzing them on different cell series in vitro. We investigated apoptosis induction and the corresponding mechanism of action focusing on leukemia and lymphoma cell lines. In our laboratory, we work with many in vitro cells in which cytostatic resistance has been developed. A comparison on the wild type cells and the corresponding resistant cells will show how far the gold compounds are able to overcome multi drug resistance. Overcoming known resistance mechanisms will provide further insight into the mode of action of the gold complexes.

2. Materials and methods

2.1. Substances

The gold (I) complexes ANB4014-4016, ANB4041 and ANB4057 (see Scheme 1) were employed as pure, crystalline materials, and were dissolved in Dimethyl sulfoxide (DMSO) (40 mM). DMSO and propidium iodide (PI) (50 µg/ml) were obtained from Serva (Heidelberg, Germany), RNase A from Qiagen (Hilden, Germany). The conventional cytostatic drugs (such as vincristine, daunorubicin, doxorubicin, methotrexate, etc.) were provided by Helios Kliniken Schwerin, prepared with DMSO or water as stock solution according to their properties, and further diluted immediately before use in the experiments. Venetoclax was obtained from TOCRIS (Bristol, UK).

2.2. Used cell lines and cell cultivation

The following cell lines were used: Nalm-6 (human b cell precursor leukemia cells); BJAB (human Burkitt like lymphoma cells); Jurkat (human T-cell leukemia cells), provided by Prof. Dr. S. Fulda, Goethe University Frankfurt; K562 (human chronic myeloid leukemia in blast crisis), provided by Prof. Dr. Dr. K.-H. Seeger, Charité Berlin; SKN-AS (human neuroblastoma cell line), provided by Prof. Dr. T. Simon, University Cologne; MCF-7 (human breast carcinoma cell line); MelHO (human melanoma cell line), provided by Dr. J. Eberle, Charité Berlin. Furthermore, in some cell lines, we induced resistance to common cytostatic drugs. We treated the cells with small amounts of the chemotherapeutic agents, in which no loss of viability was observed. The concentration was then raised until the cells were no longer susceptible to cytotoxic concentrations. The Nalm-6 cells were made resistant to Vincristine (VCR), Daunorubicin (Dauno), Methotrexate (MTX); the BJAB cells to VCR and Doxorubicin (Doxo); the K562 cells to Dauno. The cells were cultured in RPMI 1640 (Gibco, Invitrogen, Karlsruhe, Germany) supplemented with 10 % (v/v) heat inactivated FBS and 1 % (v/v) penicillin streptomycin at 37 °C and 5 % CO_2. Cell cultures were subcultured every 3–4 days to a concentration of 0.5×10^5/ml. To establish uniform growth conditions, the cells were brought to a concentration of 3×10^5/ml 24 h prior to an experimental set-up. The cells were used for test preparation the next day and were brought to appropriate concentrations.

2.3. Necrosis exclusion via LDH detection

The measurement of lactate dehydrogenase (LDH) in the medium, which leaks out of the cells when cell integrity is lost, is a reasonable way to rule out necrosis [19,20] and can be done with an ELISA-based coupled enzymatic test [21]. We used the Cytotoxicity Detection Kit (Roche, Mannheim, Germany) according to the manual. Substances incubated for 1 h. A positive control with Triton-X100 was carried out and defined 100 % cell necrosis. Test samples were correlated to this.

2.4. Determination of cell concentration and cell viability

Cell concentration as well as cell viability were investigated using the CASY®CellCounter and Analyzer System (OMNI Life Science, Bremen, Germany). Cells could be analyzed according to their respective characteristics in a defined setup and differentiated in a single measurement

between cell debris, dead cells and viable cells. For the analysis of cell proliferation after 24 h the cells were prepared in 1×10^5/ml and incubated with the respective test substances at 37 °C and 5 % CO_2. A DMSO control was carried out at the highest concentration and was equivalent to no more than 0.5 %. After 24 h cell suspension was properly resuspended, and 100 µL were transferred into 10 ml CASYton (ready-to-use-isotonic saline solution) and measured. The control or DMSO-control determined a cell proliferation of 100 %. Test approaches were devised in relation to this. The IC_{50} was determined with the AAT Bioquest Tool [22].

2.5. Measurement of apoptosis via modified cell cycle analysis

We analyzed DNA fragmentation as a late apoptotic stage [23]. The DNA fragmentation was calculated using a modified cell cycle analysis, which detects DNA fragmentation at the single-cell level as described [24]. DNA fragmentation was investigated as follows. Cell cultures were placed in 1×10^5/ml, treated with the respective test substances in appropriate concentrations and incubated for 72 h at 37 °C and 5 % CO_2. A DMSO control was carried out at the highest concentration used and was equivalent to no more than 0.5 %. The cells were collected via centrifugation (8000 rpm, 4 °C, 5 min) and fixed on ice with formaldehyde (2 %, (v/v)) in 1 × PBS for 30 min. After incubation the cells were centrifuged (1500 rpm, 4 °C, 5 min) and incubated with 1 × PBS/ethanol (1:2, (v/v)) on ice for 15 min. Cells were centrifuged (1500 rpm, 4 °C, 5 min) and resuspended in RNase A (40 µg/ml) in 1 × PBS. RNase was incubated for 30 min at 37 °C. The cells were centrifuged (1500 rpm, 4 °C, 5 min) and resuspended in 1 × PBS with Propidium iodide (PI) (50 µg/ml). DNA fragmentation was analyzed and quantified as hypodiploid DNA content (subG1) by flow cytometry (FACScan, Becton Dickinson, Heidelberg, Germany). The data evaluation was performed by the Cell Quest software.

2.6. Annexin V/Propidium iodide (PI) double staining

We used the Annexin-V-FLUOS staining (Roche, Mannheim, Germany). The experimental setup was as follows: Cells were plated out in 1×10^5/ml and treated with appropriate substances, which incubated on the cells for 48 h at 37 °C and 5 % CO_2 content. After incubation, cells were collected (5 min, 4 °C, 8000 rpm), the pellet was washed in 1 × PBS and centrifuged again (5 min, RT, 1500 rpm). Four control sets were included (incubation buffer only, Annexin-V-FITC in incubation buffer, PI in incubation buffer, Annexin-V-FITC + PI in incubation buffer). The concentration series was incubated with Annexin-V-FITC + PI in incubation buffer (15 min, RT). The data evaluation was performed by flow cytometry (FACScan, Becton Dickinson, Heidelberg, Germany). The data evaluation was performed by the Cell Quest software.

2.7. Measurement of the mitochondrial transmembrane potential ($\Delta\psi_m$)

The cells were prepared in 1×10^5/ml and treated with test substances. After 48 h of incubation at 37 °C and 5 % CO_2 concentration the cells were collected by centrifugation (3000 rpm, 5 min, 4 °C). The pellets were resuspended in phenol red-free RPMI and 5,5′,6,6′-Tetrachlor-1,1′,3,3′-tetraethylbenzimidazolylcarbocyaniniodid (JC-1) (0.2 mg/ml in DMSO) was added by pipetting. The samples were briefly vortexed and incubated at 300 rpm and 37 °C for 30 min in a thermal mixer. After the incubation period the cells were centrifuged (4000 rpm, 4 °C, 5 min) and resuspended in 1xPBS. The mitochondrial transmembrane potential was analyzed in flow cytometry using FACScan (Becton Dickinson, Heidelberg, Germany) and the CELL Quest software.

2.8. Isolation of human leukocytes

Leukocytes were isolated from the human blood of a healthy individual. 50 ml of fresh blood was collected and diluted with RPMI 1640 medium supplemented with 20 % FCS (v/v). 4 ml of bicoil separating solution was placed in Falcons and carefully overlaid with 5 ml of diluted blood. Samples were centrifuged (18 min, 18 °C, 2000 rpm) and leukocytes were then collected using a Pasteur pipette and washed with 10 ml of medium (20 % FCS). Leukocytes were centrifuged again (5 min, 18 °C, 2000 rpm) and resuspended again in 10 ml medium (20 % FCS). The cell count was determined using CASY®CellCounter and Analyzer System from OMNI Life Science (Bremen, Germany) and the leukocytes were then taken into culture at a count of 3×10^5 cells/ml. The remainder of the experiment was the same as for DNA fragmentation. The blood is donated by a member of our working group. The experiment was confirmed by an ethics committee (EK_MR_150321_Neubauer).

2.9. Immunoblotting

After 24 h incubation of the substance at appropriate concentrations on Nalm-6 cells, protein purification was performed. Cells were pelleted (5 min, 4 °C, 1500 rpm), washed with 1x PBS, and pelleted again (5 min, 4 °C, 8000 rpm). Cells were then incubated for one hour in lysis buffer (Tris/HCl (10 mM Tris-HCl, pH 7.5), EDTA (2 mM), 0.1 % (w/v) SDS, 1 × Complete Protease Inhibitor Cocktail) and were then centrifuged for 30 min (4 °C, 13,200 rpm). Protein concentration in the supernatant was determined by BSA standard calibration and ELISA measurement according to a Pierce® BCA Protein Assay (ThermoFisher Scientific Inc., Waltham, USA). The appropriate amount of protein was denatured in sample buffer and water for 5 min at 95 °C and 300 rpm. Protein separation was performed by SDS-polyacrylamide gel electrophoresis (SDS-PAGE). A standard protein marker was included for molecular weight. We used gradient gels (Serva Electrophoresis GmbH, Heidelberg, Germany), and the pockets were filled with 20 µL protein sample or 7 µL marker each. Electrophoresis was run at 120 V for 10 min and then at 160 V for 45 min. Subsequently, the separated proteins were transferred to a nitrocellulose membrane by semidry blot (65 min, 100 mA). The membrane was washed in 1 × PBS and blocked for one hour in PBST (PBS, 0.05 % Tween-20) containing BSA. Various primary antibodies were then incubated for one hour. Used were Caspase 3 antibody (Enzo, Farmingdale, USA), Beta-actin-antibody (Sigma-Aldrich, St. Louis, USA), Harakiri antibody (USBiological, Salem, USA). The membrane was washed 3 times again in PBST, and the secondary antibodies in PBST were incubated for one hour. The following antibodies were used: anti-mouse IgG HRP (Promega, Madison, USA), anti-Rabbit IgG HRP (Sigma-Aldrich, St. Louis, USA). After washing again (3 ×), the bands were detected using ECL solution (GE Healthcare, Chicago, USA) and Chemigenius-2 bio-imaging system (Syngene, Cambridge, UK).

2.10. Cytochrome c release

The Mitochondria Isolation Kit for Mammalian Cells (Pierce, Rockford, USA) was used to separate the mitochondrial fraction from the cytosolic fraction and performed according to the manual. After isolation, the procedure coincides with immunoblotting from the BSA standard calibration line. As the first antibodies we used anti-Smac (Santa Cruz Biotechnology, Inc., Dallas, USA), anti-cytochrome c (BD Pharmingen, San Diego, USA), anti-beta-actin (Sigma-Aldrich, St. Louis, USA). We used anti-mouse IgG HRP (Promega, Madison, USA) as a second antibody.

2.11. RT qPCR

We used the RT^2 profiler array PAHS-212Z (Human Cell Death PathwayFinder, Qiagen, Hilden, Germany) according to the instruction. Cells were plated out in 1×10^5/ml and incubated with ANB4014 for 14 h. A substance-free control was also incubated for 14 h. RNA was

Table 1
Screening of gold complexes after 72 h of incubation on Nalm-6 cells. Apoptosis was determined by modified cell cycle analysis. Shown are the AC_{50} (concentration causing apoptosis in 50 % of the cells) concentrations of the corresponding complexes. The AC_{50} was calculated using the AAT Bioquest tool [22] from the value greater than and less than the AC_{50} (n = 3). Thus, the AC_{50} here corresponds only to an approximate value. For corresponding graphs see Supplement 1.

Compound	AC_{50} values (μM)
ANB4014	0.36
ANB4015	0.7
ANB4016	0.22
ANB4041	0.7
ANB4057	2.2

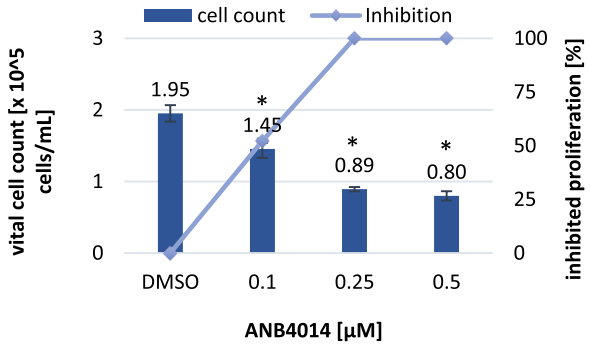

Fig. 1. Antiproliferative effect of ANB4014 after 24 h incubation on Nalm-6 cells. Cells were plated out in 1 × 10^5/ml. After 24 h a doubling of the cell number can be expected. If the final cell number is below 1 × 10^5/ml cytotoxic effects of the substance can be assumed. IC_{50} = 0.1 μM. The IC_{50} was calculated using the AAT Bioquest tool [1]. For calculation the concentrations were normalized to DMSO, because DMSO showed antiproliferative effects to a small extent. n = 3 ± SD. (*: $p < 0.05$ vs. DMSO, two-tailed t-test).

isolated and purified using Pure RNA Isolation KIT (Roche Molecular Systems Inc., Rotkreuz, Switzerland). RNA was measured photometrically in a quality control to verify purity and determine concentration. The cDNA synthesis was performed using the RT^2 First Strand Kit from Qiagen, and an SYBR Green Mastermix (RT^2 SYBR Green Mastermix, Qiagen, Hilden, Germany) was prepared. An appropriate amount was pipetted into the wells of the RT^2 PCR Array (Qiagen, Hilden, Germany). PCR was performed in LightCycler® 96 (Roche Molecular Systems Inc., Rotkreuz, Switzerland), and analysis was performed using the ΔΔCt method by the GeneGlobe Data Analysis Center (Qiagen, Hilden, Germany).

2.12. Statistics

The results shown correspond to a triplicate determination (except Western blots and PCR). The standard deviation (SD) is shown as error bars. If SD is very small, error bars may not be seen. Significance was calculated after normalization to DMSO using a two-tailed t-test with a significance level of 0.05. Graphs and statistics were performed using Microsoft Office Excel.

3. Results

3.1. Screening of gold compounds

To get an overview of the cytotoxicity of the different gold complexes, we screened the compounds on leukemia cells Nalm-6. We analyzed DNA fragmentation as late apoptotic stage by modified cell

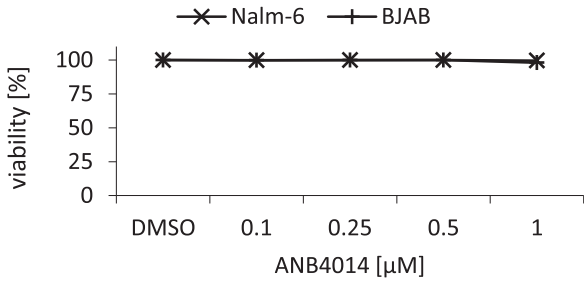

Fig. 2. Exclusion of necrosis-induced cell death by ANB4014 on Nalm-6 and BJAB after 1 h of incubation. LDH leaks from the cell during lost cell integrity and was measured by coupled enzymatic assay in the medium. An increase in LDH concentration in the medium corresponds to a decrease in viability. This is not observed with the substance ANB4014. n = 3.

cycle analysis via propidium iodide (PI) staining and cytometry after 72 h of incubation [23,24]. All compounds showed effects in the nano- or low micromolar range (see Table 1). The most promising compounds were ANB4014 and ANB4016, which showed similar apoptotic effects already in the nanomolar concentration range.

3.2. The IC_{50} of ANB4014 and ANB4016 are in the nanomolar range

To investigate the antiproliferative effects of the ANB4014 and ANB4016 complexes, we determined the cell number after 24 h of incubation of the compounds compared with an entrained control. We assayed both compounds on leukemia and lymphoma cell lines. IC_{50} (half maximal inhibitory concentration) values in the nanomolar range were shown on both cell series and with both compounds (IC_{50}s: ANB14 on Nalm-6 = 0.1 μM, ANB4014 on BJAB= 0.18 μM, ANB4016 on Nalm-6 = 0.2 μM, ANB4016 on BJAB= 0.29 μM). For both compounds, cytotoxic effects can already be observed after 24 h when the cell number drops below the seeded cell number. This is exemplified here using the compound ANB4014 on Nalm-6 cells (see Fig. 1). The other graphs can be seen in Supplement 2. For further experiments, we focused on the substance ANB4014.

3.3. Specification of cytotoxic and cytostatic effects via LDH measurement and Annexin V/PI double staining

To rule out the nonspecific cytotoxic effects of the compounds, we examined lactate dehydrogenase (LDH) extraction from cells after 1 h of incubation of the compounds on Nalm-6 and BJAB cells. LDH can leave the cell and be detected in the medium in the course of lost cell integrity and thus serves here as a necrosis indicator [21]. ANB4014 does not show unspecific cytotoxic effects in the relevant concentration range on the mentioned cell lines after 1 h of incubation. Viability is 100 % in Nalm-6 cells at the highest concentration tested (1 μM) and slightly lower in BJAB cells (98.04 %) (see Fig. 2). To confirm and characterize more precise cytotoxicity (vital vs. apoptosis vs. necrosis) we additionally performed Annexin V/Propidium iodide double staining [25,26]. After 48 h of incubation of ANB4014 on Nalm-6, a concentration-dependent decrease in vital cells was observed, with a concomitant increase in mainly early apoptotic stages (see Supporting information Supplement 4, Supplement 5).

3.4. ANB4014 acts on various cancer cell lines in vitro

We compared the apoptotic effect of the gold complex ANB4014 on different tumor cell lines. ANB4014 was incubated for 72 h on the corresponding cells. We analyzed DNA fragmentation as late apoptotic stage. The approximate AC_{50} (concentration causing apoptosis in 50 % of the cells) ranges are given in Table 2.

Table 2
AC_{50} values of ANB4014 on different tumor cell lines. Apoptosis was determined by modified cell cycle analysis. The gold compound incubated for 72 h in each case. The AC_{50} was calculated using the AAT Bioquest tool [22] from the value greater than and less than the AC_{50}. Thus, the AC_{50} here corresponds only to an approximate value. n = 3. AC_{50} (concentration causing apoptosis in 50 % of the cells). For corresponding graphs see Supplement 1, Supplement 3.

Cell line	Tumor	AC_{50} values (μM)
Nalm-6	B-ALL	0.35
BJAB	Burkitt-like Lymphoma	0.4
Jurkat	T-ALL	2.4
SKN-A-S	Neuroblastoma	6.1
MCF-7	Breast cancer	28
MelHO	Melanoma	34

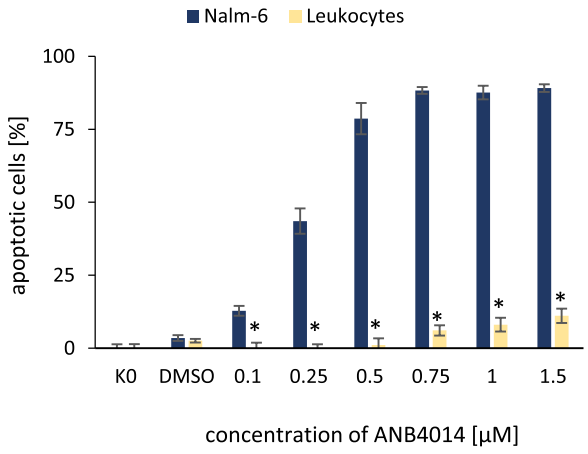

Fig. 3. ANB4014 shows only minor apoptotic effects on healthy human leukocytes compared to leukemia cells. We isolated the leukocytes from 50 ml of healthy human blood and took them into culture. ANB4014 incubated for 72 h on the leukocytes and leukemia cells. Apoptosis was determined by modified cell cycle analysis. n = 3 ± SD. (*: $p < 0.05$ vs. analogous concentration on Nalm-6, two-tailed t-test).

3.5. ANB4014 shows little apoptosis on healthy human leukocytes compared to leukemia cells

To exclude cytotoxic effects on healthy leukocytes, we extracted leukocytes from healthy human blood, cultured them and incubated ANB4014 on them for 72 h. In the concentration range corresponding to more than three times the AC_{50} for Nalm-6, only minor apoptotic effects by ANB4014 were seen on the leukocytes. From a concentration of 0.75 μM, a saturation effect can be observed on the Nalm-6 cells (see Fig. 3).

3.6. Gold complex acts via the intrinsic apoptosis pathway

Intrinsic apoptosis leads to the permeabilization of the mitochondrial membrane, in the course of which the mitochondrial transmembrane potential (Δψm) also collapses [15]. This can be visualized by means of JC-1 staining [27]. ANB4014 incubated for 48 h on Nalm-6 cells and showed a concentration-dependent loss of mitochondrial transmembrane potential and thus involvement of mitochondrial apoptosis (see Fig. 4). If mitochondrial membrane permeabilization occurs, the pro-apoptotic proteins cytochrome c and Smac are released from the mitochondrion into the cytoplasm and activate downstream the further signaling chain [5]. After 24 h of incubation of ANB4014 on Nalm-6 a cytochrome c and Smac release into the cytosol could be observed in the Western blot, confirming the involvement of the intrinsic pathway (see

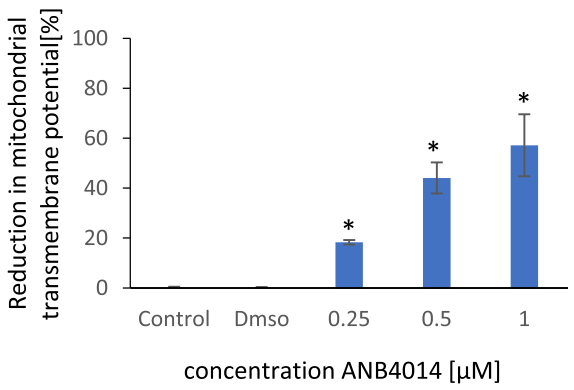

Fig. 4. ANB4014 leads to reduction of mitochondrial transmembrane potential in Nalm-6. The compounds incubated for 48 h. Loss of membrane potential was determined by JC-1 and flow cytometry. n = 3 ± SD. (*: $p < 0.05$ vs. DMSO, two-tailed t-test).

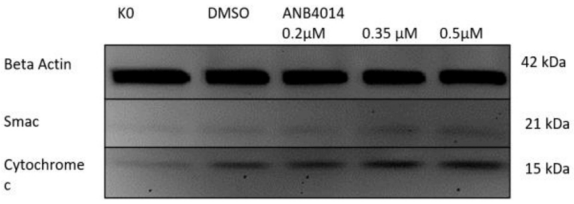

Fig. 5. Cytochrome c and Smac release into the cytosol by ANB4014 on Nalm-6 after 24 h of incubation. A concentration-dependent increase of Smac and especially cytochrome c can be seen in the Western Blot.

Fig. 5).

3.7. N-acetylcysteine prevents apoptosis, taurine leads to effect reduction

Tumor cells, in the course of their increased metabolism, also form increased ROS and counteract these by an increase in redox systems, including the Thioredoxin (Trx) system [28]. Based on the large body of work showing that gold complexes inhibit thioredoxin reductase (TrxR) and induce ROS [29–31], as well as that N-acetylcysteine (NAC) can completely inhibit the effect of gold [32], we also investigated an effect-reducing impact by the antioxidants NAC and taurine. NAC acts on the ROS levels of the cell in several ways: for example, as a direct radical scavenger, as a reducing agent, or by increasing glutathione levels [33]. Taurine, on the other hand, is not a classical free radical scavenger but acts on the ROS status of the cell via various indirect mechanisms. For example, taurine reduces ROS production in the respiratory chain, but also protects the cell's antioxidant defense system by protecting the enzymes involved from oxidative stress [34]. We compared the apoptotic effect of ANB4014 on Nalm-6 alone and in combination with NAC or taurine, thus indirectly demonstrating an effect relationship with ROS. NAC completely prevents apoptosis by ANB4014 (see Fig. 6, A), whereas taurine just leads to a reduction in effect on Nalm-6 cells (see Fig. 6, B).

3.8. Involvement of different proteins of the Bcl-2 family

The Bcl-2 family proteins are the key enzymes in both the initiation and inhibition of the mitochondrial apoptosis pathway and encompass three groups: anti-apoptotic members (as Bcl-2, Bcl-xL, Mcl-1), pro-apoptotic pore-formers (as Bax, Bak), and pro-apoptotic BH3-only proteins (as BIM, Bid, Puma, HRK) [35]. So, we examined ANB4014 on cytostatic-resistant leukemia cells, which are characterized by up- or downregulation of members of the Bcl-2 family as a resistance mechanism. These cytostatic resistances are induced by our laboratory and by

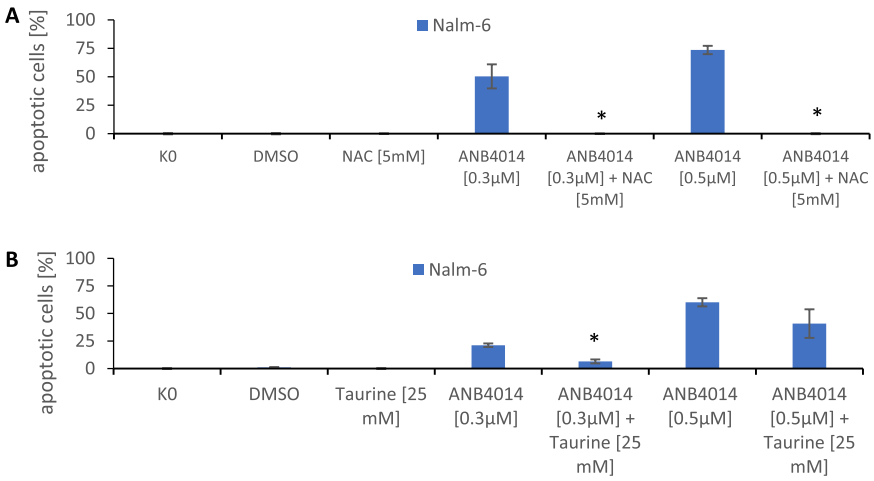

Fig. 6. Antioxidants reduce the apoptotic effect of ANB4014. A: N-Acetylcysteine (NAC) completely abolishes the apoptotic effect of ANB4014 on Nalm-6. Apoptosis was determined by modified cell cycle analysis after 72 h of incubation. n = 3 ± SD. **B:** Taurine partially abolishes the apoptotic effect of ANB4014 on Nalm-6. Apoptosis was determined by modified cell cycle analysis after 72 h of incubation. n = 3 ± SD. (* < 0.05 vs correspond concentration without antioxidant, two-tailed t-test).

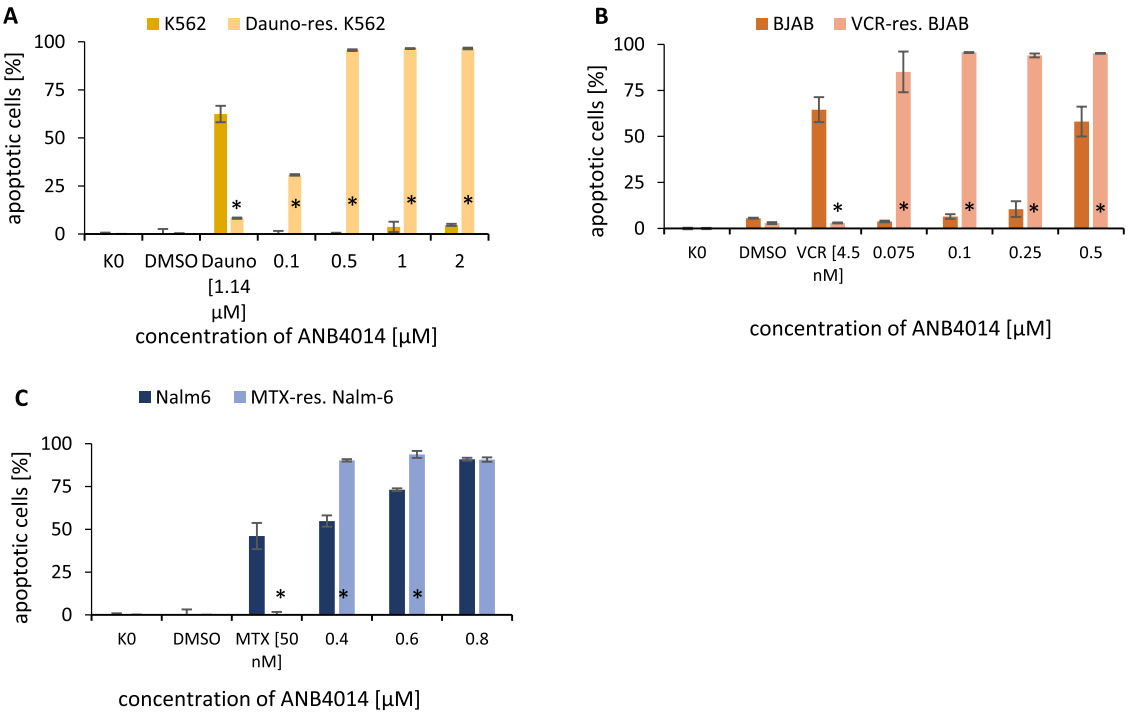

Fig. 7. Effect increase of ANB4014 on cytostatic-resistant cells. Apoptosis was determined by modified cell cycle analysis after 72 h of incubation. The resistant cell lines show a clear sensitization to the gold complex. n = 3 ± SD. (*: p < 0.05 vs. analogous concentration on baseline cell line, two-tailed t-test). **A**: ANB4014 on K562 and Dauno-res. K562: While the starting cells K562 are almost resistant to ANB4014 up to a concentration of 2 μM the Dauno-res. K562 already show high apoptotic levels at lower concentrations. **B**: ANB4014 on BJAB and VCR-res. BJAB. ANB4014 reaches high apoptotic levels already at low concentrations, whereas it has hardly any effect on the initial cells. **C**: ANB4014 on Nalm-6 and MTX-res. Nalm-6. The MTX-res. cells are more sensitive to ANB4014 than Nalm-6.

comparison of ANB4014 on the initial cell line and the resistant cell line, a correlation of mechanism of action and mechanism of resistance can be drawn. DNA fragmentation was examined for ANB4014 on K562 (chronic myeloid leukemia in blast crisis) and Dauno-res. K562, for which we found a down-regulation of the BH3-only protein harakiri [36], on BJAB and VCR-res. BJAB cells for which we found upregulation of the anti-apoptotic Bcl-2 and on Nalm-6 and MTX-res. Nalm-6, for which we found overexpression of the anti-apoptotic Mcl-1 as well as p53 underexpression. We observed not only a resistance overcoming but also a clear sensitization to the gold complex ANB4014 in all of these resistant cell lines: At concentrations where on the wild type cells no or less apoptosis is observed, in the resistant cells almost all cells are already apoptotic. While ANB4014 hardly induces apoptosis on K562 up to a concentration of 2 μM, it has an effect on the resistant cell line Dauno-res. K562 to a high degree. Even at a lower concentration of 0.5 μM, almost all cells in the resistant cells are apoptotic (see Fig. 7, A). Dauno-res. K562 are also resistant to anthracyclines and vinca alkaloids. In Western blot studies, we could confirm an upregulation of the BH3-only protein harakiri (HRK) after 24 h of incubation of ANB4014 on Nalm-6 (see Fig. 8). BH3-only proteins belong to the Bcl-2 family and depending on the BH3-only protein, they activate apoptosis by either inhibiting anti-apoptotic members or activating pro-apoptotic members of the Bcl-2 family [37,38]. On the cell line MTX-res. Nalm-6, ANB4014 is also more effective than on the wild-type cells. At a concentration of 0.4 μM, an apoptosis of 55.11 ± 6.10 % was observed on the wild-type cells, and an apoptosis of 90.26 ± 1.06 % on the MTX-res. cells (see Fig. 7, C). Also on the VCR-res. BJAB cells that show Bcl-2 upregulation, the AC_{50} is lower than on BJAB: below 0.075 μM. At 0.1 μM, hardly any

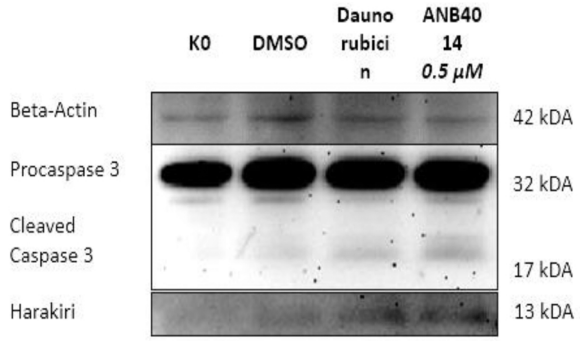

Fig. 8. Up-regulation of Harakiri and cleaved Caspase 3. Shown is the Western blot after 24 h of incubation of ANB4014 in Nalm-6.

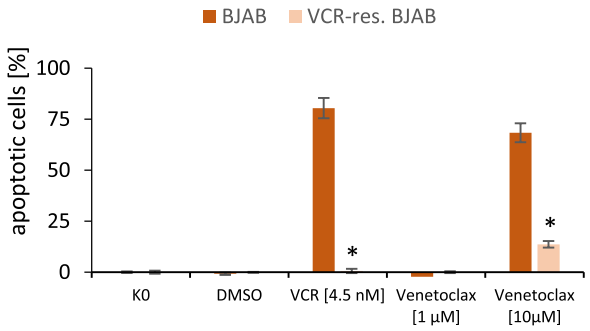

Fig. 9. Venetoclax is less effective on VCR-res. BJAB than on BJAB wild-type cells. Apoptosis was determined by modified cell cycle analysis after 72 h of incubation. n = 3 ± SD. (*: $p < 0.05$ vs. analogous concentration on baseline cell line, two-tailed t-test).

apoptosis takes place in the wild-type cells, whereas in the resistant cells almost all cells are apoptotic (BJAB 6.51 ± 1,24 % apoptosis, VCR-res. BJAB 95.54 ± 0,23 % apoptosis) (see Fig. 7, B). VCR-res. BJAB show co-resistance to vinca alkaloids. Since Bcl-2 overexpression is a frequently observed resistance mechanism [13,39] and ANB4014 has been shown to increase resistance in VCR-res. BJAB so clearly, we were interested in comparison with the BH3 mimetic venetoclax, which selectively binds Bcl-2 [37]. In tumor cells characterized by over-expression of anti-apoptotic proteins like Bcl-2, intrinsic apoptosis can thus be directly activated by targeted therapy, since the actual apoptosis mechanism is usually intact [13,40]. Venetoclax is approved for the treatment of chronic lymphocytic leukemia and acute myeloid leukemia and is also being investigated in clinical trials for non-Hodgkin lymphoma [37,41]. On lymphoma cell cultures with high Bcl-2 expression it acts at low nanomolar levels [41]. We compared venetoclax on BJAB and VCR-res. BJAB. Interestingly, not only is the effect of venetoclax on the VCR-resistant BJAB lower than on the wild-type BJAB cells, but the VCR-resistant BJAB cells are also resistant to venetoclax despite Bcl-2 upregulation (see Fig. 9). Thus, we were interested in whether venetoclax, through Bcl-2 binding, could re-sensitize VCR-res. BJAB to vincristine. The VCR-res. BJAB cells are resistant to vincristine up to a concentration of 4.5 nM. We tested the synergistic effect of vincristine (4.5 nM) and venetoclax (1 µM respectively 10 µM) on VCR-res. BJAB cells. While the substances alone on the VCR-res. BJAB hardly induce apoptosis, the combination of the two compounds shows synergistic effects. The apoptosis rate is comparable to the levels induced by vincristine or venetoclax in the BJAB cell line (see Fig. 10).

3.9. ANB4014 activates caspase 3

Downstream of the intrinsic as well as extrinsic pathway, effector caspases are activated. Caspase 3 is one of these, which ultimately leads to proteolytic cleavage of the cell [7]. After 24 h of incubation, an activation of caspase 3 in the form of a proteolytic cleavage into the active form by ANB4014 can already be observed in the Western blot (see Fig. 8). A Doxo-res. BJAB cell line we generated is characterized by a caspase-3 down-regulation. We examined ANB4014 on this cell line to investigate a caspase 3 dependency and found that Doxo-res. BJAB are almost completely resistant to ANB4014 at a concentration of 0.5 µM (58.05 ± 8.1 % apoptosis in BJAB vs. 6.18 ± 1.07 % apoptosis in

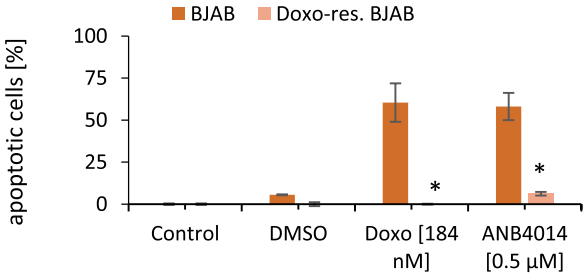

Fig. 11. ANB4014 is Caspase 3 dependent. Shown is the apoptotic effect of ANB4014 on the wild-type cells BJAB and the corresponding Doxo-res. BJAB which are characterized by a Caspase 3 downregulation. Doxorubicin induces little or no apoptosis on the corresponding resistant cell line. Apoptosis was determined by modified cell cycle analysis after 72 h of incubation. n = 3 ± SD. (*: $p < 0.05$ vs. analogous concentration on baseline cell line, two-tailed t-test).

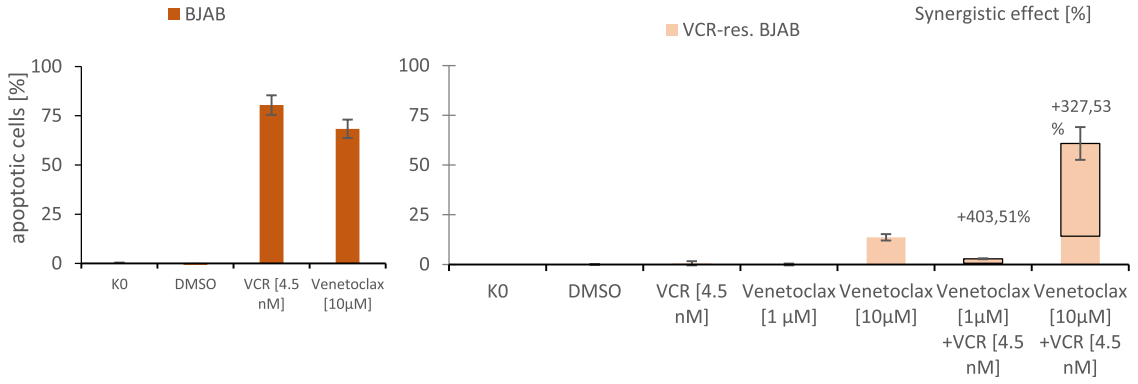

Fig. 10. Re-sensitization of VCR-res. BJAB for vincristine by BH3 mimetic venetoclax. The left graph shows the effect of VCR and venetoclax on BJAB. The right graph shows the respective effect of VCR and venetoclax on VCR-res. BJAB alone and in combination with each other. When the substances are combined, a bipartite graph is shown. The lower part corresponds to the additive effect, the upper circled part shows the synergistic effect. While the substances alone on the VCR-res. BJAB hardly induce apoptosis, the combination of the two compounds shows synergistic effects (right). The apoptosis rate is comparable to the levels induced by vincristine or venetoclax in the BJAB cell line (left). Apoptosis was determined by modified cell cycle analysis after 72 h of incubation. n = 3 ± SD.

Table 3
Over- or underexpression of apoptosis-associated genes by ANB4014 after 14 h incubation on Nalm-6 analyzed by RT-qPCR. Fold regulation compared to control.

	Fold regulation
Overexpression of pro-apoptotic Genes	
BCL2L11 (BIM)	+ 4.2
Caspase 7	+ 7.8
GADD45A	+ 25.8
Underexpression of anti-apoptotic Genes	
Bcl-2	-4.7

Doxo-res. BJAB, see Fig. 11).

3.10. ANB4014 leads to over- and underexpression of pro- and anti-apoptotic genes

Furthermore, we examined apoptosis-related genes for over- or under expression induced by ANB4014 in an RT-qPCR. We used the cell death pathway finder array from Qiagen (Hilden, Germany). ANB4014 was incubated at a concentration of 0.8 μM on Nalm-6 for 14 h. The analysis revealed a large number of genes that were over- or underexpressed compared to the control. Table 3 lists some selected genes showing an overexpression of pro-apoptotic and an underexpression of anti-apoptotic genes.

3.11. ANB4014 overcomes multiple cytostatic resistances in vitro

Cytostatic resistance in tumor cells is a frequently observed complication and often limits the success of therapy [42]. In our laboratory, we induced resistance to common chemotherapeutic agents in different cell lines, which are thus acquired. All resistances are characterized by further co-resistances to various cytostatic drugs. We investigated ANB4014 for its ability to overcome these resistances. The gold compound was incubated for 72 h on the initial cell lines and the resistant cell lines and apoptosis were evaluated by PI staining and flow cytometry. For some resistant cell lines, we know their resistance mechanisms, or partial mechanisms of resistance, and for some, the discovery is still pending. Resistance and resistance overcoming allow further conclusions to be drawn about the mechanisms of action of the gold complexes. We determined resistance for a concentration at which at least the apoptotic effect of the parent compound (VCR, Dauno, MTX and so on) could be observed on the wild-type cells or at least one AC_{50}. ANB4014 overcomes a range of cytostatic drug resistance. For an overview, see Supplement 6 of the Supporting information.

3.12. ANB4014 is not a substrate of P-gp

A VCR-res. Nalm-6 as well as a Dauno-res. Nalm-6 are characterized by upregulation of the multidrug transporter P-glycoprotein (P-gp). P-gp is a multidrug efflux pump that is upregulated in many tumor cells and through which the tumor cell can actively efflux a variety of substrates, especially hydrophobic, amphipathic natural drugs. These include anthracyclines (doxorubicin, daunorubicin, epirubicin), vinca alkaloids (vincristine, vinblastine), epipodophyllotoxins (etoposides, teniposides), paclitaxel and colchicine [39,43]. This is consistent with our observations regarding the co-resistance of VCR-res. and Dauno-res. Nalm-6 to other established cytostatic drugs [44]. ANB4014 shows similar effects on both cell lines mentioned above and thus complete resistance overcoming (see Fig. 12 A + B).

4. Discussion

We demonstrated that the gold compounds are cytostatic and cytotoxic on leukemia and lymphoma cells in the nanomolar concentration range, and they have promising potential as anticancer agents.

We found that complexes induce apoptosis in tumor cells but not in healthy leukocytes and that the intrinsic apoptosis pathway plays a crucial role. Via JC-1 staining and cytochrome c and Smac release, we detected a concentration-dependent breakdown of the mitochondrial transmembrane potential and leakage of pro-apoptotic proteins from the mitochondrion. This is in agreement with the observations of other work on gold(I) complexes [45–47]. The major regulators of the intrinsic apoptosis pathway are the proteins of the Bcl-2 family [48]. These are divided into pro- and anti-apoptotic members. The anti-apoptotic ones include Bcl-2, Mcl-1 or Bcl-xL. They prevent oligomerization of the pro-apoptotic proteins Bax and Bak, which leads to permeabilization of the mitochondrial membrane and activates the further signaling pathway [37]. Other important players are the BH3-only proteins, which can activate apoptosis by binding anti-apoptotic proteins or by directly activating pro-apoptotic proteins [5,13,37]. In Western blot, we detected upregulation of the BH3-only protein HRK, and in PCR, we found overexpression of the BH3-only protein BIM and downregulation of Bcl-2. HRK acts as a sensitizer protein by blocking Bcl-2 or Bcl-xL and thus activating apoptosis indirectly [49]. BIM, on the other hand, inhibits all anti-apoptotic Bcl-2 proteins equally and binds Bax and Bak directly as activator proteins [35]. The resistance overcoming on cells MTX-res. Nalm-6 (Mcl-1 overexpression, p53 underexpression), VCR-res. BJAB (Bcl-2 upregulation) and Dauno-res. K562 (HRK downregulation) with clear sensitization to ANB4014 highlight the consideration that the intrinsic apoptosis pathway via members of the Bcl-2 family is relevant for action. The three cell series are characterized by

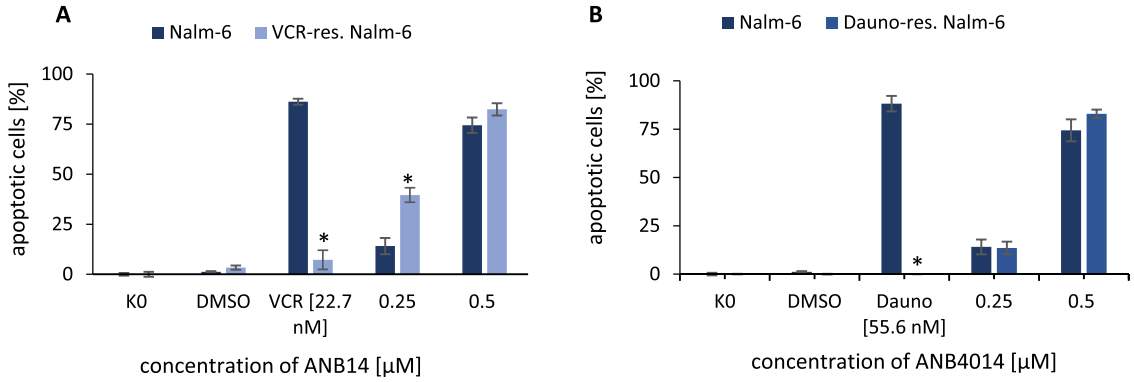

Fig. 12. Resistance overcoming by ANB4014 on cytostatic-resistant leukemia cells in vitro characterized by upregulation of the multidrug transporter P-glycoprotein (p-gp). Shown is the apoptotic effect of ANB4014 on the wild-type cells and the corresponding cytostatic-resistant cells. The parent cytostatic drug induces little or no apoptosis on the corresponding resistant cell line. Apoptosis was determined by modified cell cycle analysis after 72 h of incubation. n = 3 ± SD. (*: $p < 0.05$ vs. analogous concentration on baseline cell line, two-tailed t-test). A: ANB4014 overcomes vincristine-induced resistance. B: ANB4014 overcomes daunorubicin-induced resistance.

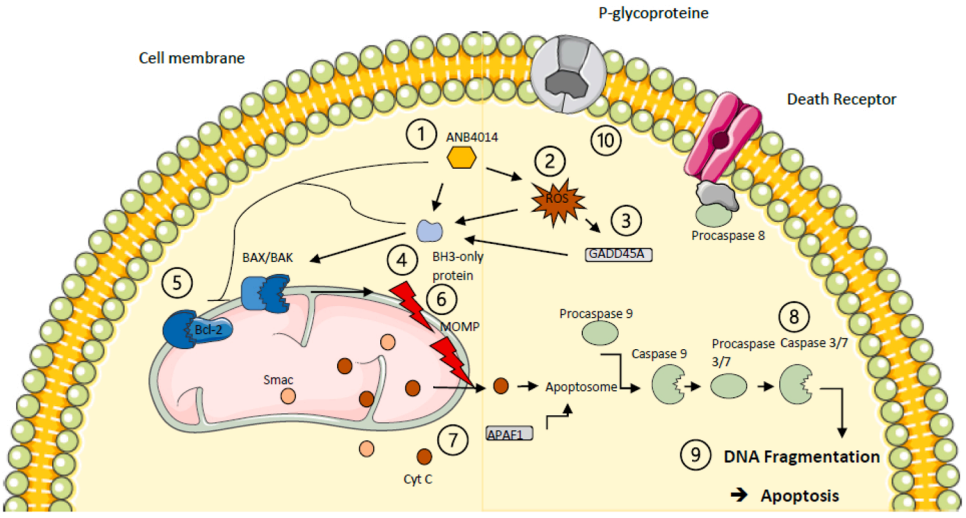

Fig. 13. The potential mechanism of action of the compound ANB4014. The figure reflects the hypothetical apoptosis induction that can be derived from the experiments studied here. The numbers draw the connections to the experiments. **1)** The Structural formulas can be found in Scheme 1. **2)** ANB4014 leads to ROS production. This is indirectly demonstrated by the antioxidant experiment in Fig. 6. **3)** The protein GADD45A is formed by ROS, which in turn leads to apoptosis via BIM, for example. Overexpression of GADD45A by ANB4014 was detected via PCR (Table 3). **4)** ANB4014 leads to activation of BH3-only proteins directly or via ROS. Evidenced by the upregulation of harakiri (HRK) in Western blot (Fig. 8), overexpression of BIM in PCR (Table 3). In addition, ANB4014 shows a significant increase in effect on Dauno-res. K562, which are characterized by under-expression of HRK (Fig. 7). **5)** Directly or via BH3-only proteins, anti-apoptotic proteins of the Bcl-2 family are inhibited and pro-apoptotic proteins such as Bax/Bak are activated. Evidence of Bcl-2 underexpression in PCR (Table 3), ANB4014 also shows a significant gain of effect on the Bcl-2 overexpressed VCR-res. BJAB as well as the Mcl-1 overexpressed MTX-res. Nalm-6 (Fig. 7). **6)** This leads to the breakdown of mitochondrial transmembrane potential (MOMP), detected by JC-1 staining (Fig. 4). **7)** Smac and cytochrome c (Cyt c) leakage occurs, detected by its release as Western blot (Fig. 5). The apoptosome is formed and **8)** the caspase cascade is activated. This was shown for caspase 3 by Western blot and for caspase 7 by PCR (Fig. 8, Table 3). In addition, Fig. 11 shows a caspase 3 dependency. **9)** The effector caspases eventually lead to proteolytic cleavage of DNA and thus inevitably to apoptosis. Detected by Annexin V/PI double staining and by modified cell cycle arrest Table 2, Supplement 5. **10)** ANB4014 is not a substrate of P-glycoprotein. Detected on the P-glycoprotein-overexpressing Dauno- and VCR-res. Nalm-6 (Fig. 12). Image created in part using Servier Medical Art provided by Servier and licensed under a Creative Commons Attribution 3.0 unported license (http://smart.servier.com, accessed 28 February 2023).

acquired resistance. A synopsis of the results from the mechanism analyses and the resistance overcomes show that the gold complexes shift the balance of the Bcl-2 proteins towards a predominance of the pro-apoptotic members and, via this mechanism, appear to be significantly more effective on the aforementioned resistant cell lines. These resistant cells thus seem to be dependent on their resistance mechanism. If the gold complexes disrupt this mechanism, the cell's survival strategies seem to be undermined and collapse. In this regard, the mitochondrial apoptosis pathway is a promising way to directly activate apoptosis in tumor cells by targeted therapy [30]. Certo et al. introduced the term "primed to death" in their work, describing a state in which the tumor cell is constantly primed with activator BH3-only proteins and thus depends on anti-apoptotic proteins of the Bcl-2 family to survive. BH3 mimetics but also common cytostatics leading to the induction of BH3-only sensitizer proteins can collapse this fragile state by releasing the activator BH3-only proteins from the anti-apoptotic Bcl-2 proteins and activating Bax and/or Bak [50]. Therefore, we compared the effect of the BH-3 mimetic venetoclax on BJAB and the VCR-res. BJAB. So far, we have been able to detect for the VCR-res. BJAB only demonstrated Bcl-2 upregulation. From the literature, BJAB is characterized by a low Bcl-2 concentration and an effect by venetoclax is only observed in micromolar ranges [41]. This is consistent with our results. The VCR-res. BJAB, however, were resistant to venetoclax. But interestingly, vincristine and venetoclax together show a synergistic effect on the VCR-res. BJAB. This could argue for a re-sensitization of the VCR-res. BJAB to vincristine by venetoclax, as venetoclax blocks upregulated Bcl-2. This suggests that overexpression of Bcl-2 in VCR-res. BJAB is not solely responsible as a resistance mechanism, but should be assumed to be a partial mechanism. It has already been shown that Bcl-2 overexpression alone does not sensitize to venetoclax. If, for example, Mcl-1-or Bcl-xL are upregulated at the same time, cells show resistance to venetoclax [48,51]. This underscores the findings that the gold complexes act through different players in the Bcl-2 family. Whether the gold complexes act directly here or upstream remains open. A large body of work reports that gold complexes inhibit thioredoxin reductase and lead to ROS. Intervening here represents a possibility for tumor control [29,30,45,47]. Thioredoxin reductase (TrxR) is a selenocysteine-containing flavoprotein that reduces Trx and other endogenous and exogenous substrates in an NADPH-dependent manner [52]. Trx functions in many signaling pathways in the cell: Not only does it act as a stabilizer of redox status as a ROS scavenger and by reducing other enzymes, Trx also serves as a growth factor or regulates DNA binding of various transcription factors [53]. Inhibition of TrxR can lead to an imbalance of the redox status with increased ROS levels, which in turn can lead to apoptosis [52,53]. We were able to detect ROS indirectly by incubating the gold compounds in combination with NAC and taurine, which completely and partially abrogated apoptosis. Oxidative stress, for example, may lead to activation of BIM and inhibition of Bcl-2 via the c-Jun N-terminal kinase (JNK) and the p38 MAPK pathways, and inhibition of thioredoxin reductase may lead to inhibition of the transcription factor NF-κB which also regulates transcription of Bcl-2 family proteins, including Bcl-2 itself [53]. The significant overexpression of GADD45a in RT qPCR (+ 25.8 fold regulation) after incubation with ANB4014 supports these previous findings. GADD45a is a rapidly regulated protein in response to cellular stress and is involved in many signaling pathways such as apoptosis, cell cycle arrest or DNA repair. GADD45a leads to apoptosis via ERK, JNK or p38 signaling pathways [54]. Direct detection of ROS and presumed inhibition of thioredoxin reductase by the gold complexes must follow. Furthermore, using different methods, we were able to show the involvement of caspase 3 and 7, both of which are activated downstream of the intrinsic and extrinsic pathways [7].

In addition to the mechanism of action analysis, a key aspect of our work was resistance overcoming analysis, which of course in turn allowed us to draw conclusions about the mechanism of action of ANB4014. Cytostatic resistance plays an important role in clinical practice and often limits the therapeutic options available [6]. The gold complexes overcame most of the resistances we investigated. The overcoming of VCR-res. and Dauno-res. Nalm-6, which are characterized by upregulation of the multidrug efflux pump P-glycoprotein (p-gp), suggests that the gold complex is not a substrate of p-gp. P-gp plays a major role in multi-drug resistance [42]. This finding is consistent with

our previous work about gold complexes [30,36]. In one such work we could also demonstrate that the gold(I) complexes investigated at that time were able to overcome the resistances in VCR-res. and Dauno-res. Nalm-6. In an experiment on cellular gold uptake, it was shown that the gold levels in VCR-res. Nalm-6 and Dauno-res. did not differ from those in Nalm-6 [30].

5. Conclusion

In a nutshell, we present the following mechanism of action for ANB4014 for discussion. Presumably, the gold substance generates ROS and thus or directly pro-apoptotic proteins of the Bcl-2 family are activated and anti-apoptotic proteins are inhibited. This eventually leads to the depletion of the mitochondrial transmembrane potential via oligomerization of Bax/Bak, resulting in the efflux of Smac and cytochrome c. This leads to the formation of the apoptosome, the caspase cascade is activated, which finally triggers DNA fragmentation. In Fig. 13 we have sketched this mechanism and linked it by numbering to the corresponding experiments in the paper.

In summary, the gold compounds presented here show promising results and potential as antitumor agents in initial preclinical studies. The complexes appear to be particularly promising in resistant cells when the resistance mechanism can be subverted. It is of interest to investigate this mechanism of action in further studies. In addition, further studies with more derivatives are needed to better understand and optimize the structure-activity relationships and possibly test them in mouse models in a next step.

CRediT authorship contribution statement

Conceptualization Aram Prokop, Albrecht Berkessel; Data curation Marie-C. Ahrweiler-Sawaryn, Corazon Frias, Aram Prokop; Formal analysis Marie-C. Ahrweiler-Sawaryn, Corazon Frias, Nicola L. Wilke, Aram Prokop; Funding acquisition Aram Prokop; Investigation Marie-C. Ahrweiler-Sawaryn, Animesh Biswas, Corazon Frias, Jerico Frias, Nicola L. Wilke, Nathalie Wilke; Methodology Aram Prokop, Marie-C. Ahrweiler-Sawaryn, Corazon Frias, Nicola L. Wilke; Project administration Aram Prokop, Albrecht Berkessel; Resources Aram Prokop, Albrecht Berkessel; Software Aram Prokop, Nicola Wilke; Supervision Aram Prokop; Validation Marie-C. Ahrweiler-Sawaryn, Corazon Frias, Aram Prokop; Visualization Marie-C. Ahrweiler-Sawaryn, Animesh Biswas, Corazon Frias, Jerico Frias; Writing – original draft Marie-C. Ahrweiler-Sawaryn, Animesh Biswas, Albrecht Berkessel; Writing – review & editing Marie-C. Ahrweiler-Sawaryn, Albrecht Berkessel, Aram Prokop.

Declaration of Competing Interest

The authors declare that they have no known competing financial interests or personal relationships that could have appeared to influence the work reported in this paper.

Data Availability

Data will be made available on request.

Acknowledgement

We gratefully thank the Foundation Blankenheimer Dorf e.v., Blankenheim, Germany, the Foundation David (Cologne), Germany the Dr. Kleist Foundation (Berlin), Germany and the Koch-Foundation (Berlin), Germany.

Appendix A. Supporting information

Supplementary data associated with this article can be found in the online version at doi:10.1016/j.biopha.2023.114507.

References

[1] B. Rosenberg, L. Vancamp, T. Krigas, Inhibition of cell division in Escherichia coli by electrolysis products from a platinum electrode, Nature 205 (1965) 698–699, https://doi.org/10.1038/205698a0.
[2] S. Dasari, P.B. Tchounwou, Cisplatin in cancer therapy: molecular mechanisms of action, Eur. J. Pharm. 740 (2014) 364–378, https://doi.org/10.1016/j.ejphar.2014.07.025.
[3] L. Galluzzi, L. Senovilla, I. Vitale, J. Michels, I. Martins, O. Kepp, et al., Molecular mechanisms of cisplatin resistance, Oncogene 31 (2012) 1869–1883, https://doi.org/10.1038/onc.2011.384.
[4] Eve Wiltshaw, Cisplatin in the treatment of cancer, Platin. Met. Rev. (1979) 90–98.
[5] S. Fulda, Targeting apoptosis signaling pathways for anticancer therapy, Front. Oncol. 1 (2011) 23, https://doi.org/10.3389/fonc.2011.00023.
[6] S.W. Lowe, E. Cepero, G. Evan, Intrinsic tumour suppression, Nature 432 (2004) 307–315, https://doi.org/10.1038/nature03098.
[7] R.C. Taylor, S.P. Cullen, S.J. Martin, Apoptosis: controlled demolition at the cellular level, Nat. Rev. Mol. Cell Biol. 9 (2008) 231–241, https://doi.org/10.1038/nrm2312.
[8] M. Redza-Dutordoir, D.A. Averill-Bates, Activation of apoptosis signalling pathways by reactive oxygen species, Biochim. Biophys. Acta 1863 (2016) 2977–2992, https://doi.org/10.1016/j.bbamcr.2016.09.012.
[9] S. van Cruchten, W. van den Broeck, Morphological and biochemical aspects of apoptosis, oncosis and necrosis, Anat. Histol. Embryol. 31 (2002) 214–223, https://doi.org/10.1046/j.1439-0264.2002.00398.x.
[10] M.O. Hengartner, The biochemistry of apoptosis, Nature 407 (2000) 770–776, https://doi.org/10.1038/35037710.
[11] G. Kroemer, L. Galluzzi, C. Brenner, Mitochondrial membrane permeabilization in cell death, Physiol. Rev. 87 (2007) 99–163, https://doi.org/10.1152/physrev.00013.2006.
[12] D. Hanahan, R.A. Weinberg, The hallmarks of cancer, Cell 100 (2000) 57–70, https://doi.org/10.1016/S0092-8674(00)81683-9.
[13] J.M. Adams, S. Cory, The Bcl-2 apoptotic switch in cancer development and therapy, Oncogene 26 (2007) 1324–1337, https://doi.org/10.1038/sj.onc.1210220.
[14] D. Hanahan, R.A. Weinberg, Hallmarks of cancer: the next generation, Cell 144 (2011) 646–674, https://doi.org/10.1016/j.cell.2011.02.013.
[15] S. Fulda, L. Galluzzi, G. Kroemer, Targeting mitochondria for cancer therapy, Nat. Rev. Drug Discov. 9 (2010) 447–464, https://doi.org/10.1038/nrd3137.
[16] A. Biswas, Universität zu Köln. Key intermediates in NHC-catalyzed reactions of activated esters and novel NHC ligands for gold catalysis, Univ. zu Köln (2020).
[17] G. Scherowsky, Die synthese von 2.4-diaryl-1.3.4-thiadiazoliumsalzen, Tetrahedron Lett. 12 (1971) 4985–4988, https://doi.org/10.1016/S0040-4039(01)97606-3.
[18] V.R. Yatham, W. Harnying, D. Kootz, J.-M. Neudörfl, N.E. Schlörer, A. Berkessel, 1,4-bis-dipp/mes-1,2,4-triazolylidenes: carbene catalysts that efficiently overcome steric hindrance in the redox esterification of α- and β-substituted α,β-enals, J. Am. Chem. Soc. 138 (2016) 2670–2677, https://doi.org/10.1021/jacs.5b11796.
[19] F.K.-M. Chan, K. Moriwaki, M.J. de. Rosa, Detection of necrosis by release of lactate dehydrogenase activity, Methods Mol. Biol. 979 (2013) 65–70, https://doi.org/10.1007/978-1-62703-290-2_7.
[20] C. Korzeniewski, D.M. Callewaert, An enzyme-release assay for natural cytotoxicity, J. Immunol. Methods 64 (1983) 313–320, https://doi.org/10.1016/0022-1759(83)90438-6.
[21] A. Prokop, W. Wrasidlo, H. Lode, R. Herold, F. Lang, G. Henze, et al., Induction of apoptosis by enediyne antibiotic calicheamicin thetaII proceeds through a caspase-mediated mitochondrial amplification loop in an entirely Bax-dependent manner, Oncogene 22 (2003) 9107–9120, https://doi.org/10.1038/sj.onc.1207196.
[22] "Quest Graph™ IC50 Calculator (v.1)." AAT Bioquest, Inc, 2021. ⟨https://www.aatbio.com/tools/ic50-calculator-v1⟩.
[23] C. Riccardi, I. Nicoletti, Analysis of apoptosis by propidium iodide staining and flow cytometry, Nat. Protoc. 1 (2006) 1458–1461, https://doi.org/10.1038/nprot.2006.238.
[24] F. Essmann, T. Wieder, A. Otto, E.C. Müller, B. Dörken, P.T. Daniel, GDP dissociation inhibitor D4-GDI (Rho-GDI 2), but not the homologous rho-GDI 1, is cleaved by caspase-3 during drug-induced apoptosis, Biochem. J. 346 (Pt 3) (2000) 777–783.
[25] Z. Darzynkiewicz, G. Juan, X. Li, W. Gorczyca, T. Murakami, F. Traganos, Cytometry in cell necrobiology: analysis of apoptosis and accidental cell death (necrosis), Cytometry 27 (1997) 1–20.
[26] I. Vermes, C. Haanen, H. Steffens-Nakken, C. Reutellingsperger, A novel assay for apoptosis flow cytometric detection of phosphatidylserine expression on early apoptotic cells using fluorescein labelled Annexin V, J. Immunol. Methods 184 (1995) 39–51, https://doi.org/10.1016/0022-1759(95)00072-I.
[27] M. Reers, T.W. Smith, L.B. Chen, J-aggregate formation of a carbocyanine as a quantitative fluorescent indicator of membrane potential, Biochemistry 30 (1991) 4480–4486, https://doi.org/10.1021/bi00232a015.
[28] J. Zhang, X. Li, X. Han, R. Liu, J. Fang, Targeting the thioredoxin system for cancer therapy, Trends Pharm. Sci. 38 (2017) 794–808, https://doi.org/10.1016/j.tips.2017.06.001.
[29] R. Rubbiani, I. Kitanovic, H. Alborzinia, S. Can, A. Kitanovic, L.A. Onambele, et al., Benzimidazol-2-ylidene gold(I) complexes are thioredoxin reductase inhibitors with multiple antitumor properties, J. Med. Chem. 53 (2010) 8608–8618, https://doi.org/10.1021/jm100801e.
[30] C. Schmidt, B. Karge, R. Misgeld, A. Prokop, R. Franke, M. Brönstrup, I. Ott, Gold(I) NHC complexes: antiproliferative activity, cellular uptake, inhibition of

mammalian and bacterial thioredoxin reductases, and gram-positive directed antibacterial effects, Chemistry 23 (2017) 1869–1880, https://doi.org/10.1002/chem.201604512.
[31] I. Ott, On the medicinal chemistry of gold complexes as anticancer drugs, Coord. Chem. Rev. 253 (2009) 1670–1681, https://doi.org/10.1016/j.ccr.2009.02.019.
[32] D. Saggioro, M.P. Rigobello, L. Paloschi, A. Folda, S.A. Moggach, S. Parsons, et al., Gold(III)-dithiocarbamato complexes induce cancer cell death triggered by thioredoxin redox system inhibition and activation of ERK pathway, Chem. Biol. 14 (2007) 1128–1139, https://doi.org/10.1016/j.chembiol.2007.08.016.
[33] M. Zafarullah, W.Q. Li, J. Sylvester, M. Ahmad, Molecular mechanisms of N-acetylcysteine actions, Cell. Mol. Life Sci. 60 (2003) 6–20, https://doi.org/10.1007/s000180300001.
[34] C.J. Jong, J. Azuma, S. Schaffer, Mechanism underlying the antioxidant activity of taurine: prevention of mitochondrial oxidant production, Amino Acids 42 (2012) 2223–2232, https://doi.org/10.1007/s00726-011-0962-7.
[35] J. Kale, E.J. Osterlund, D.W. Andrews, BCL-2 family proteins: changing partners in the dance towards death, Cell Death Differ. 25 (2018) 65–80, https://doi.org/10.1038/cdd.2017.186.
[36] J.F. Schlagintweit, C.H.G. Jakob, N.L. Wilke, M. Ahrweiler, C. Frias, J. Frias, et al., Gold(I) bis(1,2,3-triazol-5-ylidene) complexes as promising selective anticancer compounds, J. Med. Chem. 64 (2021) 15747–15757, https://doi.org/10.1021/acs.jmedchem.1c01021.
[37] B.A. Carneiro, W.S. El-Deiry, Targeting apoptosis in cancer therapy, Nat. Rev. Clin. Oncol. 17 (2020) 395–417, https://doi.org/10.1038/s41571-020-0341-y.
[38] M. Giam, D.C.S. Huang, P. Bouillet, BH3-only proteins and their roles in programmed cell death, Oncogene 27 Suppl 1 (2008) S128–S136, https://doi.org/10.1038/onc.2009.50.
[39] C. Holohan, S. van Schaeybroeck, D.B. Longley, P.G. Johnston, Cancer drug resistance: an evolving paradigm, Nat. Rev. Cancer 13 (2013) 714–726, https://doi.org/10.1038/nrc3599.
[40] A.C. Faber, H. Ebi, C. Costa, J.A. Engelman, Apoptosis in targeted therapy responses: the role of BIM, Adv. Pharm. 65 (2012) 519–542, https://doi.org/10.1016/B978-0-12-397927-8.00016-6.
[41] L.V. Pham, S. Huang, H. Zhang, J. Zhang, T. Bell, S. Zhou, et al., Strategic therapeutic targeting to overcome venetoclax resistance in aggressive B-cell lymphomas, Clin. Cancer Res. 24 (2018) 3967–3980, https://doi.org/10.1158/1078-0432.CCR-17-3004.
[42] D.B. Longley, P.G. Johnston, Molecular mechanisms of drug resistance, J. Pathol. 205 (2005) 275–292, https://doi.org/10.1002/path.1706.
[43] S.V. Ambudkar, S. Dey, C.A. Hrycyna, M. Ramachandra, I. Pastan, M. M. Gottesman, Biochemical, cellular, and pharmacological aspects of the multidrug transporter, Annu. Rev. Pharm. Toxicol. 39 (1999) 361–398, https://doi.org/10.1146/annurev.pharmtox.39.1.361.
[44] S.M. Hopff, Q. Wang, C. Frias, M. Ahrweiler, N. Wilke, N. Wilke, et al., A metal-free salalen ligand with antitumor and synergistic activity in resistant leukemia and solid tumor cells via mitochondrial pathway, J. Cancer Res. Clin. Oncol. 147 (2021) 2591–2607, https://doi.org/10.1007/s00432-021-03679-3.
[45] F. Caruso, R. Villa, M. Rossi, C. Pettinari, F. Paduano, M. Pennati, et al., Mitochondria are primary targets in apoptosis induced by the mixed phosphine gold species chlorotriphenylphosphine-1,3-bis(diphenylphosphino)propanegold(I) in melanoma cell lines, Biochem. Pharm. 73 (2007) 773–781, https://doi.org/10.1016/j.bcp.2006.11.018.
[46] M.J. McKeage, Gold opens mitochondrial pathways to apoptosis, Br. J. Pharm. 136 (2002) 1081–1082, https://doi.org/10.1038/sj.bjp.0704822.
[47] M.P. Rigobello, G. Scutari, A. Folda, A. Bindoli, Mitochondrial thioredoxin reductase inhibition by gold(I) compounds and concurrent stimulation of permeability transition and release of cytochrome c, Biochem. Pharm. 67 (2004) 689–696, https://doi.org/10.1016/j.bcp.2003.09.038.
[48] G.S. Choudhary, S. Al-Harbi, S. Mazumder, B.T. Hill, M.R. Smith, J. Bodo, et al., MCL-1 and BCL-xL-dependent resistance to the BCL-2 inhibitor ABT-199 can be overcome by preventing PI3K/AKT/mTOR activation in lymphoid malignancies, Cell Death Dis. 6 (2015), e1593, https://doi.org/10.1038/cddis.2014.525.
[49] N. Inohara, L. Ding, S. Chen, G. Núñez, Harakiri, a novel regulator of cell death, encodes a protein that activates apoptosis and interacts selectively with survival-promoting proteins Bcl-2 and Bcl-X(L), EMBO J. 16 (1997) 1686–1694, https://doi.org/10.1093/emboj/16.7.1686.
[50] M. Certo, V. Del Gaizo Moore, M. Nishino, G. Wei, S. Korsmeyer, S.A. Armstrong, A. Letai, Mitochondria primed by death signals determine cellular addiction to antiapoptotic BCL-2 family members, Cancer Cell 9 (2006) 351–365, https://doi.org/10.1016/j.ccr.2006.03.027.
[51] M. Hormi, R. Birsen, M. Belhadj, T. Huynh, L. Cantero Aguilar, E. Grignano, et al., Pairing MCL-1 inhibition with venetoclax improves therapeutic efficiency of BH3-mimetics in AML, Eur. J. Haematol. 105 (2020) 588–596, https://doi.org/10.1111/ejh.13492.
[52] D. Mustacich, G. Powis, Thioredoxin reductase, Biochem. J. 346 (2000) 1–8.
[53] K.F. Tonissen, G. Di Trapani, Thioredoxin system inhibitors as mediators of apoptosis for cancer therapy, Mol. Nutr. Food Res. 53 (2009) 87–103, https://doi.org/10.1002/mnfr.200700492.
[54] J.M. Salvador, J.D. Brown-Clay, A.J. Fornace, Gadd45 in stress signaling, cell cycle control, and apoptosis, Adv. Exp. Med. Biol. 793 (2013) 1–19, https://doi.org/10.1007/978-1-4614-8289-5_1.

Supporting Information

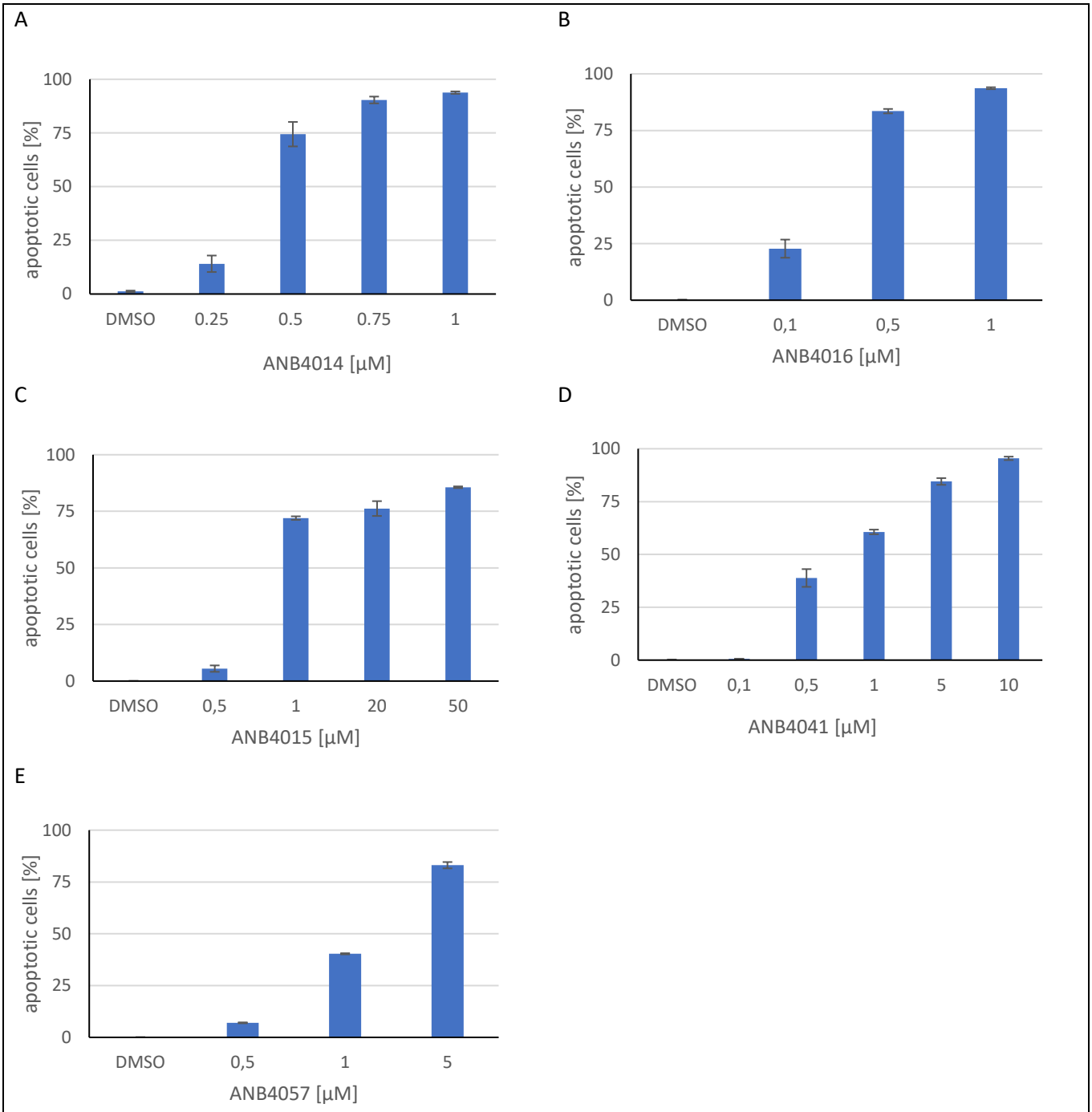

Supplement 1: **Apoptosis induction on Nalm-6 by different gold complexes.** Shown are graphs that served as the basis for calculating the AC_{50} (see **Fehler! Verweisquelle konnte nicht gefunden werden.**). The different gold complexes incubated for 72 hours on Nalm-6 cells. Apoptosis was determined by modified cell cycle analysis. For the calculation of AC_{50}, the values were normalized to DMSO. The DMSO control was equal to the highest DMSO concentration used, but never more than 0.5%. A: ANB4014 on Nalm-6. B: ANB4016 on Nalm-6. C: ANB4015 on Nalm-6. D: ANB4041 on Nalm-6. E: ANB4057 on Nalm-6. n=3 ± SD.

A

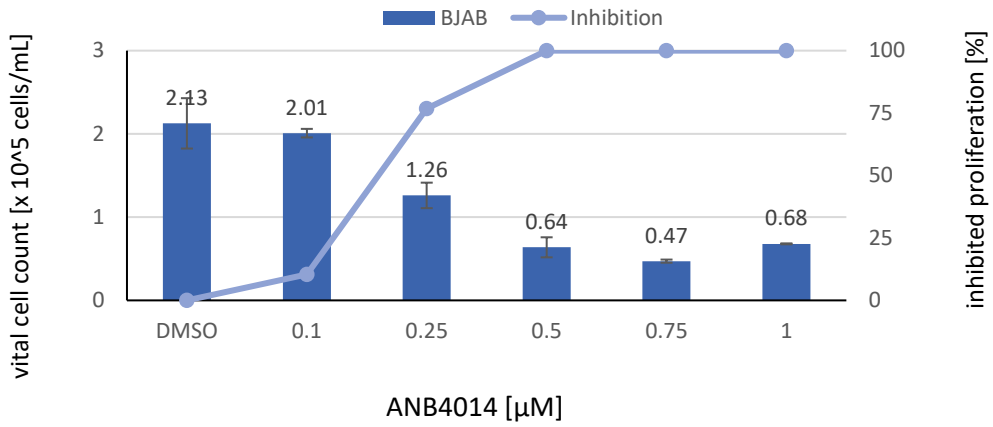

B

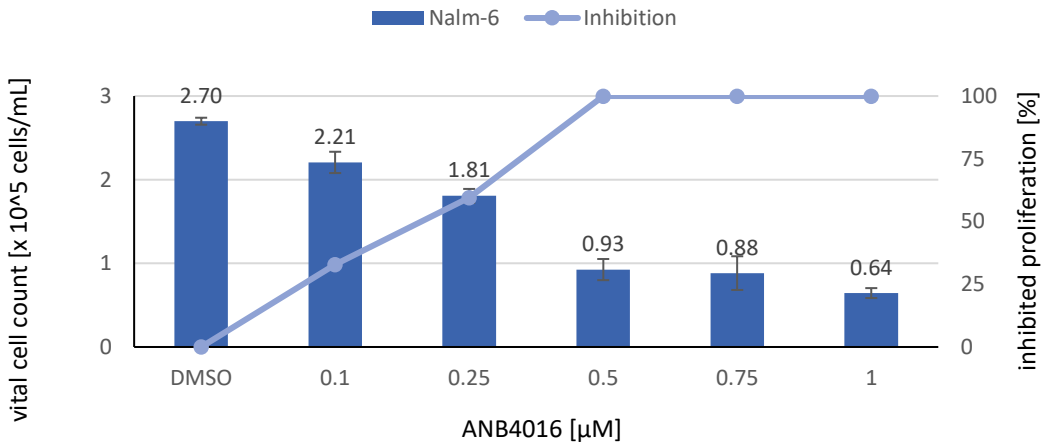

C

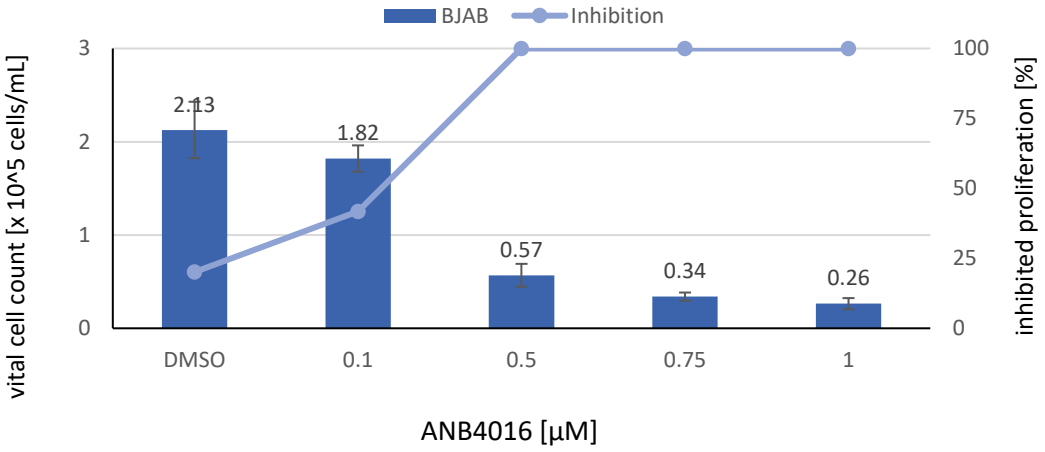

Supplement 2: **Antiproliferative effect of ANB4014 and ANB4016 on Nalm-6 and BJAB.** The graphs show the calculation basis for the IC_{50} values. Cells were plated out in $1x10^5$/ml. The substances incubated on the cells for 24 hours. Cell proliferation was determined by CASY®CellCounter and Analyzer System (OMNI Life Science, Bremen, Germany). The DMSO control was equal to the highest DMSO concentration used, but never more than 0.5%. The values were normalized to DMSO. n=3 ± SD. A: ANB4014 on BJAB. B: ANB4016 on Nalm-6. C: ANB4016 on BJAB.

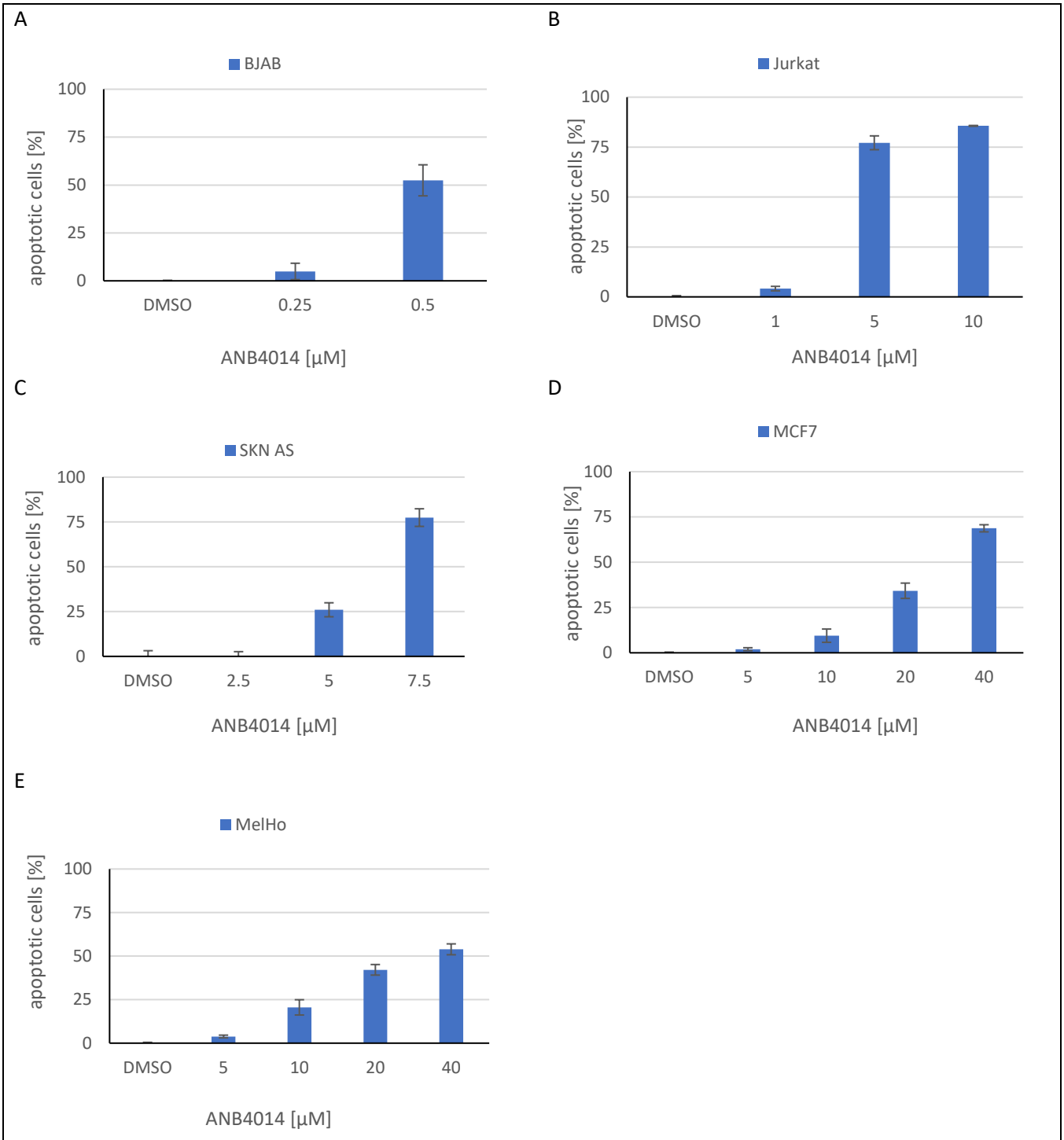

Supplement 3: **Apoptosis induction by ANB4014 on different tumor cell lines**. Shown are graphs that served as the basis for calculating the AC_{50} (see **Fehler! Verweisquelle konnte nicht gefunden werden.**). The different gold complexes incubated for 72 hours on Nalm-6 cells. Apoptosis was determined by modified cell cycle analysis. For the calculation of AC_{50}, the values were normalized to DMSO. The DMSO control was equal to the highest DMSO concentration used, but never more than 0.5%. n=3 ± SD. A: ANB4014 on BJAB. B: ANB4014 on Jurkat. C: ANB4014 on SKN AS. D: ANB4014 on MCF7. E: ANB4014 on MelHO.

Control

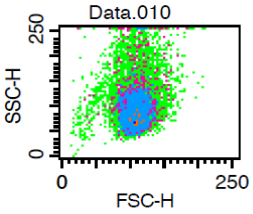

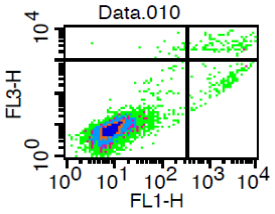

Quad	Events	% Gated
UL	25	0.25
UR	114	1.14
LL	9734	97.34
LR	127	1.27

ANB4014 [1µM]

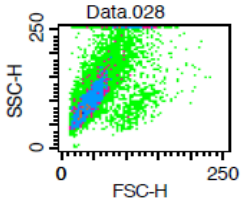

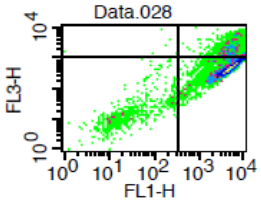

Quad	Events	% Gated
UL	6	0.06
UR	1552	15.52
LL	736	7.36
LR	7706	77.06

Supplement 4: Dot plot Annexin V/PI double staining of Control and ANB4014 [1µM] on Nalm-6 after 48 hours of incubation. UL= upper left (PI pos/Annexin V neg), UR = upper right (PI pos/ Annexin V neg.), LL= lower left (PI neg./Annexin V neg.), LR = lower right (PI neg./ Annexin).

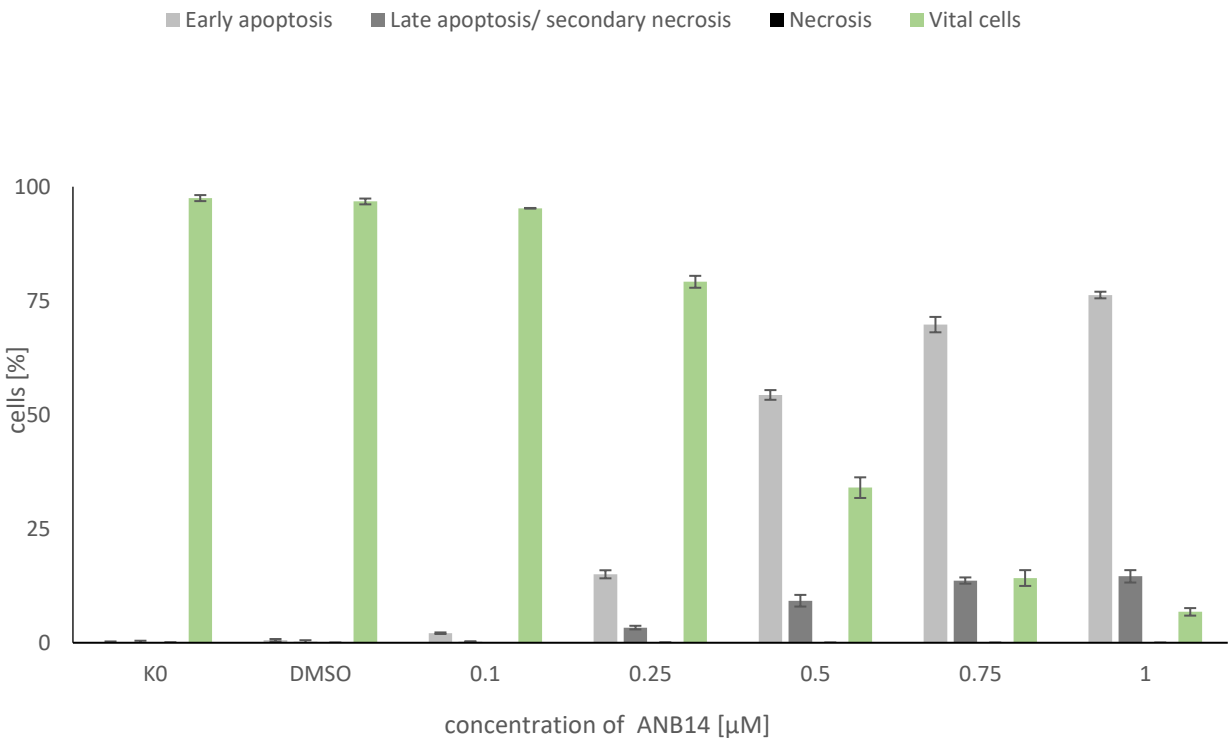

Supplement 5: Concentration-dependent decrease in vital cells and increase in lethal cells after 48 hours of incubation of ANB4014 on Nalm-6. The following stages can be detected by annexin V/PI- double staining: Vital cells (Annexin/PI neg/neg), early apoptosis (Annexin V/PI pos/neg), late apoptosis or necrosis (Annexin V/PI pos/pos; Annexin V/PI neg/pos). An increase in apoptotic stages can be seen, with a decrease in vital cells. n=3 ±SD.

Initial cell line	Resistant cell line	Resistance mechanism	Effect
Nalm-6	VCR-res. Nalm-6	P-gp overexpression	S
	Dauno-res. Nalm-6	P-gp overexpression	S
	MTX-res. Nalm-6	p53- underexpression, Mcl-1 overexpression	S
BJAB	VCR-res. BJAB	Bcl-2-overexpression	S
	Doxo-res. BJAB	Caspase 3 underexpression	R
K562	Dauno-res. K562	Harakiri underexpression	S

Supplement 6: Overview of resistance overcomes of ANB4014 to multi-cytostatic drug-resistant cell lines. We defined the terms resistant, sensitive, and intermediate as follows: Resistant (R)= In a concentration range where an AC_{50} or at least the apoptotic effect of the parent cytostatic is achieved on the wild-type cell line, the apoptotic effect of ANB4014 on the resistant cell line corresponds to at most half. Sensitive (S)= In a range where at least one AC_{50} or at least the effect of the parent cytostatic agent on the wild-type cell line is achieved on the wild-type cell line, the apoptotic effect of ANB4014 on the resistant cell line is at least equal to the apoptotic effect on the wild-type cell line. Intermediate (I) corresponds to the apoptotic effect between R and S.

Publikation 2

Die nachfolgende Publikation "Gold(I) Bis(1,2,3-Triazol-5-yliden) Complexes as Promising Selective Anticancer Compounds" wurde nachgedruckt mit Genehmigung von J. Med. Chem. 2021, 64, 21, 15747-15757. Datum der Veröffentlichung: 20. Oktober 2021, https://doi.org/10.1021/acs.jmedchem.1c01021, Article on request Link: https://pubs.acs.org/articlesonrequest/AOR-YHIJVRTKIYABCJ8C9TJ8.

Journal of Medicinal Chemistry

pubs.acs.org/jmc

Article

Gold(I) Bis(1,2,3-triazol-5-ylidene) Complexes as Promising Selective Anticancer Compounds

Jonas F. Schlagintweit, Christian H. G. Jakob, Nicola L. Wilke, Marie Ahrweiler, Corazon Frias, Jerico Frias, Marcel König, Eva-Maria H. J. Esslinger, Fernanda Marques, João F. Machado, Robert M. Reich, Tânia S. Morais, João D. G. Correia, Aram Prokop,* and Fritz E. Kühn*

Cite This: https://doi.org/10.1021/acs.jmedchem.1c01021

Read Online

ACCESS | Metrics & More | Article Recommendations | Supporting Information

ABSTRACT: The synthesis and antiproliferative activity of Mes- and iPr-substituted gold(I) bis(1,2,3-triazol-5-ylidene) complexes in various cancer cell lines are reported, showing nanomolar IC_{50} values of 50 nM (lymphoma cells) and 500 nM (leukemia cells), respectively (Mes < iPr). The compounds exclusively induce apoptosis (50 nM to 5 μM) instead of necrosis in common malignant blood cells (leukemia cells) and do not affect non-malignant leucocytes. Remarkably, the complexes not only overcome resistances against the well-established cytostatic etoposide, cytarabine, daunorubicin, and cisplatin but also promote a synergistic effect of up to 182% when used with daunorubicin. The present results demonstrate that gold(I) bis(1,2,3-triazol-5-ylidene) complexes are highly promising and easily modifiable anticancer metallodrugs.

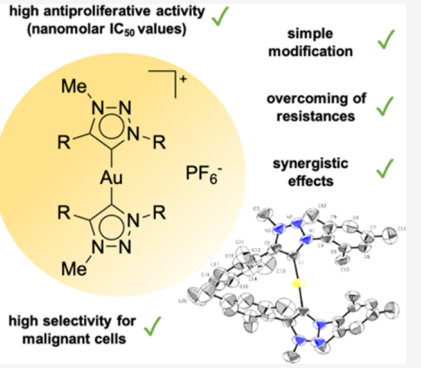

INTRODUCTION

Cancer is still a major global public health problem.[1] Its treatment often involves therapy with well-known cisplatin.[2−4] However, due to its mechanism of action and low selectivity for cancer cells, severe side-effects are associated with a cisplatin treatment leading to the demand for less harmful alternatives.[4] Organometallic gold compounds have been shown to be promising candidates.[5−7] In particular, *N*-heterocyclic carbene (NHC) complexes got into the focus of research due to their good anticancer activity, facile synthesis, and high stability.[5−8] Their steric and electronic properties as well as their lipophilicity are tunable *via* wingtip variation which has been proven to impact the cytotoxicity of the respective gold(I) complexes.[5,7−9] For instance, Berners-Price et al. reported a correlation between the anticancer activity and the ability of Au(I) imidazol-2-ylidene (NHC_{im}) complexes to inhibit thioredoxin reductase (TrxR).[5,8−10]

Recently, Au(I) complexes bearing a newer NHC ligand class of 1,2,3-triazol-5-ylidenes (NHC_{trz}) have been shown to be moderately active against bacteria.[11] Despite this first biological application and although various studies have been conducted using NHC_{im} ligands, surprisingly little is known about the antiproliferative effects of gold(I) complexes with NHC_{trz} ligands against cancer cells.[12−17] In fact, the only study of their anticancer properties was published in 2018, describing ferrocene-modified heterobimetallic NHC_{trz} Au(I) complexes.[17] Owing to the fact that ferrocenes are known to induce oxidative stress leading to cell death even without the involvement of gold, the reported study does not provide direct and unequivocal information about the effectiveness of NHC_{trz} Au(I) compounds.[17,18] Since their first description in 2008, NHC_{trz} ligands have become popular in homogeneous catalysis due to their exceptionally simple modifiability *via* "click" chemistry and subsequent alkylation.[19−22] Contrary to most NHC_{im} complexes having only two substituents, they bear three substituents which can be varied by the choice of alkyne, azide, and alkyl-halide applied throughout synthesis. In this way, additional modification sites are available, which might also be advantageous for biological applications potentially enabling a simple conjugation of efficacy and selectivity enhancing targeting vectors like antibodies and peptides in the future.[23−27][19,21,22]

As only very few gold(I) NHC_{trz} compounds have been described and little is known concerning their therapeutic properties, herein, the first detailed study on the assessment of bis(NHC_{im}) Au(I) complexes as potential anticancer compounds is presented. Their cytotoxicity and selectivity for various cancer cell lines focusing on blood tumors as well as an unequivocal identification of the form of cell death are reported. In addition, the overcoming of resistances against the

Received: June 7, 2021

commonly applied drugs etoposide, cytarabine, daunorubicin, and cisplatin as well as potential synergistic effects is investigated.

Well-studied benzimidazole-based gold(I) NHC complexes commonly bear aliphatic or aromatic wingtips, sterically shielding the metal center.[5,7,9] Therefore, in this work, isopropyl (R = iPr, **1**) and mesityl (R = Mes, **2**) are applied as wingtips of novel gold(I) bis(NHC_{trz}) compounds as representatives of aliphatic and aromatic substituents (Scheme 1). Due to its simple accessibility, methyl (Me) is chosen as the third 1,2,3-triazole substituent.

RESULTS AND DISCUSSION

Synthesis and Characterization of 1 and 2. **1** and **2** are readily accessible *via* the silver oxide route, subsequent transmetalation with Au(tht)Cl, and anion exchange with NH_4PF_6 (Scheme 1, tht = tetrahydrothiophene).

Scheme 1. Synthesis of 1,2,3-Triazolium Iodides *via* "Click" Chemistry and Methylation[a]

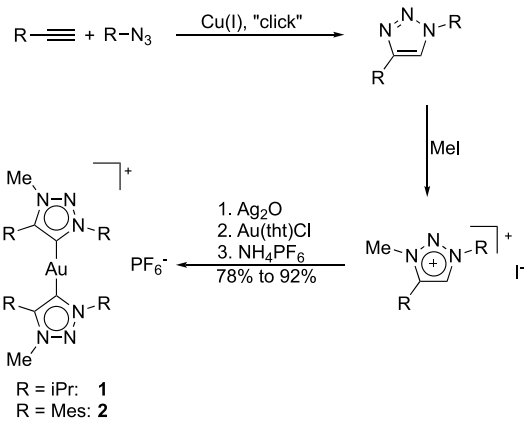

[a]Synthesis of gold(I) complexes 1 and 2 *via* the Ag_2O route, transmetalation with Au(tht)Cl, and anion exchange (see the Supporting Information for details).

In addition to matching elemental analyses, analytical high-performance liquid chromatography (HPLC) and electrospray ionization mass spectrometry (ESI-MS), the absence of the acidic triazolium protons in ^{1}H NMR spectra as well as the observation of characteristic carbene signals in ^{13}C NMR spectra at 168.3 ppm (**1**) and 176.0 ppm (**2**) confirms the successful synthesis (Supporting Information, Figures S5−S8). The crystal structure of **2** is illustrated in Figure 1. As expected for a gold(I) bis(NHC), the complex exhibits a nearly linear structure with a C−Au−C angle of 176.9(3)°. The Au−C distance of 2.011(7) Å is in the range of other Au(I) bis(NHC_{trz}) compounds.[22,28]

Anticancer Activity. The anticancer activity of **1** and **2** is evaluated by monitoring the viability of the respective cell lines *via* the MTT assay in breast-(MCF7 and MDAMB231), prostate-(PC3), and ovarian-(A2780) human cancer cell lines (Table 1). It is strongly affected by the substituents with the Mes-substituted compound **2** being significantly more active than its iPr counterpart **1**. As shown by Berners-Price et al., the lipophilicity of Au(I) bis(NHC_{im}) complexes correlates with the activity.[5,8,9] Therefore, mesityl-substituted imidazole and benzimidazole-based NHC complexes are reported to be more active than their isopropyl counterparts.[5,8,9,29] Accordingly, the more lipophilic complex **2** (log $P_{octanol/water}$: 0.264 ± 0.002 vs 1.592 ± 0.030, see the Supporting Information) shows better antiproliferative activity than **1**, significantly exceeding that of reference metallodrugs cisplatin and auranofin and reaching nanomolar IC_{50} values in all studied cell lines. Overall, both compounds and **2** in particular are among the most active Au compounds against cancer cells including NHC_{im} complexes.[5,30,31]

Stability Studies and TrxR Inhibition. In contrast to the cancer types of Table 1, leukemia is not commonly treated with cisplatin, one of the most effective anticancer drugs against many solid tumors, and thus requires alternatives.[4] Among these, auranofin, the most advanced gold(I) metallodrug, is currently in clinical trials against different blood cancers but lacks stability against thiol-containing proteins in the blood.[32] In contrast, benzimidazole-based gold(I) NHC complexes are reported to be significantly more stable.[13] As shown by ^{1}H NMR kinetics, the highly antiproliferative compounds **1** and **2** are also stable against cysteine and glutathione (Supporting Information, Figures S9−S18).

Aiming to get a first insight into the mechanism of action, the ability of these complexes to inhibit the selenoprotein TrxR is studied. This enzyme is considered a major target for several cytotoxic gold compounds and an important mechanism responsible for their antiproliferative activity.[33,34] Complexes **1** and **2** are moderate inhibitors of the enzyme, with IC_{50} values for the TrxR inhibition of 1.0 and 1.6 μM, respectively (Supporting Information, Figures S25 and S26). However, the complexes are considerably less active than auranofin (17 nM) and show an inverse correlation between the TrxR inhibition and cytotoxicity. This is likely related to the fact that another, more dominant, mechanism of action is involved for these NHC_{trz}-Au(I) complexes and in stark contrast to studies of Berners-Price on normal NHC_{im}-Au(I) complexes.[8]

Induction of Apoptosis as Cell Death Type. The high activity and stability of the more active complex **2** prompted its evaluation as a potential antiproliferative agent against blood cancer cells. Therefore, human acute lymphoblastic leukemia (ALL) cells (Nalm-6) **2** are incubated (24 h) with increasing concentrations of complex **2** and the cell count and viability are determined. The complex already causes a significant proliferation inhibition at low concentration (0.05 μM). Moreover, it inhibits cell proliferation in a dose-dependent manner, and at 0.5 μM, the proliferation inhibition reaches 100%, with the cell number being reduced below the initial cell count (Supporting Information, Figure S27). The cell count decrease is caused by cell death induced by the compound. There are two main types of cell death: apoptosis and necrosis, which can be differentiated with annexin-V/propidium iodide (PI) double-staining experiments (see the Supporting Information for explanation).[35−37] After 48 h of incubation with **2**, the flow cytometric analysis shows that the largest number of cells is in early apoptosis, a large number is already in late apoptosis, and no necrosis is detectable (Figure 2).

Another characteristic step of the programmed cell death induced by **2**, namely, the detection of DNA fragmentation, is also observed.[38] The process, which can be triggered by various mechanisms, ultimately lead to the decay of the DNA into fragments of 180 bp length and formation of apoptotic bodies *via* proteolytic enzymes called effector caspases.[39,40] Flow cytometric measurement of these hypodiploid DNA fragments follows specific labeling by staining with PI.[41] After incubation of Nalm-6 cells for 72 h with **2**, flow cytometric

https://doi.org/10.1021/acs.jmedchem.1c01021
J. Med. Chem. XXXX, XXX, XXX−XXX

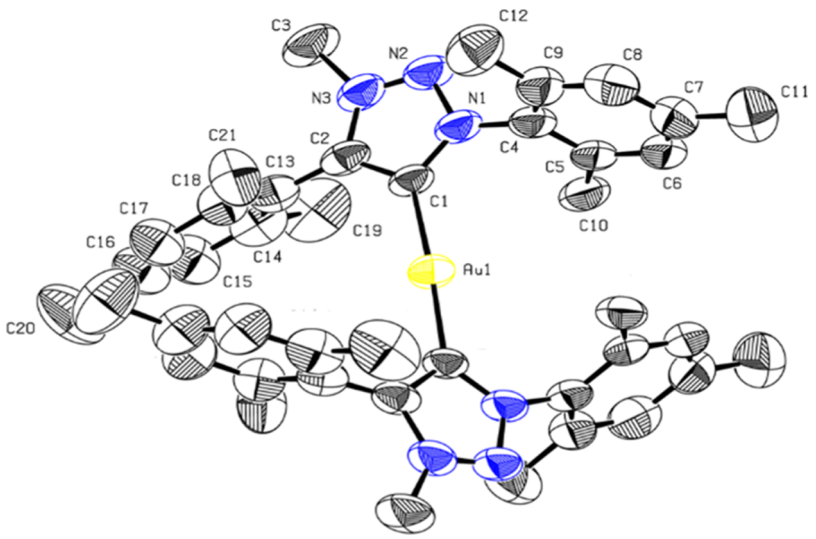

Figure 1. ORTEP-style representation of the cationic fragment of compound **2**. Hydrogen atoms and hexafluorophosphate anions are omitted for clarity. CCDC: 2082048.

Table 1. IC_{50} Values ± SD (μM) of 1 and 2 and Metallodrugs Cisplatin and Auranofin in Human Cancer Cell Lines after 48 h of Incubation Determined by the MTT Assay (Supporting Information, Figure S24)

	A2780	MCF7	MDAMB231	PC3
1	1.30 ± 0.28	0.42 ± 0.11	3.65 ± 0.75	5.10 ± 1.8
2	0.36 ± 0.09	0.084 ± 0.016	0.063 ± 0.02	0.4 ± 0.09
cisplatin	3.6 ± 1.3	21 ± 6.3	13.8 ± 4.5	34 ± 5.5
auranofin	0.43 ± 0.23	0.28 ± 0.14	1.9 ± 0.7	2.4 ± 1.9

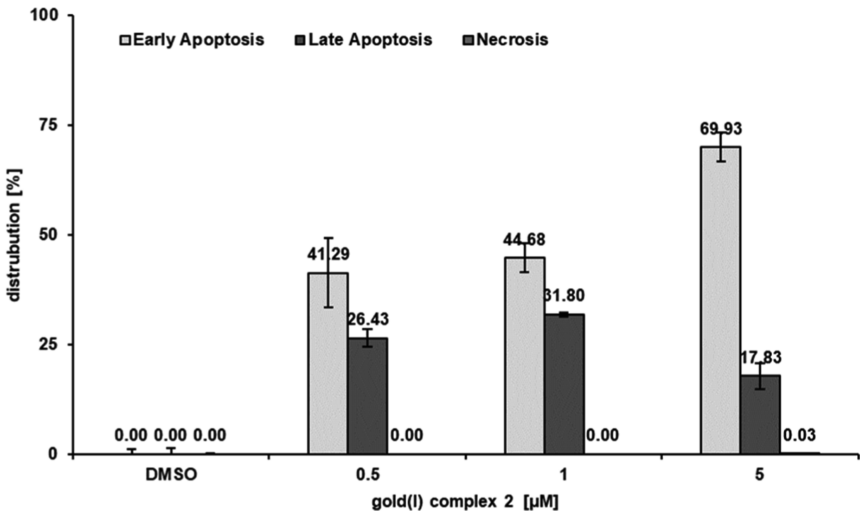

Figure 2. Nalm-6 cells were treated and incubated with increasing concentrations of **2** for 48 h. Solvent-treated cells [0.5% dimethyl sulfoxide (DMSO)] served as the control. The distribution of counted cells according to the cell status was measured by flow cytometric analysis. Vital cells, representing the remaining fraction, are not shown. Depicted values are mean values ± SD (n = 3).

analysis shows that the percentage of apoptotic cells increased continuously in a dose-dependent manner starting at 0.05 μM. The number of apoptotic cells increases to above 80% and reaches a plateau at 10 μM (Figure 3).

Overcoming of Important Resistances. The development of chemoresistance to conventional and commonly used cytostatic drugs *via* different mechanisms is one of the main problems in modern cancer therapy.[42,43] Therefore, current research is largely focused on the development of novel compounds that can overcome such resistances in cancer cells *via* different targets in the cells.[44] To test the ability of **2** to overcome such resistances, cells without known resistance as the control cell line and one cell line each with a known resistance are incubated with increasing concentrations of the compound. After 72 h of incubation, the induced DNA fragmentation is determined as an indicator for apoptosis.

In comparison to the control cells Nalm-6, **2** achieves similar or even higher amounts of apoptotic cells on the drug-resistant cell line JeFri (Figure 4a). In addition to resistance against the cytostatic drug etoposide, JeFri also exhibits coresistances against other cytostatics of the anthracycline group such as daunorubicin, doxorubicin, idarubicin, epirubicin, and mitox-

https://doi.org/10.1021/acs.jmedchem.1c01021
J. Med. Chem. XXXX, XXX, XXX−XXX

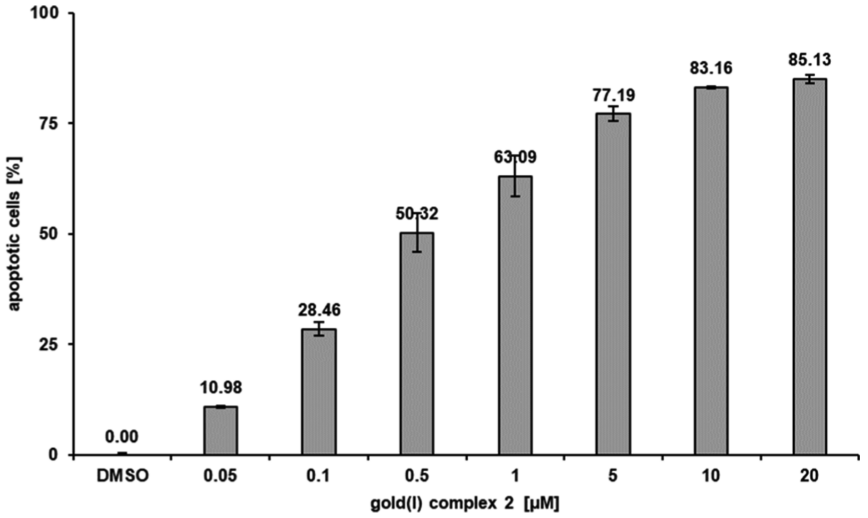

Figure 3. Nalm-6 cells were treated with different concentrations of **2** and incubated for 72 h. Solvent-treated cells (0.5% DMSO) served as the control. Apoptosis induction was measured by flow cytometric analysis of nuclear DNA fragmentation. Values are given in percentage of hypoploidy (subG1), which reflects the number of apoptotic cells as mean values ± SD (n = 3).

antrone. Previous experiments reveal that the resistance of JeFri cells results from the underexpression of the GADD45A (Growth Arrest and DNA Damage-inducible 45 proteins) gene (Supporting Information, Table S3). The proteins play an important role in the regulation of cell cycle control and DNA repair and may act as tumor suppressors through proapoptotic properties.[45,46] The underexpression or lack of GADD45A proteins could potentially abolish their mediating effect on chemotherapeutic drugs.[45]

On the cytarabine-resistant cell line MaKo, **2** shows, at a concentration of 0.5 μM, even higher apoptotic effects than on the control cells (Figure 4b). At the higher concentrations on the MaKo cells, the measurement showed similarly high or slightly lower rates of apoptosis, so that the reaching of a plateau can be recognized. This can be explained by the fact that the high concentrations of the substance trigger very high rates of apoptosis and the cells may already be in a late stage of apoptosis. The resulting cell remnants and debris have minimal DNA fluorescence and smaller diameters and thus are not visualized in the hypodiploid (sub-G1) portion of the measurement.[39] MaKo cells show additional coresistance to the antimetabolites cladribine and clofarabine as well as to the vinca alkaloid vincristine. The mechanism of resistance shown by these cells may be due to downregulation or underexpression of the FOXI1 (Forkhead box I1) gene, which was demonstrated in a previous PCR analysis (Supporting Information, Table S3). Studies in gastric cancer tissue have shown that FOXI1 is involved as a transcription factor in the positive regulation of microRNAs (miRNAs) that may act as antioncogenes.[47] In addition, there is evidence that FOXI1 is involved in the regulation of cell growth and proliferation and can induce cell cycle arrest or apoptosis.[47] Thus, the underexpression of the FOXI1 gene, resulting in a decreased level of the FOXI1 protein, may abrogate its potential effect as a tumor suppressor.

To test the effect of the compound on other cell types, **2** is applied in three concentrations to the chronic myeloid leukemia (CML) cell line K562 and the subline NiWi-Dau generated by us. In addition to resistance to daunorubicin, the cell line also shows numerous coresistances not only to other anthracyclines (idarubicin, doxorubicin, and epirubicin) and mitoxanthrone but also to the vinca alkaloids (vincristine, vinblastine, vindesine, and vinorelbine) and the steroid prednisone. The resistances are likely caused by the underexpression of the protein harakiri (Hrk), which was detected in previous investigations (Supporting Information, Figures S20 and S22). Hrk is a proapoptotic protein that can induce cell death and interacts, for example, with the antiapoptotic protein bcl-2.[48,49] Interestingly, **2** also causes apoptosis at higher concentrations and overcomes the resistance of NiWi-Dau cells to daunorubicin at a concentration of 5 μM (Figure S19).

Effects on Neuroblastoma Cells. To evaluate the effect of **2** for other potential therapeutic applications besides blood cancer, the neuroblastoma cells (SK-N-AS) and the cisplatin-resistant subline (LiOn) are incubated with the compound. The LiOn cells showed underexpression of caspase-8 in previous experiments (Supporting Information, Figures S21 and S23). It plays a central role as an initiator caspase in the extrinsic pathway of apoptosis and, when inactivated, can lead to tumor progression or resistance to cancer therapy.[50−52] These cells also show apoptosis after incubation with **2**, which therefore overcomes the resistances despite the caspase-8 deficiency; treatment with the compound results in a significantly higher number of apoptotic cells in the resistant cell line compared to that in the control cell line (Figure 5).

Selectivity for Malignant Cells. In order to investigate the selectivity of **2** toward malignant cells, Nalm-6 cells, BJAB mock lymphoma cells, and healthy human leukocytes are incubated with different concentrations of the compound. The following measurement of DNA fragmentation shows a very clear selectivity toward the cancer cells. The proportion of apoptotic cells among the healthy leukocytes remains below 2% even at a concentration of 5 μM. Interestingly, the substance has an even higher effect in the Burkitt-like lymphoma cells compared to that in the leukemia cells (Figure 6).

Synergistic Effects with Daunorubicin. To determine whether 2 exhibits a synergistic effect with commonly used cytostatic drugs, Nalm-6 cells are treated with minimal doses of the complex, the established cytostatic drug daunorubicin, and the combination of both. The individual concentrations do not result in more than 12% apoptosis. However, the combination

https://doi.org/10.1021/acs.jmedchem.1c01021
J. Med. Chem. XXXX, XXX, XXX−XXX

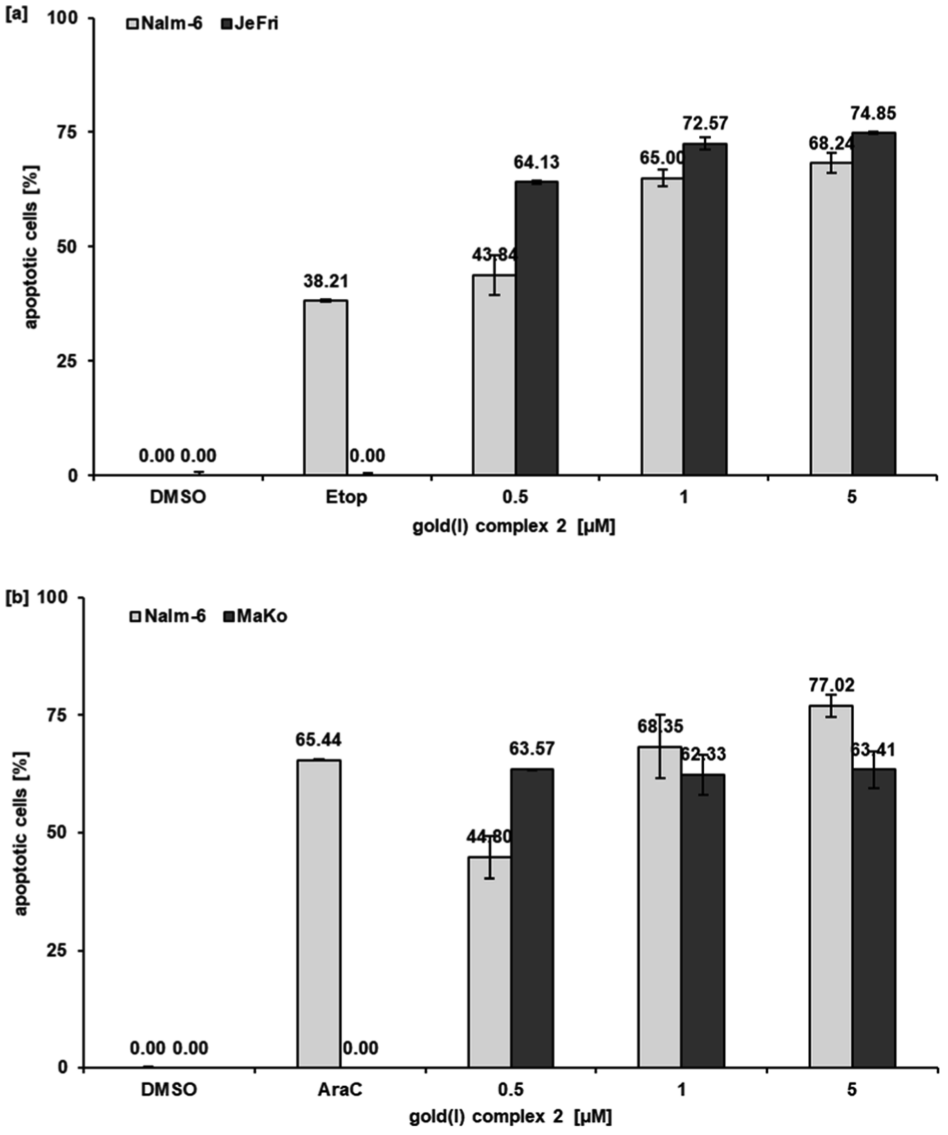

Figure 4. To prove the overcoming of etoposide and cytarabine resistance in leukemia cells, Nalm-6 and JeFri [**a**] or MaKo [**b**] cells were treated with 0.5, 1, and 5 μM **2**. Solvent-treated cells (0.5% DMSO) served as the control. 0.36 μM etoposide (Etop) [**a**] and 1.4 μM cytarabine (AraC) [**b**], respectively, were used as the positive control to prove the resistance. After 72 h of incubation, DNA fragmentation was measured by flow cytometric analysis. Values are given in percentage of apoptotic cells as mean values ± SD (n = 3).

of both results in a clear synergistic effect. Compared to the sum of the individual doses, an increase in the apoptotic effect of 182 and 128%, respectively, is achieved (Figure 7). Daunorubicin, which belongs to the anthracyclines, reaches its cytostatic effect by intercalating with DNA and as a direct inhibitor of topoisomerase II.[53]

More detailed studies on the mechanism of action of 2 are pending, but a mechanism *via* the intrinsic pathway, that is, an effect on mitochondria, is assumed. The effect of two different mechanisms of action could explain the synergistic effect of daunorubicin and **2** since the cells are attacked in two ways, resulting in more effective apoptosis induction.

CONCLUSIONS

For the first time, a series of gold(I) bis(1,2,3-triazol-5-ylidene) complexes is investigated as potential anticancer compounds showing high anticancer activity in the range of the most active gold compounds against a variety of solid tumor cell lines and blood cancer cells with IC_{50} values in the nanomolar range. The more lipophilic mesityl-substituted compound **2** is more effective than its isopropyl counterpart **1** in all tested cell lines. Interestingly, in contrast to the more common imidazole-based Au(I) NHCs, TrxR inhibition does not seem to play the main role in the observed antiproliferative activity hinting to another, more dominant, mechanism of action. Complex **2** exclusively induces the highly selective cell death pathway apoptosis in ALL cells (Nalm6). A significant inhibition is already observed at concentrations as low as 0.05 μM. Remarkably, **2** overcomes resistances against the common cytostatic etoposide, cytarabine, daunorubicin, and cisplatin. With daunorubicin, a significant synergistic effect of up to 182% is determined. Moreover, the compound is not only highly effective against leukemia and lymphoma cells but also does not affect non-malignant leukocytes even at high concentrations (5 μM). These results prove gold(I) bis-(1,2,3-triazol-5-ylidene) complexes as highly promising anticancer compounds, suitable for upcoming *in vivo* studies. In addition to their high activity, selectivity, stability, and ability

https://doi.org/10.1021/acs.jmedchem.1c01021
J. Med. Chem. XXXX, XXX, XXX−XXX

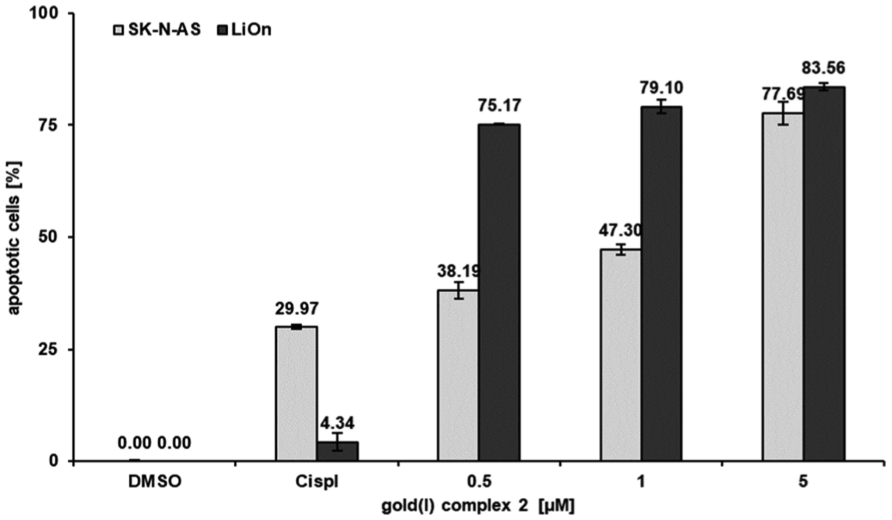

Figure 5. SK-N-AS and LiOn cells were treated with 0.5, 1, and 5 μM **2**. Solvent-treated cells (0.5% DMSO) served as the control. 7.5 μM cisplatin (Cispl) was pipetted in both cell lines to prove the resistance. After 72 h of incubation, DNA fragmentation was measured by flow cytometric analysis. Values are given in percentage of apoptotic cells as mean values ± SD (n = 3).

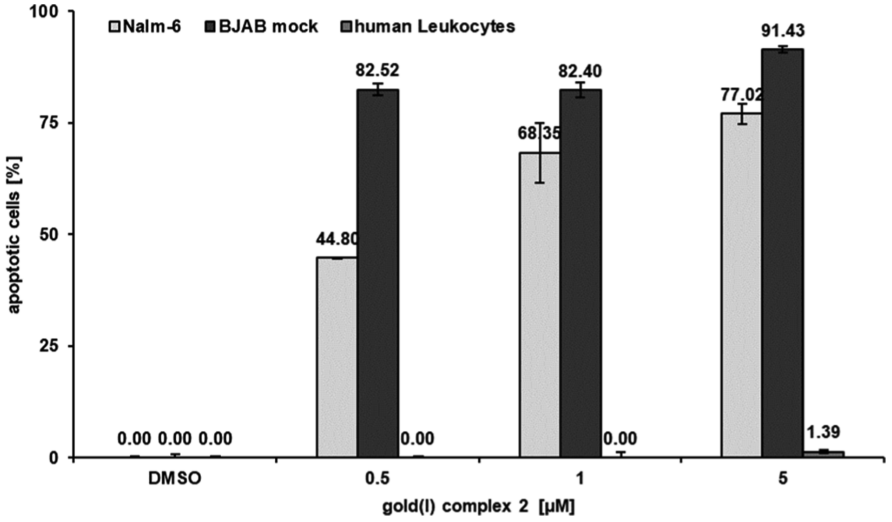

Figure 6. Nalm-6 cells, BJAB mock cells, and human leukocytes were treated with different concentrations of **2**. Solvent-treated cells (0.5% DMSO) served as the control. All cells were incubated for 72 h. Then, induction of apoptosis was measured by flow cytometric analysis of cellular content. Values are given as percentage of cells with hypodiploid DNA as mean values ± SD (n = 3).

to overcome common resistances, the newly investigated compound class offers more potential sites for modifications than benzimidazole-based compounds. Replacing the methyl substituent with functional groups containing linkers could allow the attachment of target-specific vectors such as peptides or antibodies to further improve the already high selectivity and efficacy. In contrast to a classical wingtip modification, usually applied for NHC_{im} ligands, this does not significantly impact the steric shielding around the gold center. The resulting potential benefit on the stability and activity is in the focus of upcoming research.

EXPERIMENTAL SECTION

General Remarks. All reagents were purchased from commercial suppliers and used without further purification. NMR spectra were recorded on a Bruker AVANCE DPX 400 (^{1}H NMR, 400.13 MHz; ^{13}C NMR, 100.53 MHz). Chemical shifts are reported in parts per million and referenced to the residual signal of the deuterated solvent (acetonitrile-d_3; 1.94 ppm). Elemental analyses (C/H/N) were performed by the microanalytical laboratory at Technische Universität München. ESI-MS data were acquired on a Thermo Fisher UltiMate 3000. Analytical reversed-phase HPLC-HESI-MS (heated ESI-MS) was performed on an UltiMate 3000 UHPLC focused chromatographic system (Dionex) connected to an LCQ Fleet mass spectrometer (Thermo Scientific) equipped with a C18 column (Hypersil GOLD aQ, 150 × 2.1 mm, 3 μm). Linear gradients (0.7 mL/min, 20 min) of acetonitrile (0.1% formic acid) and water (0.1% formic acid) were used for analytical purposes. 1,4-Diisopropyl-3-methyl-1,2,3-triazolium iodide and Au(tht)Cl were synthesized according to literature procedures.[54−56] The identity and purity (>95%) of all biologically studied compounds were confirmed by analytical HPLC in conjunction with elemental analysis and NMR spectroscopy.

1,4-Diisopropyl-1,2,3-triazole. In a round-bottom flask, NaN_3 (4.77 g, 73.4 mmol, 2.50 equiv) was dissolved in 15 mL of water and mixed with a solution of isopropyl bromide (6.14 g, 49.9 mmol, 1.70 equiv) in 5 mL of THF. The mixture was stirred at 90 °C for 3 h. After being cooled to room temperature, 10 mL of DCM was added. The organic phase was separated and washed with 5 mL of water. Subsequently, copper turnings (18.7 g, 293 mmol, 10.0 equiv), 3-

https://doi.org/10.1021/acs.jmedchem.1c01021
J. Med. Chem. XXXX, XXX, XXX−XXX

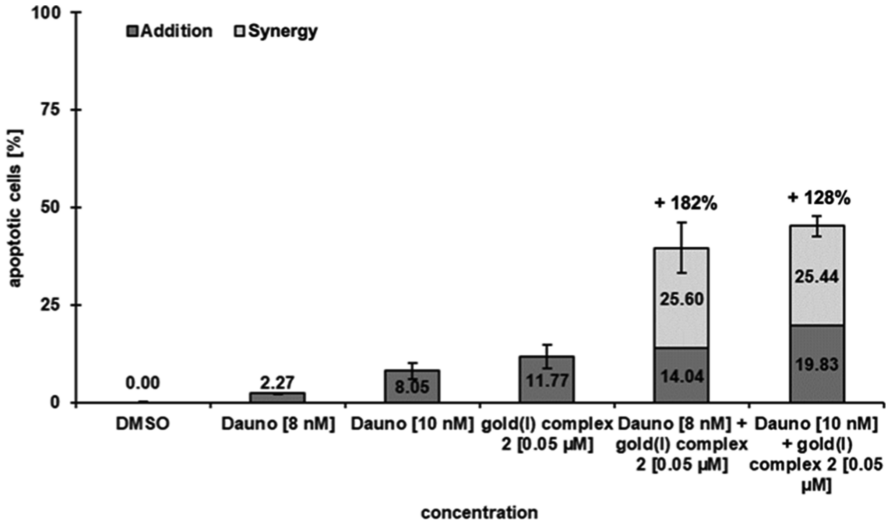

Figure 7. Nalm-6 cells were treated with 0.05 μM **2** and 8 nM and 10 nM daunorubicin (Dauno), respectively. The synergistic effect is shown as the percentages of the additional number of apoptotic cells relative to the sum of the individual number of apoptotic cells. Solvent-treated cells (0.5% DMSO) served as the control.

methylbut-1-yne (2.00 g, 29.4 mmol, 1.00 equiv), and 20 mL of water were added. The mixture was stirred in a sealed round-bottom flask for 48 h. After filtration through Celite, a 30 mL aqueous solution of NH_3 (10%) and ethylenediaminetetraacetate (EDTA) (10%) were added. After being stirred for 1 h, the mixture and 30 mL of DCM were added to a separatory flask. The organic phase was separated, and the aqueous phase was extracted with DCM (3 × 30 mL). The combined organic phases were washed with a 20 mL aqueous solution of NH_3 (10%) and EDTA (10%) and 20 mL of water. After drying with Na_2SO_4, all volatiles were removed in vacuo. 1,4-Diisopropyl-1,2,3-triazole was obtained as a white solid in 65% yield (2.92 g, 19.1 mmol). ^{1}H NMR (400 MHz, $CDCl_3$): δ(ppm): 7.20 (s, 1H, H_{trz}), 4.73 (hept, ^{3}J = 6.8 Hz, 1H, CH(CH$_3$)$_2$), 3.03 (hept, ^{3}J = 6.9 Hz, 1H, CH(CH$_3$)$_2$), 1.49 (d, ^{3}J = 6.8 Hz, 6H, CH(CH_3)$_2$), 1.24 (d, ^{3}J = 6.9 Hz, 6H, CH(CH_3)$_2$). ^{13}C NMR (400 MHz, $CDCl_3$): δ(ppm): 154.4 (C_{trz}CH$_{trz}$), 116.5 (C$_{trz}$CH_{trz}), 52.9 (CH(CH3)2), 26.04 (CH-(CH$_3$)$_2$), 22.9 (CH$_3$), 22.8 (CH$_3$). Anal. Calcd for $C_8H_{15}N_3$: C 62.71; H 9.87; N 27.42. Found: C 62.80; H 9.98; N 27.53. MS-ESI (m/z): [$C_8H_{15}N_3$ + H$^+$]$^+$ calcd, 154.13; found, 153.98.

1,4-Diisopropyl-3-methyl-1,2,3-triazolium Iodide. In a pressure tube, 400 mg of 1,4-diisopropyl-1,2,3-triazole (2.61 mmol, 1.00 equiv) and 4.63 g of methyl iodide (32.6 mmol, 12.5 equiv) were dissolved in 20 mL of MeCN. The solution was heated to 60 °C for 5 d. After the removal of volatiles in vacuo, 1,4-diisopropyl-3-methyl-1,2,3-triazolium iodide was obtained as a pale-yellow solid in 98% yield (770 mg, 2.61 mmol). ^{1}H NMR (400 MHz, DMSO): δ(ppm): 8.92 (s, 1H, H_{trz}), 5.00 (hept, ^{3}J = 6.8 Hz, 1H, NCH(CH$_3$)$_2$), 4.24 (s, 3H, NCH_3), 3.26 (hept, ^{3}J = 6.8 Hz, 1H, CCH(CH$_3$)$_2$), 1.57 (d, ^{3}J = 6.8 Hz, 6H, CH(CH_3)$_2$), 1.29 (d, ^{3}J = 6.8 Hz, 6H, CH(CH_3)$_2$). ^{13}C NMR (101 MHz, DMSO): δ(ppm): 149.7 (NCHC$_{iPr}$), 126.0 (NCHC$_{iPr}$), 57.6 (NCH(CH$_3$)$_2$), 42.7 (NCH$_3$), 26.4 (CH(CH$_3$)$_2$), 24.9 (CH(CH$_3$)$_2$), 22.5 (CH(CH$_3$)$_2$), 20.9 (CH(CH$_3$)$_2$). Anal. Calcd for $C_9H_{18}N_3I$: C 36.62; H 6.19; N 14.24. Found: C 36.67; H 6.01; N 14.14. MS-ESI (m/z): [$C_9H_{18}N_3^+$]$^+$ calcd., 168.15; found, 168.25.

1. In a round-bottom flask, 326 mg of 1,4-diisopropyl-3-methyl-1,2,3-triazolium iodide (1.10 mmol, 2.00 equiv) and 141 mg of Ag_2O (607 μmol, 1.10 equiv) were suspended in 20 mL of DCM and stirred under exclusion of light for 30 min. Au(tht)Cl (177 mg, 552 μmol, 1.00 equiv) was added to the flask. After stirring for an additional 16 h under exclusion of light, the suspension was filtered through Celite. All volatiles were removed in vacuo. The light brown solid was dissolved in 10 mL of MeCN and treated with a solution of 180 mg of NH_4PF_6 (1.10 mmol, 2.00 equiv) in water. MeCN was removed in vacuo, resulting in the formation of an off-white solid. After filtration and dissolving in 5 mL of MeCN, the solution was added to 50 mL of water. The white precipitate was filtered off, washed with water (2 × 30 mL), and dried in vacuo. **1** was obtained as a white solid in 78% yield (306 mg, 453 μmol). ^{1}H NMR (400 MHz, $CDCl_3$): δ(ppm): 5.08 (hept, ^{3}J = 6.9 Hz, 4H, N(CH(CH3)2), 4.12 (s, 6H, NCH_3), 3.24 (hept, ^{3}J = 6.8 Hz, 4H, CCH(CH3)2), 1.67 (d, ^{3}J = 6.8 Hz, 12H, CH(CH_3)$_2$), 1.49 (d, ^{3}J = 6.9 Hz, 12H, CH(CH_3)$_2$). ^{13}C NMR (126 MHz, CD_3CN): δ(ppm): 168.3 ($C_{Carbene}$), 155.3 (NC$_{iPr}$), 59.7 (NCH(CH$_3$)$_2$), 37.2 (NCH$_3$), 25.8 (CCH(CH$_3$)$_2$), 23.6 (CH(CH$_3$)$_2$), 23.1 (CH(CH$_3$)$_2$). Anal. Calcd for $C_{18}H_{34}N_6AuPF_6$: C 31.96; H 5.07; N 12.42. Found: C 31.75; H 4.96; N 12.20. MS-ESI (m/z): [**1** − PF_6^-]$^+$ calcd 531.25; found, 531.49. RP-HPLC (50−100% MeCN/H2O with 0.1% TFA, 20 min) t_R = 3.32 min.

2. In a round-bottom flask, 326 mg of 1,4-dimesityl-3-methyl-1,2,3-triazolium iodide (671 μmol, 2.00 equiv) and 85.5 mg of Ag_2O (369 μmol, 1.10 equiv) were suspended in 20 mL of DCM and stirred under exclusion of light for 30 min. Au(tht)Cl (107 mg, 335 μmol, 1.00 equiv) was added to the flask. After stirring for an additional 16 h under exclusion of light, the suspension was filtered through Celite. All volatiles were removed in vacuo. The light brown solid was dissolved in 10 mL of MeCN and treated with a solution of 109 mg of NH_4PF_6 (671 μmol, 2.00 equiv) in water. MeCN was removed in vacuo, resulting in the formation of an off-white solid. After filtration and dissolving in 5 mL of MeCN, the solution was added to 50 mL of water. The white precipitate was filtered off, washed with water (2 × 30 mL), and dried in vacuo. **2** was obtained as a white solid in 92% yield (303 mg, 308 μmmol). Single crystals suitable for single-crystal X-ray diffraction were obtained by slow vapor diffusion of pentane in a solution of **2** in chloroform. ^{1}H NMR (400 MHz, CD_3CN): δ(ppm) 6.99 (s, 2H, CH_{Ar}), 6.96 (s, 2H (CH_{Ar}), 3.81 (s, 6H, NCH_3), 2.42 (s, 6H, p-CH_3), 2.41 (s, 6H, p-CH_3), 1.82 (s, 12H, o-CH_3), 1.76 (s, 12H, o-CH_3). ^{13}C NMR (126 MHz, CD_3CN): δ(ppm): 176.0 ($C_{Carbene}$), 147.3 (CC_{Mes}), 141.6 (C_{Ar}), 141.5 (C_{Ar}), 139.1 (C_{Ar}), 136.3 (C_{Ar}), 135.0 (C_{Ar}), 129.9 (C_{Ar}), 129.5 (C_{Ar}), 123.1 (C_{Ar}), 37.7 (NCH$_3$), 21.4 (CCH$_3$), 21.4 (CCH$_3$), 20.1 (CCH$_3$), 17.2 (CCH$_3$). Anal. Calcd. for $C_{42}H_{50}N_6AuPF_6$: C 51.43; H 5.14; N 8.57. Found: C 51.76; H 5.14; N 8.69. MS-ESI (m/z): [**2** − PF_6^-]$^+$ calcd, 835.38; found, 835.75. RP-HPLC (50−100% MeCN/H2O with 0.1% formic acid, 20 min) t_R = 14.84 min.

Single-Crystal X-ray Diffraction. X-ray diffraction measurements were performed on a single-crystal X-ray diffractometer with the following installation: a CMOS detector (Bruker APEX III, κ-CMOS), a TXS rotating anode, and a Helios optic using the APEX3 software package.[57] The measurement used MoK$_\alpha$ radiation (λ = 0.71073 Å) and was performed on single crystals coated with perfluorinated ether. The crystal was fixed on the top of a glass fiber

https://doi.org/10.1021/acs.jmedchem.1c01021
J. Med. Chem. XXXX, XXX, XXX−XXX

and frozen under a stream of cold nitrogen. A matrix scan was used to determine the initial lattice parameters. Reflections were corrected for Lorentz and polarization effects, scan speed, and background using SAINT.[58] Absorption corrections, including odd and even ordered spherical harmonics, were performed using SADABS.[58] Space group assignments were based upon systematic absences, E statistics, and successful refinement of the structures. The structures were solved by direct methods (SHELXS) or charge flipping (SHELXT) with the aid of successive difference Fourier maps and were refined against all data using SHELXL-2013 in conjunction with ShelXle.[59,60] Hydrogen atoms were analyzed in ideal positions as follows: Methyl hydrogen atoms were refined as part of rigid rotating groups, with a C−H distance of 0.98 Å and Uiso(H) = 1.5·Ueq(C). Other H atoms were placed in calculated positions and refined using a riding model, with methylene and aromatic C−H distances of 0.99 and 0.95 Å, respectively, and other C−H distances of 1.00 Å and Uiso(H) = 1.2·Ueq(C). Nonhydrogen atoms were refined with anisotropic displacement parameters. Full-matrix least-squares refinements were carried out by minimizing $\Sigma w(F_o^2 - F_c^2)^2$ with the SHELXL weighting scheme.[59] Neutral-atom scattering factors for all atoms and anomalous dispersion corrections for the nonhydrogen atoms were taken from International Tables for Crystallography.[61] The unit cell contains six disordered molecules of chloroform, which were treated as a diffuse contribution to the overall scattering without specific atom positions using the PLATON/SQUEEZE procedure.[62] Images of the crystal structures were generated with PLATON.[62] CCDC 2082048 contains the supplementary crystallographic data for this paper. These data can be obtained free of charge via www.ccdc.cam.ac.uk/data_request/cif or by emailing data_request@ccdc.cam.ac.uk or by contacting The Cambridge Crystallographic Data Centre, 12 Union Road, Cambridge CB2 1EZ, UK; fax: +44 1223 336033.

Stability Studies. 100 μL of a 10 mM stock solution of **1** and **2** in DMSO-d_6 was prepared and diluted with deuterated PBS buffer to a final concentration of 0.1 mM. **1** and **2** were dissolved (2.5 mg in 0.5 mL of D_2O) and 5.0 eq L-cysteine or glutathione (GSH) were added, respectively. The samples were incubated at 37 °C for 72 h and analyzed by ^{1}H NMR spectroscopy and ESI-MS. Both complexes showed remarkable stability against L-cysteine and GSH, respectively.

Biological Studies. *Materials.* All chemicals and solutions used for synthesis were purchased from common suppliers. Dimethyl sulfoxide (DMSO) and propidium iodide (50 μg/ml) were obtained from Serva (Heidelberg, Germany), RNase A from Qiagen (Hilden, Germany). The conventional cytostatic drugs (daunorubicin, cytarabine, and etoposide) were provided by Helios Clinics Schwerin and were dissolved in DMSO as stock solutions directly before use in the experiments. The investigated substances and auranofin were dissolved in DMSO to prepare a stock solution of 10 or 40 mM. Cisplatin was dissolved in water (1 mg/mL, 3.33 mM).

Cell Lines and Cell Culture. Different human cell lines and their chemoresistant sublines were used. The leukemia B-cell precursor (Nalm-6) cells were kindly provided by Dr. Seeger/AG Henze, Charité Berlin, Germany. Cytarabine- (MaKo) and etoposide- (JeFri) resistant sublines were generated in our working group and conditioned by treatment with increasing doses of the cytostatic drug while maintaining a high level of vitality. BJAB mock (Burkitt-like lymphoma) cells were kindly donated by AG Daniel, Charité Berlin, Germany. Furthermore, SK-N-AS neuroblastoma cells were kindly provided by Professor Simon, University Cologne, Germany, and the cisplatin-resistant subline LiOn was generated by our working group. Moreover, immortalized K562 (CML) cells were kindly provided by Dr. Seeger/AG Henze, Charité Berlin, Germany, and the daunorubicin-resistant subline NiWi-Dau was also generated in our working group. Leukocytes were attained from a blood sample of a healthy test person. The ovarian cancer cells A2780 (sensitive to cisplatin) were obtained from Sigma-Aldrich. The breast cancer cells MCF7 (hormone-dependent) and MDAMB231 (hormone-independent) and prostate cancer cells PC3 (hormone-independent) were obtained from ATCC. All suspension cell lines were cultured in RPMI 1640 medium supplemented with fetal calf serum (FCS, 10%); for the leukocytes, RPMI 1640 medium was supplemented with 20% FCS (v/v). The adherent cancer cell lines A2780, MCF7, MDAMB231, and PC3 were cultured in DMEM + GlutaMAX-I (breast cells) or RPMI 1640 (ovarian and prostate cells) medium supplemented with fetal bovine serum (10%). All cells were kept in a humidified atmosphere at 37 °C and 5% CO_2.

Isolation of Healthy Human Leukocytes. 10 mL of RPMI 1640 medium (20%) was added to 50 mL of fresh blood taken from a healthy test person. Leukocytes were separated from the other blood components using Ficoll (Biocoll separating solution, Biochrom, Merck, Darmstadt, Germany) and density gradient centrifugation (18 min, 2000 rpm, 18 °C). The leukocytes were collected from the buffy coat, and 20 mL of RPMI 1640 medium (20%) was added before centrifugation at 1500 rpm and 18 °C for 5 min. The cell count and viability were determined by the CASY cell counter and analyzer system (Roche, Mannheim, Germany). Cells were seeded at a density of 3×10^5 cells per mL prior to the experiment.

Determination of Cell Concentration and Cell Viability. For the suspension cell lines, cell count and viability were determined using the CASY cell counter and analyzer system from Roche (Mannheim, Germany). Settings were specifically defined for the requirements of the cells used. With this system, the cell concentration can be analyzed in three different size ranges: cell debris, dead cells, and viable cells can be determined in one measurement. Cells were seeded at a density of 1×10^5 cells per mL and were treated with different concentrations of the compounds; untreated cells and cells treated with the solvent DMSO served as controls. A maximum DMSO concentration of 0.5% was reached in each sample. After 24 h of incubation, the cells were resuspended, and 100 mL of each well was diluted in CASYton (10 mL, ready-to-use isotonic saline solution) for immediate automated count.

MTT Assay. For the adherent cell lines (A2780, MCF7, MDAMB231, and PC3 − 20.000 cells/well), cell viability was determined using the tetrazolium dye MTT that is reduced to its insoluble formazan by metabolic active cells. Cells were seeded at a density of 2×10^4 cells in 200 μL of appropriate medium and were treated with different concentrations of the compounds; untreated cells and cells treated with the solvent DMSO (0.5%) served as controls. After 48 h of incubation, the medium was discarded, and the cells were incubated with 200 μL of a MTT solution in PBS (0.5 mg/mL). After 3 h at 37 °C, the solution was removed, and 200 μL of DMSO was applied to each well to solubilize the purple formazan crystals formed. The absorbance at 570 nm was measured using a plate spectrophotometer (PowerWave XS, BioTek). The IC_{50} values were calculated using the GraphPad Prism software (v. 5.0).

Annexin-V/Propidium Iodide Double Staining. Phosphatidylserine, which is normally located in the inner membrane of the cell, is translocated to the outside in the early phase of apoptosis and can be bound by annexin V in a calcium-dependent manner.[36] Propidium iodide (PI) intercalates into the DNA and can only bind to it when the membrane is permeable, that is, in the late apoptotic or necrotic state. Thus, living cells are annexin-V and PI negative, early apoptotic cells are annexin-V positive and PI negative, and late apoptotic cells are annexin-V and PI positive. In contrast, necrotic cells are annexin-V negative and PI positive.[37] This allows one to distinguish between the proportion of early apoptosis, late apoptosis, and nonspecific necrosis in the samples. To determine the number of apoptotic cells in the sample, the cells were stained with annexin-V conjugated to the fluorescent dye fluorescein isothiocyanate (FITC) and PI and analyzed by flow cytometry. Cells were seeded at a density of 1×10^5 cells per mL and treated with different concentrations of the compound. After incubation for 48 h at 37 °C and 5% CO_2, cells were collected by centrifugation (5 min, 4 °C, 8000 rpm) and washed in PBS. After repelleting, Annexin-V-FITC/PI solution (Annexin-V-FLUOS Staining Kit, Roche, Mannheim, Germany) prepared in incubation buffer was added to each sample. As controls, four samples were incubated with either incubation buffer, Annexin-V-FITC in incubation buffer, PI in incubation buffer, or annexin-V-FITC and PI in incubation buffer for 10 min. For the detection of the cells, a flow cytometric analysis was performed using a FACScan (FACSCalibur,

https://doi.org/10.1021/acs.jmedchem.1c01021
J. Med. Chem. XXXX, XXX, XXX−XXX

Becton Dickinson, Heidelberg, Germany) equipped with the CellQuest software (Figure S25).

Measurement of DNA Fragmentation. Apoptotic cell death was determined by using a modified cell cycle analysis that detects DNA fragmentation at the single-cell level. For the measurement of DNA fragmentation, cells were seeded at a density of 1×10^5 cells per mL and treated with different concentrations of the compound. After 72 h of incubation, cells were collected by centrifugation at 8000 rpm and 4 °C for 5 min and fixed in PBS/formaldehyde (2%, v/v) on ice for 30 min. After being fixed, the cells were incubated with ethanol/PBS (2:1, v/v) for 15 min, centrifuged, and resuspended in PBS containing RNase A (40 μg per mL). After incubation for 30 min at 37 °C, cells were centrifuged again and finally resuspended in PBS containing PI (50 μg per mL). Nuclear DNA fragmentation was then quantified by flow cytometric determination of hypodiploid DNA (Figure S26). Data were collected and analyzed using a FACScan (FACSCalibur, Becton Dickinson, Heidelberg, Germany) equipped with the CellQuest software. Data are given in percentage of hypoploidy (subG1), which reflects the number of apoptotic cells. Apoptosis specifically induced by the compounds was calculated by subtracting background apoptosis observed in solvent control (0.5% DMSO) cells from total apoptosis detected in the treated cells.

TrxR Activity Assay. To determine the inhibition of TrxR by the gold complexes, a TrxR Assay Kit (Sigma-Aldrich) was used with minor modifications for a 96-well plate format assay. 200 μL of reaction mixture contained 2 μL of TrxR solution, 11 μL of assay buffer (phosphate buffer pH 7.0 containing 50 mM EDTA), 180 μL of working buffer (phosphate buffer containing 0.25 mM reduced nicotinamide adenine dinucleotide phosphate), and 1 μL of the complexes' solutions. The enzymatic reaction was started with the addition of 6 μL DTNB (0.1 M in DMSO). A blank sample (without enzyme) and a positive control (without compounds) were included in the assays. After proper shaking for 30 min, the formation of TNB was monitored at 412 nm with a plate spectrophotometer.

■ ASSOCIATED CONTENT

Supporting Information

The Supporting Information is available free of charge at https://pubs.acs.org/doi/10.1021/acs.jmedchem.1c01021.

NMR spectra, crystal data, and biological assays (PDF)

CCDC 2082048 contains the supplementary crystallographic data for this paper. These data can be obtained free of charge via www.ccdc.cam.ac.uk/data_request/cif or by emailing data_request@ccdc.cam.ac.uk or by contacting The Cambridge Crystallographic Data Centre, 12 Union Road, Cambridge CB2 1EZ, UK; fax: +44 1223 336033 (CIF)

Molecular formula strings file containing the SMILE structures of **1** and **2** (CSV)

■ AUTHOR INFORMATION

Corresponding Authors

Aram Prokop − *Department of Pediatric Hematology/Oncology, Children's Hospital Cologne, Cologne 50735, Germany; Department of Pediatric Oncology/Hematology, Helios Clinics Schwerin, 19049 Schwerin, Germany; MSH Medical School Hamburg, 20457 Hamburg, Germany*; Phone: 0385 520 6396; Email: aram.prokop@helios-gesundheit.de; Fax: 0385 520 2704

Fritz E. Kühn − *Molecular Catalysis, Catalysis Research Center and Department of Chemistry, Technische Universität München, Garching bei München D-85748, Germany*; orcid.org/0000-0002-4156-780X; Phone: (+49) 89 289 13096; Email: fritz.kuehn@ch.tum.de; Fax: (+49) 89 289 13247

Authors

Jonas F. Schlagintweit − *Molecular Catalysis, Catalysis Research Center and Department of Chemistry, Technische Universität München, Garching bei München D-85748, Germany*

Christian H. G. Jakob − *Molecular Catalysis, Catalysis Research Center and Department of Chemistry, Technische Universität München, Garching bei München D-85748, Germany*

Nicola L. Wilke − *Department of Pediatric Hematology/Oncology, Children's Hospital Cologne, Cologne 50735, Germany; Department of Pediatric Oncology/Hematology, Helios Clinics Schwerin, 19049 Schwerin, Germany; MSH Medical School Hamburg, 20457 Hamburg, Germany*

Marie Ahrweiler − *Department of Pediatric Hematology/Oncology, Children's Hospital Cologne, Cologne 50735, Germany; Department of Pediatric Oncology/Hematology, Helios Clinics Schwerin, 19049 Schwerin, Germany*

Corazon Frias − *Department of Pediatric Hematology/Oncology, Children's Hospital Cologne, Cologne 50735, Germany; Department of Pediatric Oncology/Hematology, Helios Clinics Schwerin, 19049 Schwerin, Germany; MSH Medical School Hamburg, 20457 Hamburg, Germany*

Jerico Frias − *Department of Pediatric Hematology/Oncology, Children's Hospital Cologne, Cologne 50735, Germany; Department of Pediatric Oncology/Hematology, Helios Clinics Schwerin, 19049 Schwerin, Germany; MSH Medical School Hamburg, 20457 Hamburg, Germany*

Marcel König − *Department of Pediatric Hematology/Oncology, Children's Hospital Cologne, Cologne 50735, Germany*

Eva-Maria H. J. Esslinger − *Molecular Catalysis, Catalysis Research Center and Department of Chemistry, Technische Universität München, Garching bei München D-85748, Germany*

Fernanda Marques − *Centro de Ciências e Tecnologias Nucleares and Departamento de Engenharia e Ciências Nucleares, Instituto Superior Técnico, Universidade de Lisboa, Bobadela LRS 2695-066, Portugal*

João F. Machado − *Centro de Ciências e Tecnologias Nucleares and Departamento de Engenharia e Ciências Nucleares, Instituto Superior Técnico, Universidade de Lisboa, Bobadela LRS 2695-066, Portugal; Centro de Química Estrutural, Faculdade de Ciências, Universidade de Lisboa, Lisboa 1749-016, Portugal*

Robert M. Reich − *Molecular Catalysis, Catalysis Research Center and Department of Chemistry, Technische Universität München, Garching bei München D-85748, Germany*; orcid.org/0000-0002-2297-2711

Tânia S. Morais − *Centro de Química Estrutural, Faculdade de Ciências, Universidade de Lisboa, Lisboa 1749-016, Portugal*; orcid.org/0000-0003-0233-8243

João D. G. Correia − *Centro de Ciências e Tecnologias Nucleares and Departamento de Engenharia e Ciências Nucleares, Instituto Superior Técnico, Universidade de Lisboa, Bobadela LRS 2695-066, Portugal*; orcid.org/0000-0002-7847-4906

Complete contact information is available at: https://pubs.acs.org/10.1021/acs.jmedchem.1c01021

Author Contributions

J.F.S., C.H.G.J., and N.L.W. contributed equally to this work. The manuscript was written through contributions of all

https://doi.org/10.1021/acs.jmedchem.1c01021
J. Med. Chem. XXXX, XXX, XXX−XXX

authors. All authors have given approval to the final version of the manuscript. Corresponding authors: A.P. and F.E.K.

Funding

Centro de Química Estrutural acknowledges Fundação para a Ciência e Tecnologia (FCT) for financial support through the Project UIDB/00100/2020. J.F. Machado thanks FCT for his doctoral grant (SFRH/BD/135915/2018). T.S. Morais thanks FCT for CEECIND 2017 Initiative for the project CEECIND/00630/2017 (acknowledging FCT as well as POPH and FSE-European Social Fund).

Notes

The authors declare no competing financial interest.

■ ACKNOWLEDGMENTS

J.F.S., C.H.G.J., and E.-M.H.J.E. thank TUM Graduate School for financial support. For the excellent technical support, we thank Ursula Schwarz-Prokop. We gratefully thank the Dr. Kleist Foundation (Berlin), the Foundation Blankenheimerdorf e.V. (Eifel), and the Otto Böcker-Foundation (Hamburg) for the financial support. J.D.G.C and F.M. thank Fundação para a Ciência e Tecnologia, Portugal, for funding through projects UID/Multi/04349/2020 and PTDC/QUI-NUC/30147/2017.

■ ABBREVIATIONS

NHC,, *N*-heterocyclic carbene; NHC_{im},, imidazol-2-ylidene; NHC_{trz},, 1,2,3-triazol-5-ylidene; cispl,, cisplatin; dauno,, daunorubicin

■ REFERENCES

(1) Siegel, R. L.; Miller, K. D.; Fuchs, H. E.; Jemal, A. Cancer Statistics, 2021. *Ca-Cancer J. Clin.* **2021**, *71*, 7−33.

(2) Rosenberg, B.; Van Camp, L.; Krigas, T. Inhibition of Cell Division in Escherichia coli by Electrolysis Products from a Platinum Electrode. *Nature* **1965**, *205*, 698−699.

(3) Rosenberg, B.; Vancamp, L.; Trosko, J. E.; Mansour, V. H. Platinum Compounds: a New Class of Potent Antitumour Agents. *Nature* **1969**, *222*, 385−386.

(4) Dasari, S.; Bernard Tchounwou, P. Cisplatin in Cancer Therapy: Molecular Mechanisms of Action. *Eur. J. Pharmacol.* **2014**, *740*, 364−378.

(5) Berners-Price, S. J.; Filipovska, A. Gold Compounds as Therapeutic Agents for Human Diseases. *Metallomics* **2011**, *3*, 863−873.

(6) Zou, T.; Lum, C. T.; Lok, C.-N.; Zhang, J.-J.; Che, C.-M. Chemical Biology of Anticancer Gold(iii) and Gold(i) Complexes. *Chem. Soc. Rev.* **2015**, *44*, 8786−8801.

(7) Dominelli, B.; Correia, J. D. G.; Kühn, F. E. Medicinal Applications of Gold(I/III)-Based Complexes Bearing N-Heterocyclic Carbene and Phosphine Ligands. *J. Organomet. Chem.* **2018**, *866*, 153−164.

(8) Hickey, J. L.; Ruhayel, R. A.; Barnard, P. J.; Baker, M. V.; Berners-Price, S. J.; Filipovska, A. Mitochondria-Targeted Chemotherapeutics: The Rational Design of Gold(I) N-Heterocyclic Carbene Complexes That Are Selectively Toxic to Cancer Cells and Target Protein Selenols in Preference to Thiols. *J. Am. Chem. Soc.* **2008**, *130*, 12570−12571.

(9) Baker, M. V.; Barnard, P. J.; Berners-Price, S. J.; Brayshaw, S. K.; Hickey, J. L.; Skelton, B. W.; White, A. H. Cationic, Linear Au(i) N-heterocyclic Carbene Complexes: Synthesis, Structure and Anti-mitochondrial Activity. *Dalton Trans.* **2006**, *30*, 3708−3715.

(10) Barnard, P. J.; Baker, M. V.; Berners-Price, S. J.; Day, D. A. Mitochondrial permeability transition induced by dinuclear gold(I)-carbene complexes: potential new antimitochondrial antitumour agents. *J. Inorg. Biochem.* **2004**, *98*, 1642−1647.

(11) Hoyer, C.; Schwerk, P.; Suntrup, L.; Beerhues, J.; Nössler, M.; Albold, U.; Dernedde, J.; Tedin, K.; Sarkar, B. Synthesis, Characterization, and Evaluation of Antibacterial Activity of Ferrocenyl-1,2,3-Triazoles, Triazolium Salts, and Triazolylidene Complexes of Gold(i) and Silver(i). *Eur. J. Inorg. Chem.* **2021**, *2021*, 1373−1382.

(12) Rubbiani, R.; Kitanovic, I.; Alborzinia, H.; Can, S.; Kitanovic, A.; Onambele, L. A.; Stefanopoulou, M.; Geldmacher, Y.; Sheldrick, W. S.; Wolber, G.; Prokop, A.; Wölfl, S.; Ott, I. Benzimidazol-2-ylidene Gold(I) Complexes Are Thioredoxin Reductase Inhibitors with Multiple Antitumor Properties. *J. Med. Chem.* **2010**, *53*, 8608−8618.

(13) Rubbiani, R.; Can, S.; Kitanovic, I.; Alborzinia, H.; Stefanopoulou, M.; Kokoschka, M.; Mönchgesang, S.; Sheldrick, W. S.; Wölfl, S.; Ott, I. Comparative in Vitro Evaluation of N-Heterocyclic Carbene Gold(I) Complexes of the Benzimidazolylidene Type. *J. Med. Chem.* **2011**, *54*, 8646−8657.

(14) Schmidt, C.; Karge, B.; Misgeld, R.; Prokop, A.; Brönstrup, M.; Ott, I. Biscarbene Gold(i) Complexes: Structure−Activity-Relationships regarding Antibacterial Effects, Cytotoxicity, TrxR Inhibition and Cellular Bioavailability. *Medchemcomm* **2017**, *8*, 1681−1689.

(15) Wragg, D.; de Almeida, A.; Bonsignore, R.; Kühn, F. E.; Leoni, S.; Casini, A. On the Mechanism of Gold/NHC Compounds Binding to DNA G-Quadruplexes: Combined Metadynamics and Biophysical Methods. *Angew. Chem., Int. Ed.* **2018**, *57*, 14524−14528.

(16) Bertrand, B.; de Almeida, A.; van der Burgt, E. P. M.; Picquet, M.; Citta, A.; Folda, A.; Rigobello, M. P.; Le Gendre, P.; Bodio, E.; Casini, A. New Gold(I) Organometallic Compounds with Biological Activity in Cancer Cells. *Eur. J. Inorg. Chem.* **2014**, *2014*, 4532−4536.

(17) Aucamp, D.; Kumar, S. V.; Liles, D. C.; Fernandes, M. A.; Harmse, L.; Bezuidenhout, D. I. Synthesis of Heterobimetallic Gold(i) Ferrocenyl-substituted 1,2,3-Triazol-5-ylidene Complexes as Potential Anticancer Agents. *Dalton Trans.* **2018**, *47*, 16072−16081.

(18) Ludwig, B. S.; Correia, J. D. G.; Kühn, F. E. Ferrocene Derivatives as Anti-infective Agents. *Coord. Chem. Rev.* **2019**, *396*, 22−48.

(19) Kolb, H. C.; Finn, M. G.; Sharpless, K. B. Click Chemistry: Diverse Chemical Function from a Few Good Reactions. *Angew. Chem., Int. Ed.* **2001**, *40*, 2004−2021.

(20) Mathew, P.; Neels, A.; Albrecht, M. 1,2,3-Triazolylidenes as Versatile Abnormal Carbene Ligands for Late Transition Metals. *J. Am. Chem. Soc.* **2008**, *130*, 13534−13535.

(21) Donnelly, K. F.; Petronilho, A.; Albrecht, M. Application of 1,2,3-triazolylidenes as versatile NHC-type ligands: synthesis, properties, and application in catalysis and beyond. *Chem. Commun.* **2013**, *49*, 1145−1159.

(22) Vivancos, Á.; Segarra, C.; Albrecht, M. Mesoionic and Related Less Heteroatom-Stabilized N-Heterocyclic Carbene Complexes: Synthesis, Catalysis, and Other Applications. *Chem. Rev.* **2018**, *118*, 9493−9586.

(23) Guisado-Barrios, G.; Soleilhavoup, M.; Bertrand, G. 1H-1,2,3-Triazol-5-ylidenes: Readily Available Mesoionic Carbenes. *Acc. Chem. Res.* **2018**, *51*, 3236−3244.

(24) Marichev, K. O.; Patil, S. A.; Bugarin, A. Recent Advances in the Synthesis, Structural Diversity, and Applications of Mesoionic 1,2,3-Triazol-5-ylidene Metal Complexes. *Tetrahedron* **2018**, *74*, 2523−2546.

(25) Shah, J.; Khan, S. S.; Blumenthal, H.; Liebscher, J. 1,2,3-Triazolium-Tagged Prolines and Their Application in Asymmetric Aldol and Michael Reactions. *Synthesis* **2009**, *2009*, 3975−3982.

(26) Koguchi, S.; Izawa, K. A New Method for the Synthesis of 1,5-Disubstituted 1,2,3-Triazoles via Triazolium Salt Intermediates. *Synthesis* **2012**, *44*, 3603−3608.

(27) Hohloch, S.; Scheiffele, D.; Sarkar, B. Activating Azides and Alkynes for the Click Reaction with [Cu(aNHC)2I] or [Cu(aNHC)-2]+ (aNHC = Triazole-Derived Abnormal Carbenes): Structural Characterization and Catalytic Properties. *Eur. J. Inorg. Chem.* **2013**, *2013*, 3956−3965.

(28) Canseco-Gonzalez, D.; Petronilho, A.; Mueller-Bunz, H.; Ohmatsu, K.; Ooi, T.; Albrecht, M. Carbene Transfer from

https://doi.org/10.1021/acs.jmedchem.1c01021
J. Med. Chem. XXXX, XXX, XXX−XXX

Triazolylidene Gold Complexes as a Potent Strategy for Inducing High Catalytic Activity. *J. Am. Chem. Soc.* **2013**, *135*, 13193−13203.
(29) Oberkofler, J.; Aikman, B.; Bonsignore, R.; Pöthig, A.; Platts, J.; Casini, A.; Kühn, F. E. Exploring the Reactivity and Biological Effects of Heteroleptic N-Heterocyclic Carbene Gold(I)-Alkynyl Complexes. *Eur. J. Inorg. Chem.* **2020**, *2020*, 1040−1051.
(30) Ott, I. On the Medicinal Chemistry of Gold Complexes as Anticancer Drugs. *Coord. Chem. Rev.* **2009**, *253*, 1670−1681.
(31) Zou, T.; Lok, C.-N.; Wan, P.-K.; Zhang, Z.-F.; Fung, S.-K.; Che, C.-M. Anticancer Metal-N-heterocyclic Carbene Complexes of Gold, Platinum and Palladium. *Curr. Opin. Chem. Biol.* **2018**, *43*, 30−36.
(32) Shaw, C. F. Gold-Based Therapeutic Agents. *Chem. Rev.* **1999**, *99*, 2589−2600.
(33) Bindoli, A.; Rigobello, M. P.; Scutari, G.; Gabbiani, C.; Casini, A.; Messori, L. Thioredoxin Reductase: A Target for Gold Compounds Acting as Potential Anticancer Drugs. *Coord. Chem. Rev.* **2009**, *253*, 1692−1707.
(34) Karaaslan, M. G.; Aktaş, A.; Gürses, C.; Gök, Y.; Ateş, B. Chemistry, Structure, and Biological Roles of Au-NHC Complexes as TrxR inhibitors. *Bioorg. Chem.* **2020**, *95*, 103552.
(35) Majno, G.; Joris, I. Apoptosis, Oncosis, and Necrosis. An Overview of Cell Death. *Am. J. Pathol.* **1995**, *146*, 3−15.
(36) Crowley, L. C.; Marfell, B. J.; Scott, A. P.; Waterhouse, N. J. Quantitation of Apoptosis and Necrosis by Annexin V Binding, Propidium Iodide Uptake, and Flow Cytometry. *Cold Spring Harb. Protoc.* **2016**, *2016*, prot087288.
(37) Rieger, A. M.; Nelson, K. L.; Konowalchuk, J. D.; Barreda, D. R. Modified Annexin V/propidium Iodide Apoptosis Assay for accurate Assessment of Cell Death. *J. Visualized Exp.* **2011**, *50*, 2597.
(38) Elmore, S. Apoptosis: A Review of Programmed Cell Death. *Toxicol. Pathol.* **2007**, *35*, 495−516.
(39) Nikoletopoulou, V.; Markaki, M.; Palikaras, K.; Tavernarakis, N. Crosstalk between Apoptosis, Necrosis and Autophagy. *Biochim. Biophys. Acta* **2013**, *1833*, 3448−3459.
(40) Hengartner, M. O. The Biochemistry of Apoptosis. *Nature* **2000**, *407*, 770−776.
(41) Riccardi, C.; Nicoletti, I. Analysis of Apoptosis by Propidium Iodide Staining and Flow Cytometry. *Nat. Protoc.* **2006**, *1*, 1458−1461.
(42) Housman, G.; Byler, S.; Heerboth, S.; Lapinska, K.; Longacre, M.; Snyder, N.; Sarkar, S. Drug Resistance in Cancer: An Overview. *Cancers* **2014**, *6*, 1769−1792.
(43) Zahreddine, H.; Borden, K. L. Mechanisms and Insights into Drug Resistance in Cancer. *Front. Pharmacol.* **2013**, *4*, 28.
(44) Holohan, C.; Van Schaeybroeck, S.; Longley, D. B.; Johnston, P. G. Cancer Drug Resistance: an Evolving Paradigm. *Nat. Rev. Cancer* **2013**, *13*, 714−726.
(45) E. Tamura, R.; F. de Vasconcellos, J.; Sarkar, D.; A. Libermann, T.; B. Fisher, P.; F. Zerbini, L.; Zerbini, L. F. GADD45 Proteins: central Players in Tumorigenesis. *Curr. Mol. Med.* **2012**, *12*, 634−651.
(46) Zhang, L.; Yang, Z.; Liu, Y. GADD45 Proteins: Roles in Cellular Senescence and Tumor Development. *Exp. Biol. Med.* **2014**, *239*, 773−778.
(47) Sun, R.; Liu, Z.; Tong, D.; Yang, Y.; Guo, B.; Wang, X.; Zhao, L.; Huang, C. miR-491-5p, mediated by Foxi1, functions as a tumor suppressor by targeting Wnt3a/β-catenin signaling in the development of gastric cancer. *Cell. Death. Dis.* **2017**, *8*, No. e2714.
(48) Barrera-Vilarmau, S.; Obregón, P.; de Alba, E. Intrinsic Order and Disorder in the Bcl-2 Member Harakiri: Insights into Its Proapoptotic Activity. *PLOS ONE* **2011**, *6*, No. e21413.
(49) Inohara, N.; Ding, L.; Chen, S.; Núñez, G. harakiri, a novel Regulator of Cell Death, encodes a Protein that activates Apoptosis and interacts selectively with Survival-promoting Proteins Bcl-2 and Bcl-XL. *EMBO J.* **1997**, *16*, 1686−1694.
(50) Fritsch, M.; Günther, S. D.; Schwarzer, R.; Albert, M.-C.; Schorn, F.; Werthenbach, J. P.; Schiffmann, L. M.; Stair, N.; Stocks, H.; Seeger, J. M.; Lamkanfi, M.; Krönke, M.; Pasparakis, M.; Kashkar, H. Caspase-8 is the Molecular Switch for Apoptosis, Necroptosis and Pyroptosis. *Nature* **2019**, *575*, 683−687.
(51) Kim, P. K. M.; Mahidhara, R.; Seol, D.-W. The Role of Caspase-8 in Resistance to Cancer Chemotherapy. *Drug Resist. Updates* **2001**, *4*, 293−296.
(52) Orning, P.; Lien, E. Multiple Roles of Caspase-8 in Cell Death, Inflammation, and innate Immunity. *J. Leukocyte Biol.* **2021**, *109*, 121−141.
(53) Gewirtz, D. A critical Evaluation of the Mechanisms of Action proposed for the Antitumor Effects of the Anthracycline Antibiotics Adriamycin and Daunorubicin. *Biochem. Pharmacol.* **1999**, *57*, 727−741.
(54) Barral, K.; Moorhouse, A. D.; Moses, J. E. Efficient Conversion of Aromatic Amines into Azides: A One-Pot Synthesis of Triazole Linkages. *Org. Lett.* **2007**, *9*, 1809−1811.
(55) Uson, R.; Laguna, A.; Laguna, M.; Briggs, D. A.; Murray, H. H.; Fackler, J. P., Jr. (Tetrahydrothiophene)Gold(I) or Gold(III) Complexes. *Inorg. Synth.* **1989**, *26*, 85−91.
(56) Nakamura, T.; Terashima, T.; Ogata, K.; Fukuzawa, S.-i. Copper(I) 1,2,3-Triazol-5-ylidene Complexes as Efficient Catalysts for Click Reactions of Azides with Alkynes. *Org. Lett.* **2011**, *13*, 620−623.
(57) *APEX3*; Bruker AXS, Inc.: Madison, Wisconsin, USA, 2016.
(58) *SAINT and SADABS*; Bruker AXS Inc.: Madison, Wisconsin, USA, 2016.
(59) Sheldrick, G. M. Crystal Structure Refinement with SHELXL. *Acta Crystallogr., Sect. A: Found. Adv.* **2015**, *71*, 3−8.
(60) Krause, L.; Herbst-Irmer, R.; Sheldrick, G. M.; Stalke, D. Comparison of Silver and Molybdenum Microfocus X-ray Sources for Single-Crystal Structure Determination. *J. Appl. Crystallogr.* **2015**, *48*, 3−10.
(61) Wilson, A. J. *International Tables for Crystallography*; Kluwer Academic Publishers: Dordrecht, The Netherlands, 1992; Vol. C Tables 6.1.1.4 (pp. 500−502), 4.2.6.8 (pp. 219−222), and 4.2.4.2 (pp. 193−199).
(62) Spek, A. L. Structure Validation in Chemical Crystallography. *Acta Crystallogr., Sect. D: Biol. Crystallogr.* **2009**, *65*, 148−155.

https://doi.org/10.1021/acs.jmedchem.1c01021
J. Med. Chem. XXXX, XXX, XXX−XXX

Supporting Information

Gold(I) bis(1,2,3-Triazol-5-ylidene) Complexes as Promising Selective Anticancer Compounds

Jonas F. Schlagintweit,[a,‡] Christian H. G. Jakob, [a,‡] Nicola L. Wilke,[b,c,d,‡] Marie Ahrweiler,[b,c] Corazon Frias,[b,c,d] Jerico Frias,[b,c,d] Marcel König,[b] Eva-Maria H. J. Esslinger,[a] Fernanda Marques,[d] João F. Machado,[e,f] Robert M. Reich,[a] Tânia S. Morais,[f] João D. G. Correia,[d] Aram Prokop[*b,c,d] Fritz E. Kühn[*,a]

a. Molecular Catalysis, Catalysis Research Center and Department of Chemistry
Technische Universität München
Lichtenbergstraße 4, D-85748 Garching bei München, Germany.
*E-mail: fritz.kuehn@ch.tum.de; Fax: (+49) 89 289 13247; Tel.: (+49) 89 289 13096.

b. Department of Pediatric Hematology/Oncology
Children's Hospital Cologne
Amsterdamer Straße 59, 50735 Cologne, Germany

c. Department of Pediatric Oncology/Hematology
Helios Clinics Schwerin
Wismarsche Straße 393 – 397, 19049 Schwerin, Germany
*E-mail: aram.prokop@helios-gesundheit.de; Fax: 0385 520 2704; Tel.: 0385 520 6396

d. MSH Medical School Hamburg, Am Kaiserkai 1, 20457 Hamburg, Germany

e. Centro de Ciências e Tecnologias Nucleares and Departamento de Engenharia e Ciências Nucleares, Instituto Superior Técnico
Universidade de Lisboa, CTN
Estrada Nacional 10 (km 139,7), 2695-066 Bobadela LRS, Portugal.

f. Centro de Química Estrutural, Faculdade de Ciências, Universidade de Lisboa, Campo Grande, 1749-016 Lisboa

Table of Contents

NMR Spectra 3
Single Crystal X-Ray Diffraction 7
Stability Studies 9
Biological Studies 14
Octanol-Water Partition Coefficients 19
Analytical HPLC 20
References 20

NMR Spectra

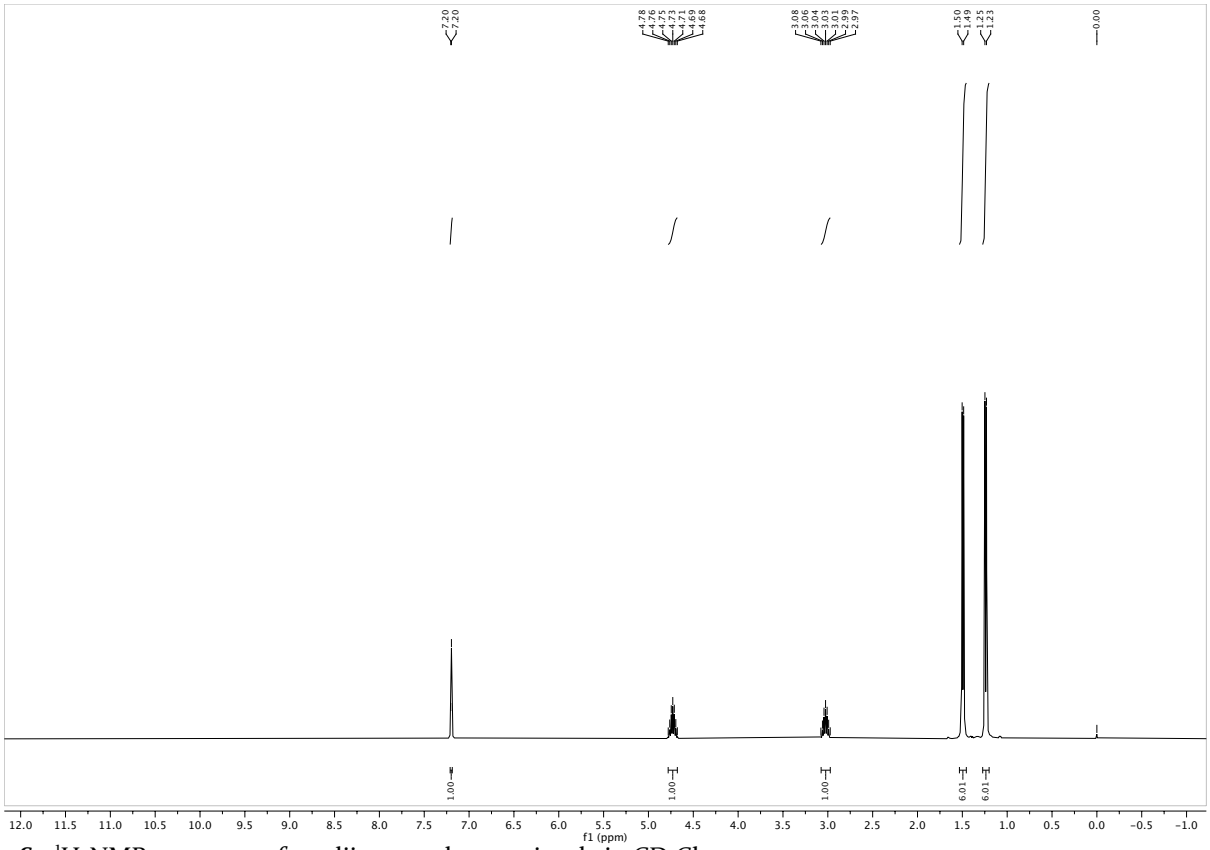

Figure S1. ^{1}H-NMR spectrum of 1,4-diisopropyl-1,2,3-triazole in CD_3Cl.

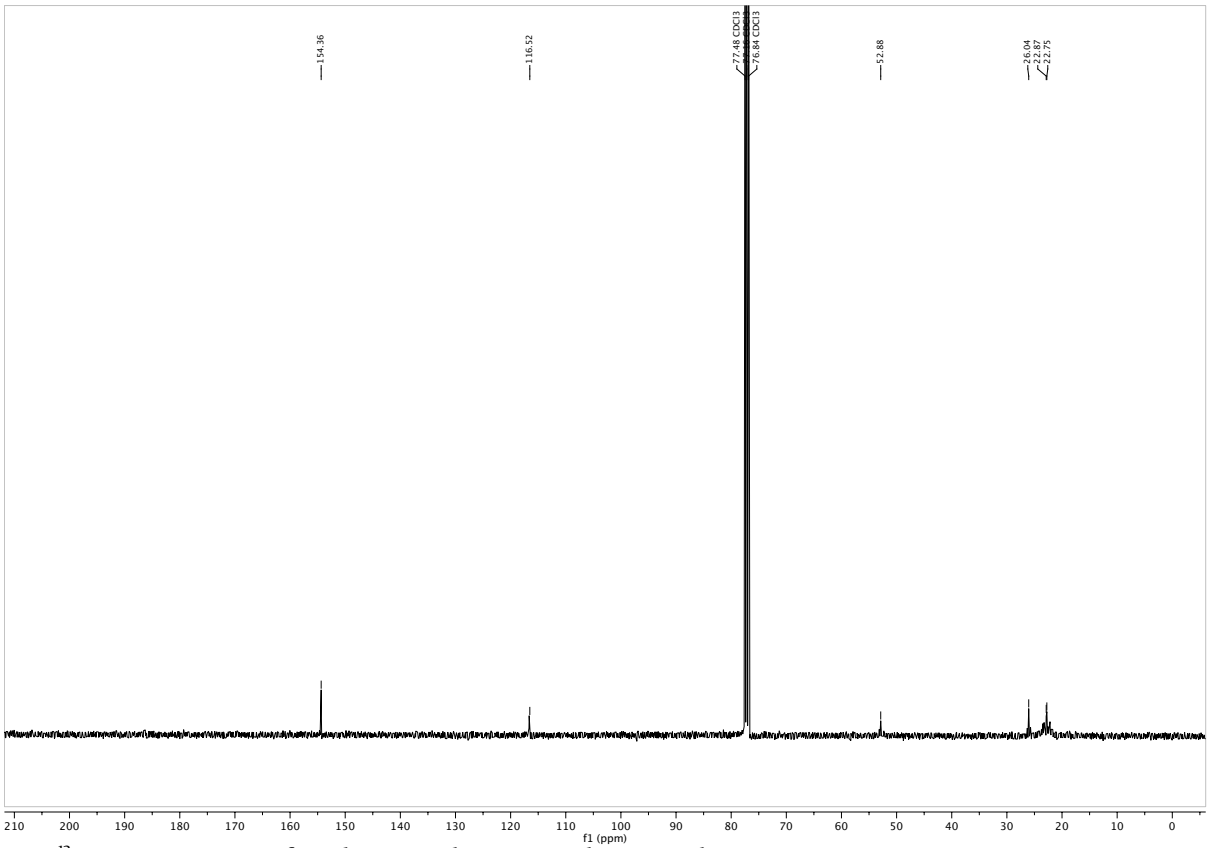

Figure S2. ^{13}C-NMR spectrum of 1,4-diisopropyl-1,2,3-triazole in CD_3Cl.

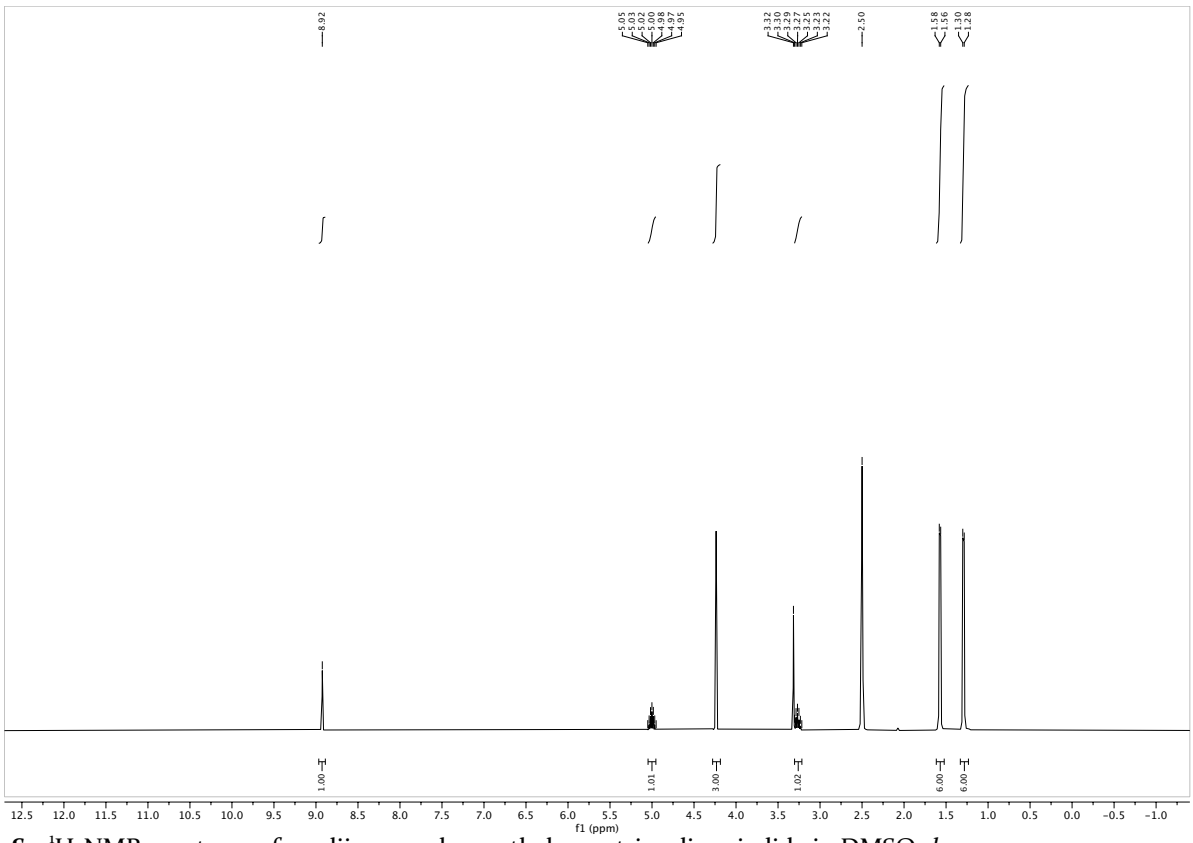

Figure S3. [1]H-NMR spectrum of 1,4-diisopropyl-3-methyl-1,2,3-triazolium iodide in DMSO-d_6.

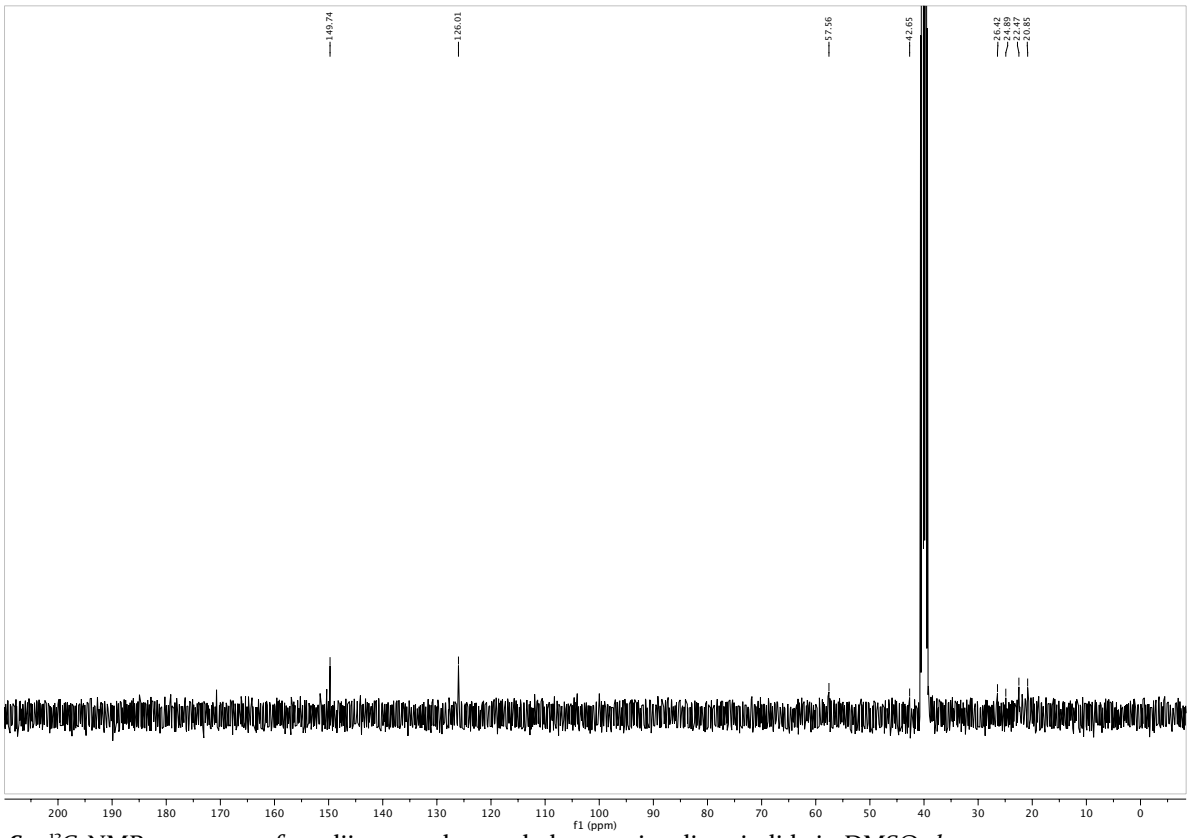

Figure S4. [13]C-NMR spectrum of 1,4-diisopropyl-3-methyl-1,2,3-triazolium iodide in DMSO-d_6.

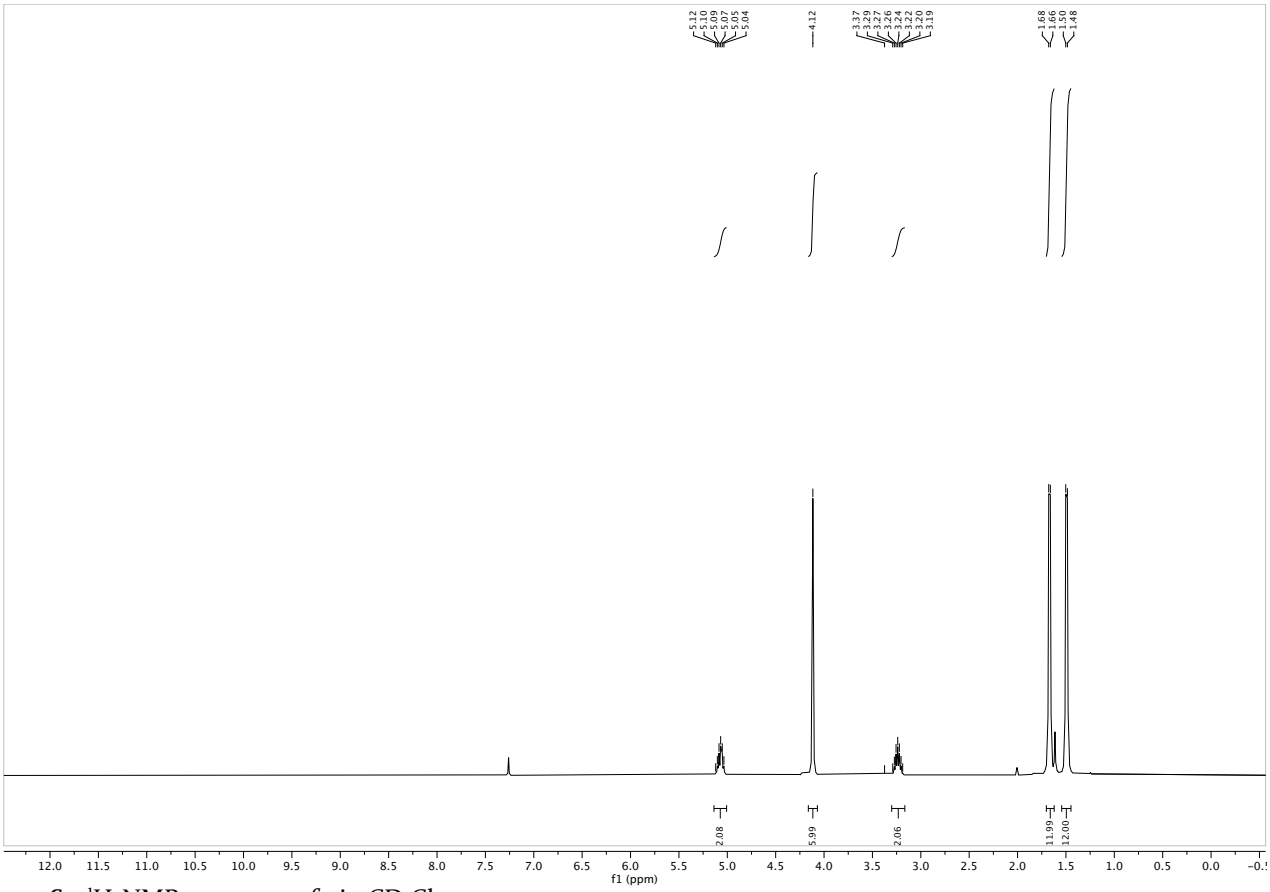

Figure S5. ^{1}H-NMR spectrum of **1** in CD_3Cl.

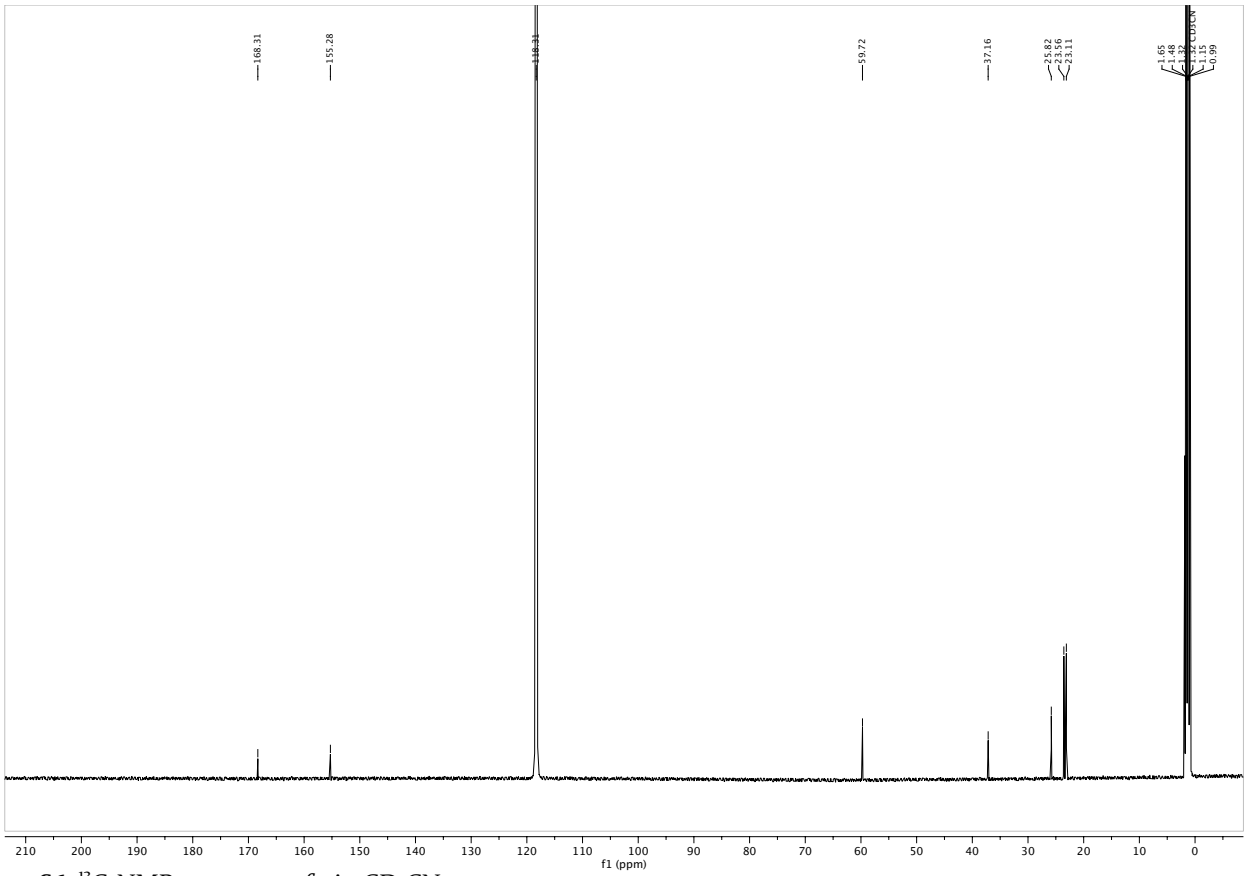

Figure S6. ^{13}C-NMR spectrum of **1** in CD_3CN.

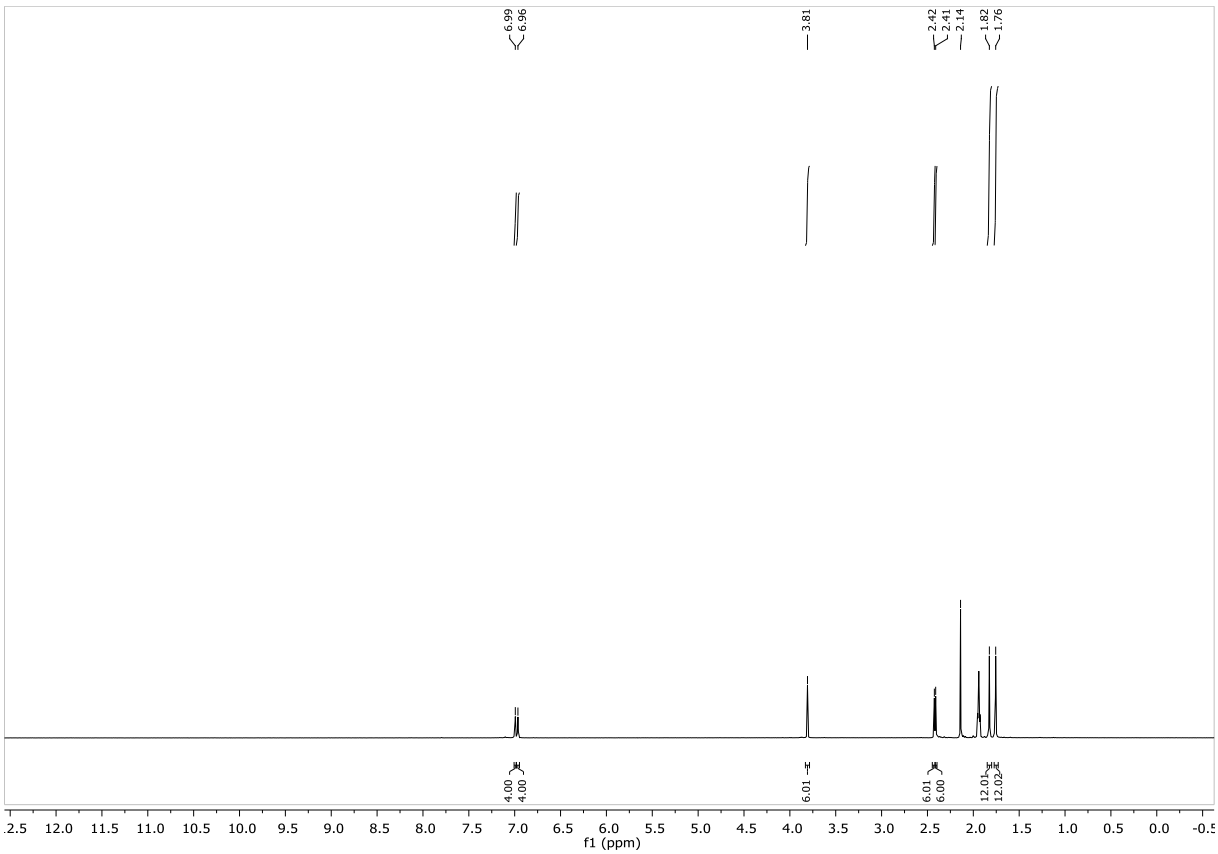

Figure S7. ^{1}H-NMR spectrum of **2** in CD_3CN.

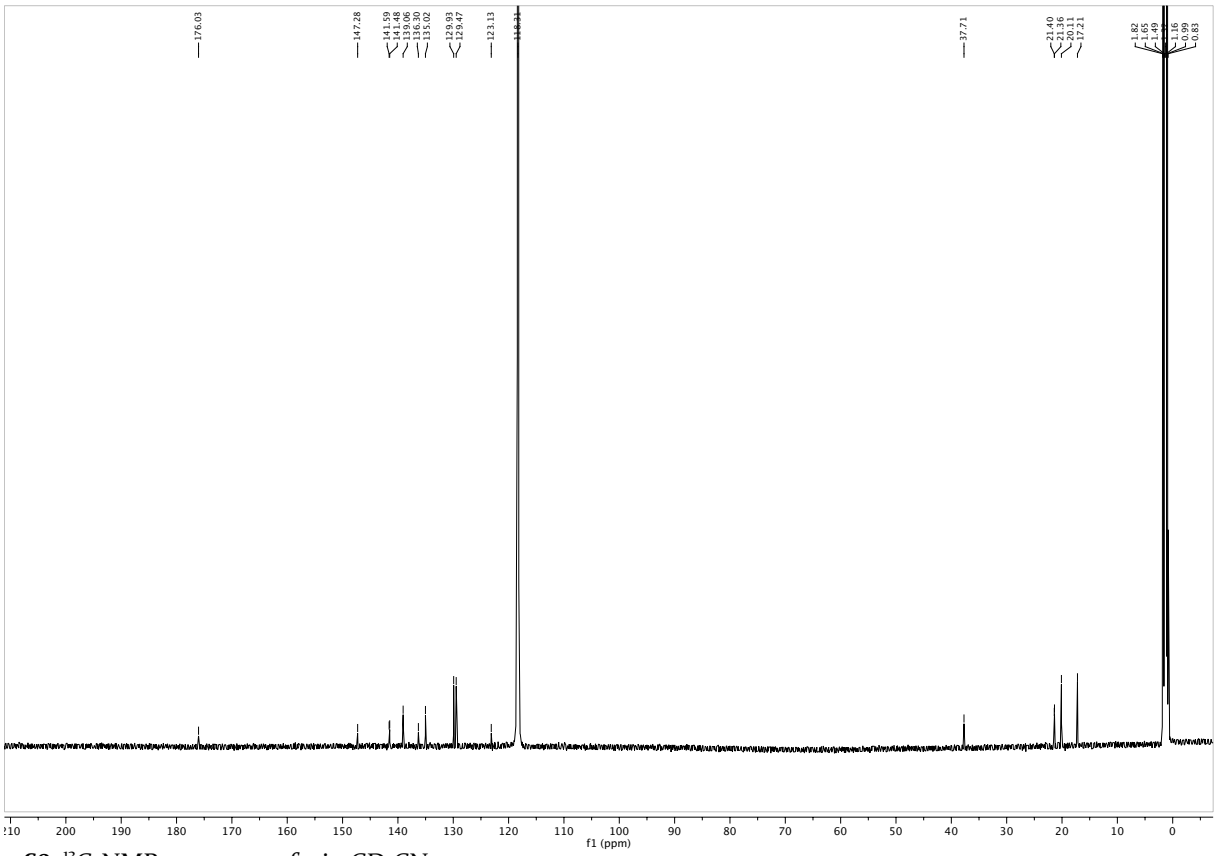

Figure S8. ^{13}C-NMR spectrum of **2** in CD_3CN.

Single Crystal X-Ray Diffraction

Table S1. Crystallographic Data of compound **2**.

Sample and Crystal Data	
Chemical formula	$C_{42}H_{50}AuF_6N_6P$
Formula weight	980.81 g mol^{-1}
Temperature	100(2) K
Wavelength	0.71073 Å
Crystal size	0.186 mm × 0.289 mm × 0.300 mm
Crystal habit	Colorless fragment
Crystal System	Monoclinic
Space group	C 1 2/c 1
Unit cell dimensions	a = 17.884(4)Å, b = 21.912(4) Å, c = 14.332(3) Å, α = 90.00(3)°, β = 123.09(3)°, γ = 90.00(3)°
Volume	4705.(2) $Å^3$
Z	1
Density (calculated)	0.346 g cm^{-3}
Absorption coefficient	0.804 mm^{-1}
F(000)	492

Table S2. Data Collection and Structure Refinement of Compound **2**.

Data Collection and Structure Refinement	
Diffractometer	Bruker D8 Venture
Radiation Source	TXS rotating anode, Mo
Theta range for data collection	2.52 to 25.35°
Index ranges	−21≤h≤21, −26≤k≤26, −17≤l≤17
Reflections collected	53185
Independent reflections	4304 [R(int) = 0.0499]
Coverage of independent reflections	99.9 %
Max. and min. transmission	0.8650 and 0.7940
Data / restraints / parameters	4304 / 0 / 257
Goodness-of-fit on F^2	1.079
Δ/σ_{max}	0.001
Final R indices (3564 data; I>2σ(I))	R_1 = 0.0517, wR_2 = 0.1190
Final R indices (all data)	R_1 = 0.0679, wR_2 = 0.1317
Largest diff. max. min.	2.184 and -1.834 eÅ^{-3}

Stability Studies

100 µL of a 10 mM stock solution of **1** and **2** in DMSO-d_6 is prepared and diluted with deuterated PBS buffer to a final concentration of 0.1 mM. **1** and **2** are dissolved (2.5 mg in 0.5 mL D_2O) and 5.0 eq *L*-cysteine or gluthatione (GSH) are added in solid (reference spectra: Figures S9 and S10), respectively. The samples are incubated at 37 °C for 72 h and analyzed by ^{1}H-NMR spectroscopy and ESI-MS.
Both complexes show remarkable stability against *L*-cysteine and GSH, respectively.

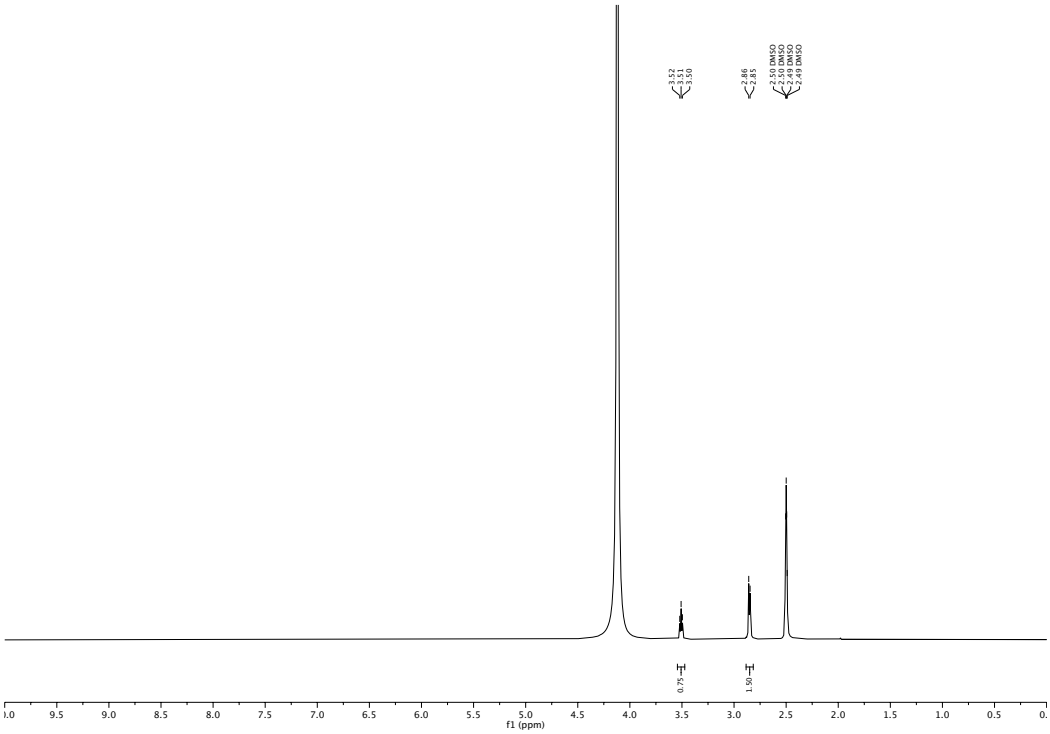

Figure S9. ^{1}H-NMR spectrum of *L*-cysteine in DMSO-d_6 and deuterated PBS buffer.

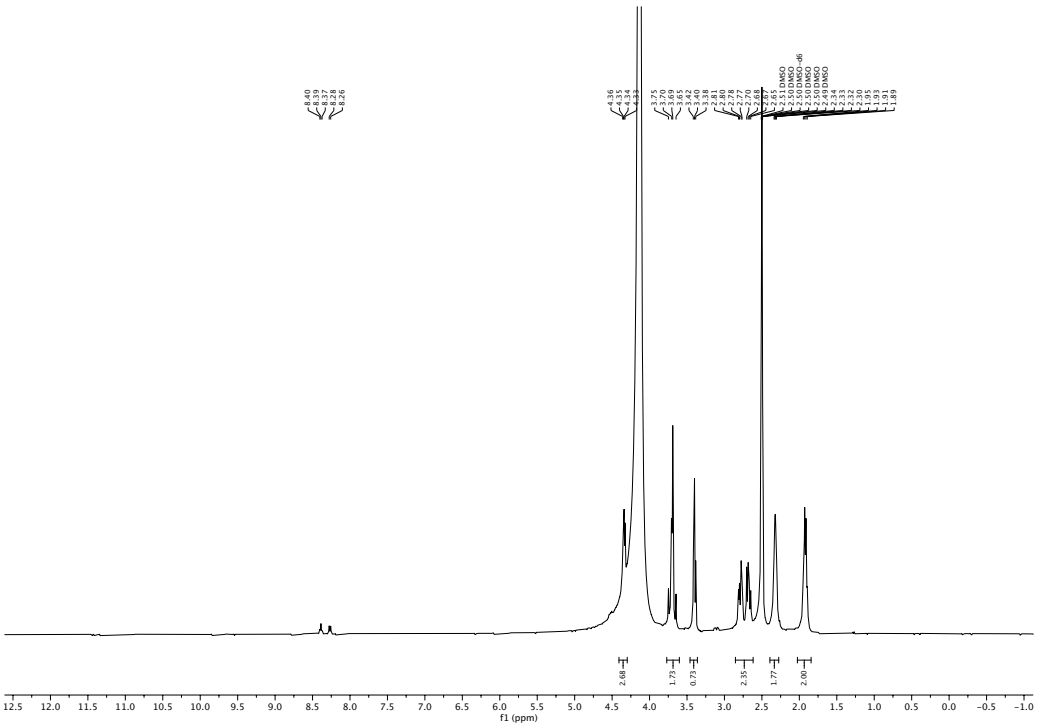

Figure S10. ^{1}H-NMR spectrum of glutathione (GSH) in DMSO-d_6 and deuterated PBS buffer.

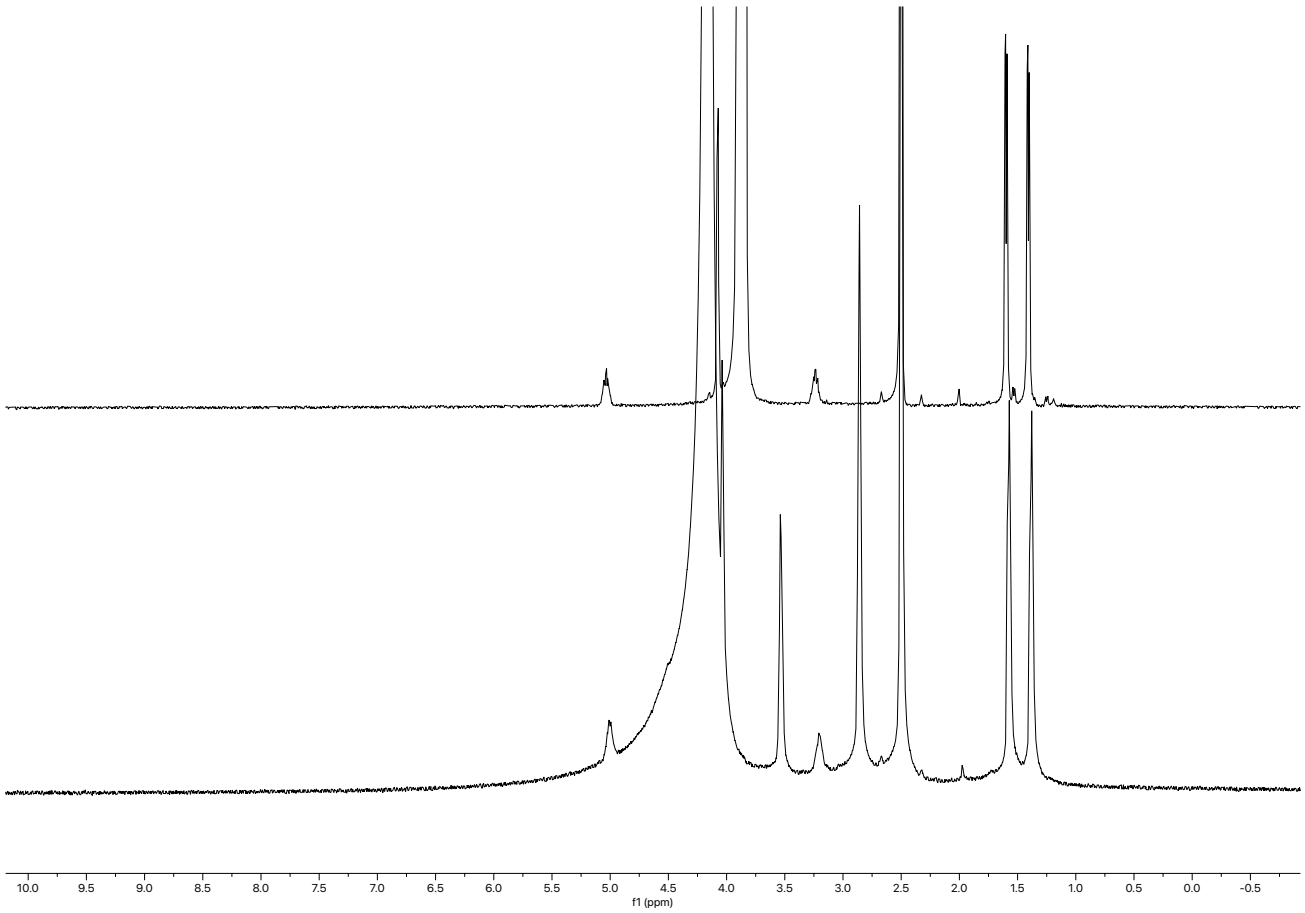

Figure S11. ^{1}H-NMR spectrum of **1** in presence of *L*-cysteine in DMSO-d_6 and deuterated PBS buffer after incubation at 37 °C: top: 72 h; bottom: 0 h. Aside from peak broadening no significant decomposition is observed.

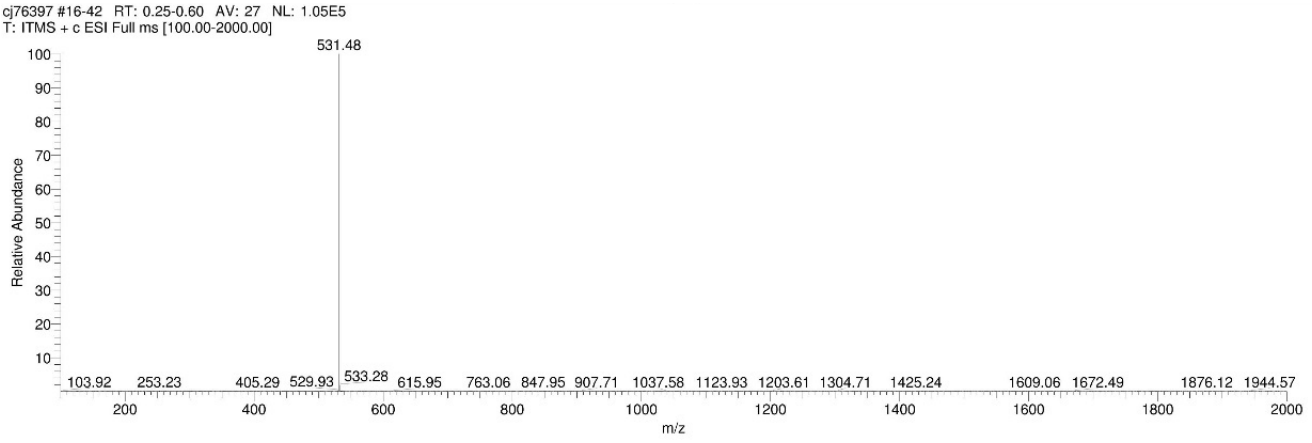

Figure S12. ESI-MS spectrum of **1** after 72 h incubation at 37 °C in presence of *L*-cysteine in DMSO-d_6 and deuterated PBS buffer. In line with the ^{1}H-NMR spectra (Figure S11) no decomposition product is observed.

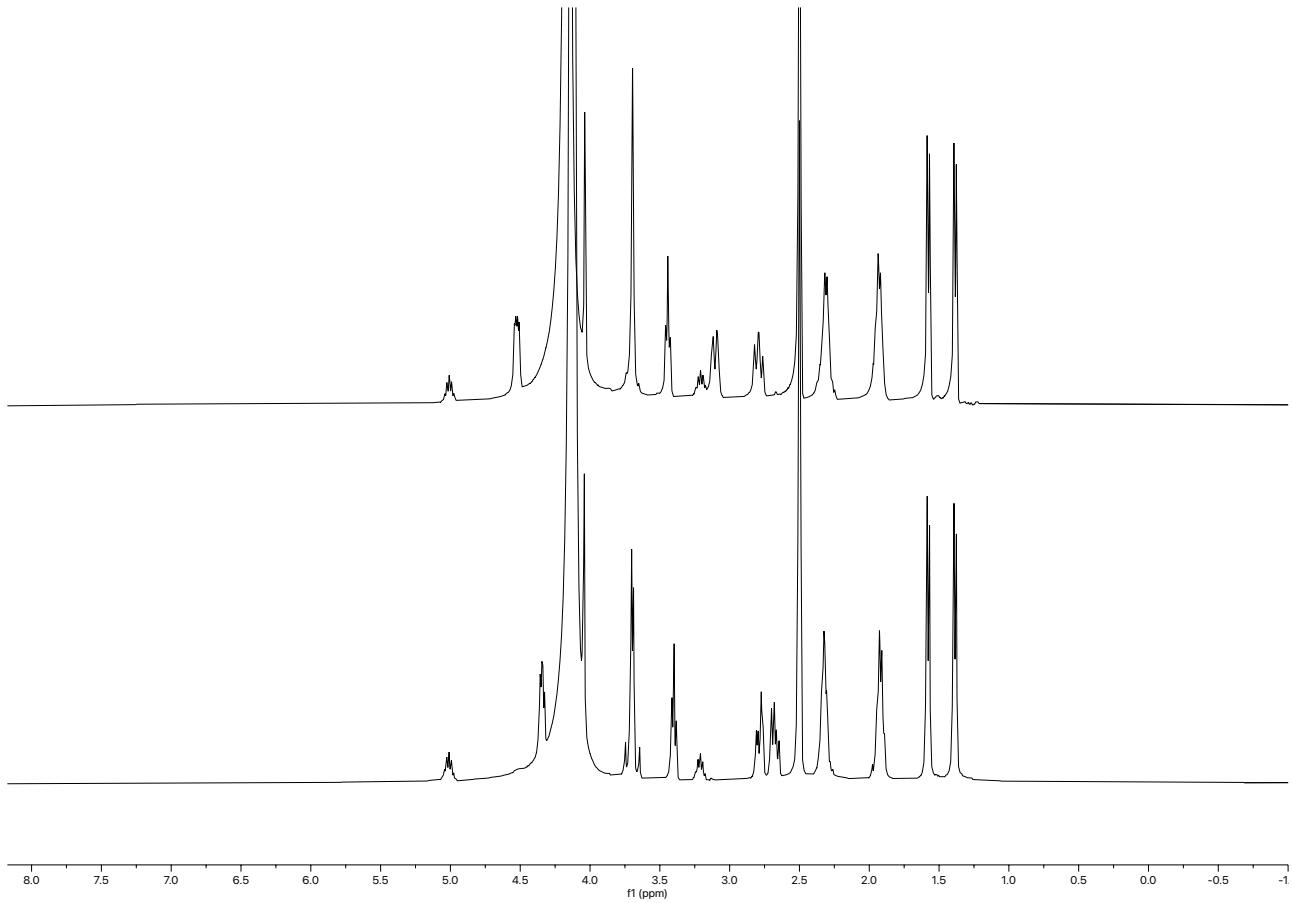

Figure S13. ^{1}H-NMR spectrum of **1** in presence of GSH in DMSO-d_6 and deuterated PBS buffer after incubation at 37 °C: top: 72 h; bottom: 0 h. No significant decomposition is observed.

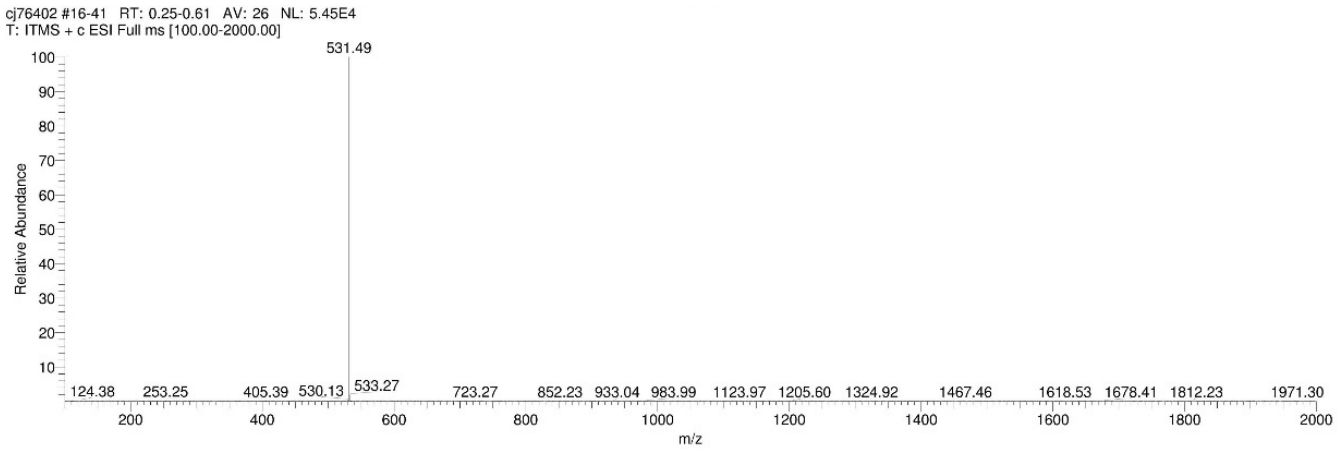

Figure S14. ESI-MS spectrum of **1** after 72 h incubation at 37 °C in presence of GSH in DMSO-d_6 and deuterated PBS buffer. In line with the ^{1}H-NMR spectra (Figure S13) no decomposition product is observed.

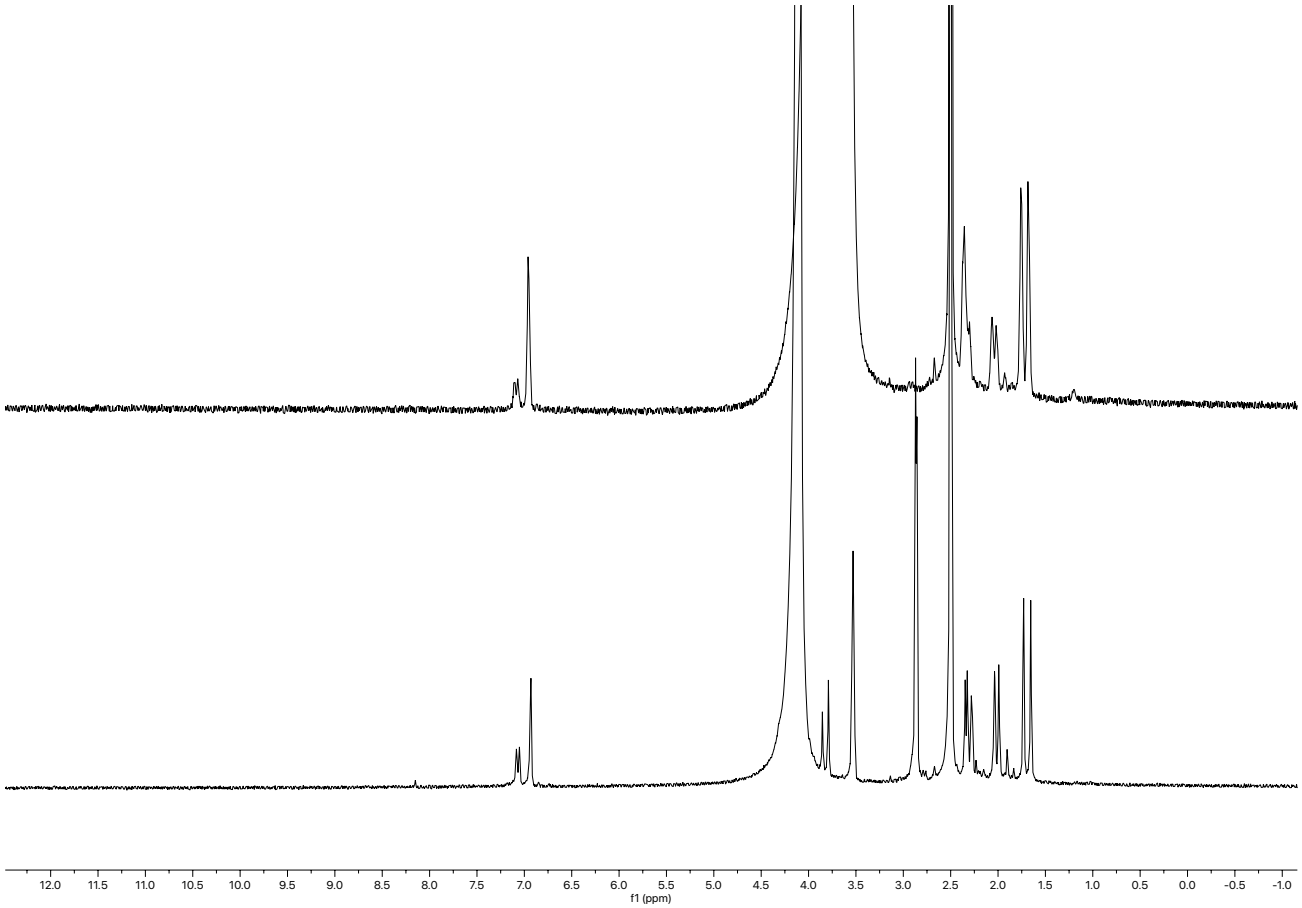

Figure S15. ^{1}H-NMR spectrum of **2** in presence of *L*-cysteine in DMSO-d_6 and deuterated PBS buffer after incubation at 37 °C: top: 72 h; bottom: 0 h. Due to peak broadening the signals in the range from 3.5 to 4.0 ppm are not visible anymore. However, no significant amount of decomposition product is observable.

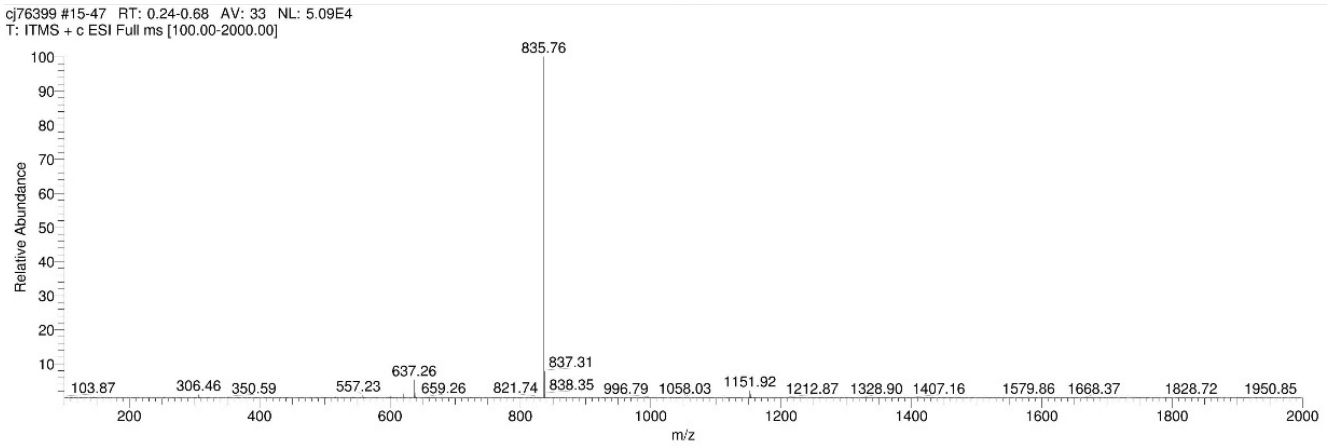

Figure S16. ESI-MS spectrum of **1** after 72 h incubation at 37 °C in presence of *L*-cysteine in DMSO-d_6 and deuterated PBS buffer. In line with the ^{1}H-NMR spectra (Figure S15) no decomposition product is observed.

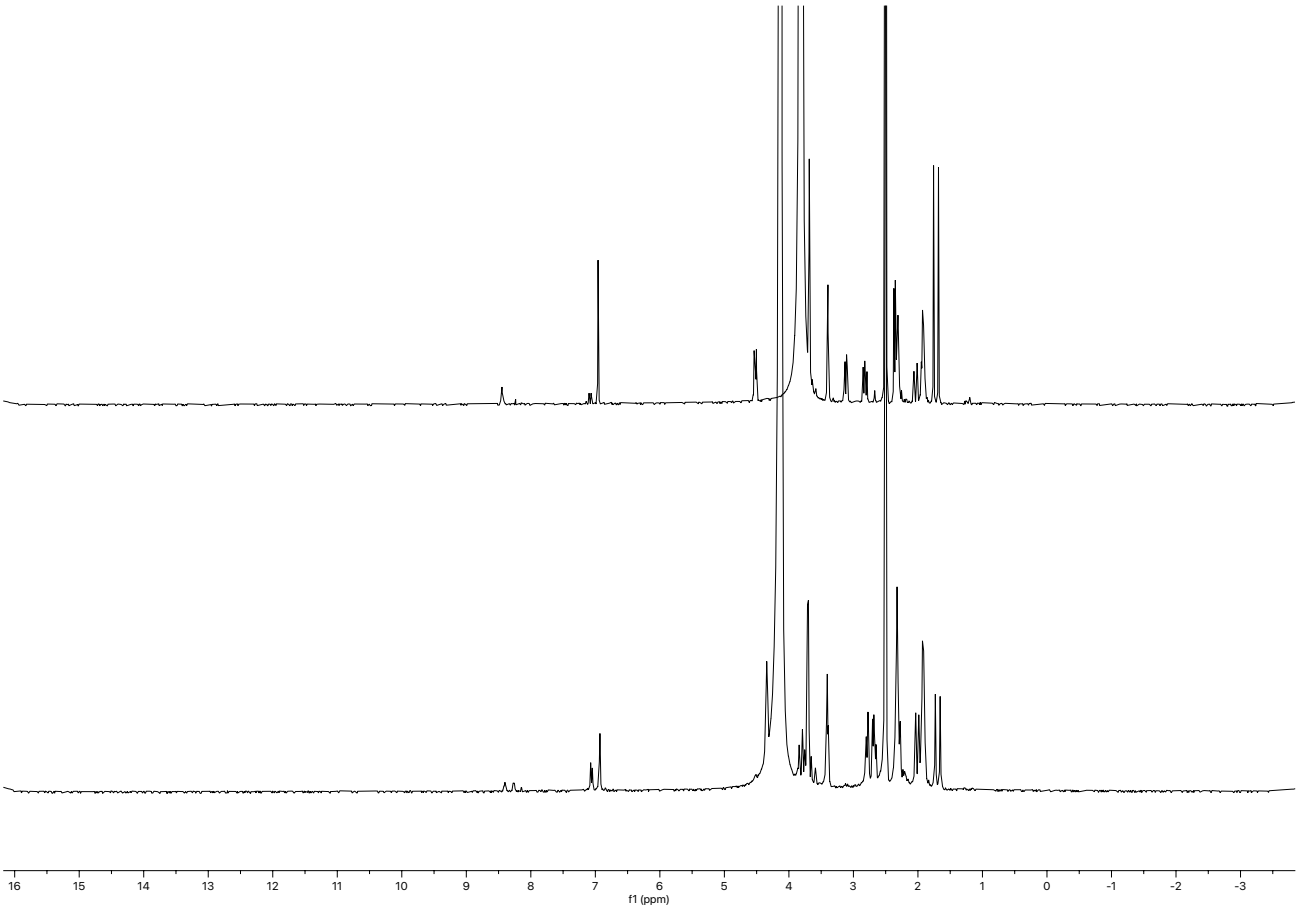

Figure S17. ^{1}H-NMR spectrum of **2** in presence of GSH in DMSO-d_6 and deuterated PBS buffer after incubation at 37 °C: top: 72 h; bottom: 0 h. Although the signals are slightly shifted, no significant decomposition is observed.

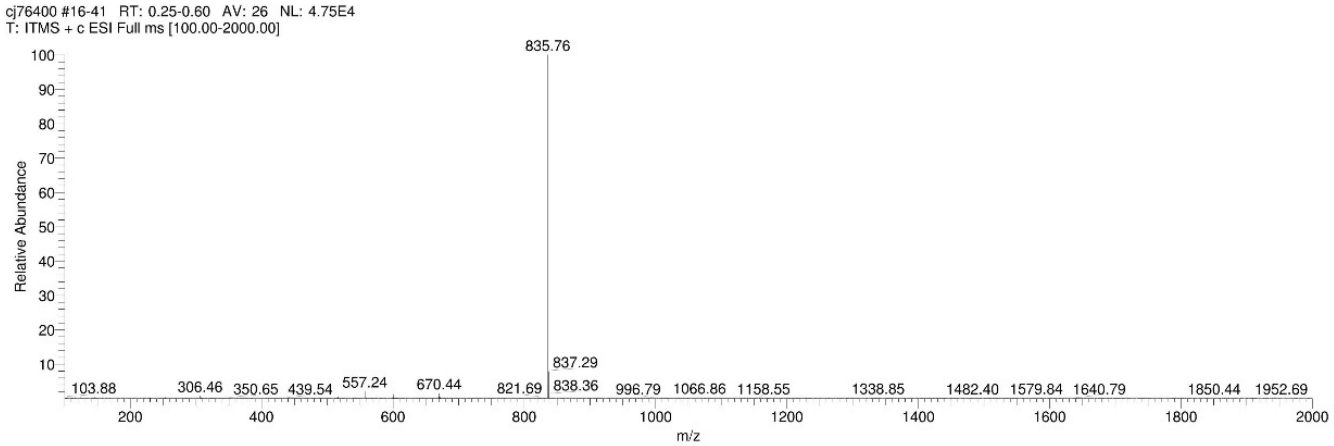

Figure S18. ESI-MS spectrum of **2** after 72 h incubation at 37 °C in presence of GSH in DMSO-d_6 and deuterated PBS buffer. In line with the ^{1}H-NMR spectra (Figure S17) no decomposition product is observed.

Biological Studies

Generation of Chemoresistant Subcell Lines

To generate a resistant cell line, the respective cytostatic drug was initially tested on the starting cell line and the concentration at which a clear apoptotic effect was stably achieved on the starting cell line, was determined.
To start, some cells were incubated with a concentration of the cytostatic agent at which no or only a very small apoptotic effect was seen on the initial cell line. In addition to the control cell line, the treated cells were continued to grow as a normal cell culture. If they showed good viability despite the pipetted amount of drug, the concentration was increased in small steps. This was continued until the previously determined concentration was reached. To reconfirm the resistance that had developed, the previously determined concentration as well as smaller and a larger concentration of the cytostatic agent both on the initial cell line and on the newly developed cell line was tested, as shown for example, in Figure S19.
In order to detect any additional co-resistance/s that may have developed during the generation of resistance, the respective starting cell line and the new cell line were tested with different concentrations of commonly used cytostatic drugs, using the previously determined concentration of the cytostatic drug of resistance as a positive control.

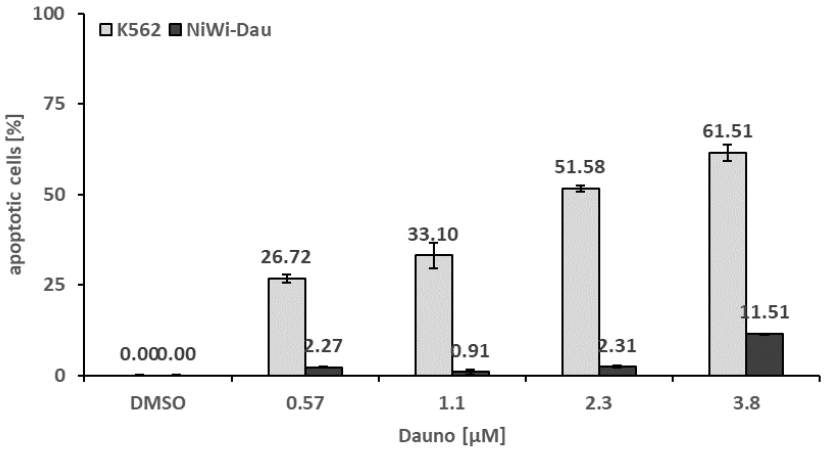

Figure S19. K562 and NiWi-Dau cells were treated with different concentrations of daunrubicin (Dauno). Solvent treated cells (0.5% DMSO) served as control. After 72 h of incubation, DNA fragmentation was measured by flow cytometric analysis. Values are given

Table S3. Gene expression analysis of resistant Nalm6 cells (JeFri and MaKo) compared to control cells Nalm6 using the RT2 profiler PCR array cell death pathway finder (96 genes profiled on 2 samples with the PAHS-212Z); α represents fold-change results in a biologically meaningful way. Fold-change values greater than one indicate a positive- or an up-regulation, negative fold-change values indicate a negative- or a down-regulation and the fold-regulation is equal to the fold-change.

Cell line	Gene	Fold regulation [α]
JeFri	GADD45A (Growth arrest and DNA-damage-inducible, alpha)	- 4.04
MaKo	FOXI1 (Forkhead box I1)	- 3.06

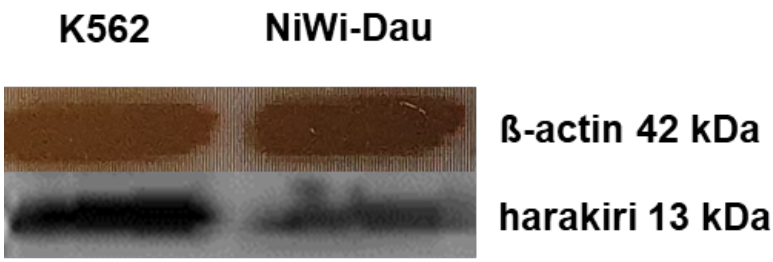

Figure S20. Cells were collected and lysed. 30 µg of cytosolic protein were separated by sodium SDS-PAGE and subjected to western blot analysis. Immunoblot developed with anti-harakiri is shown. The position of the 13 kDa harakiri band is indicated. Equal loading and blotting were verified by detection of ß-actin (42 kDa).

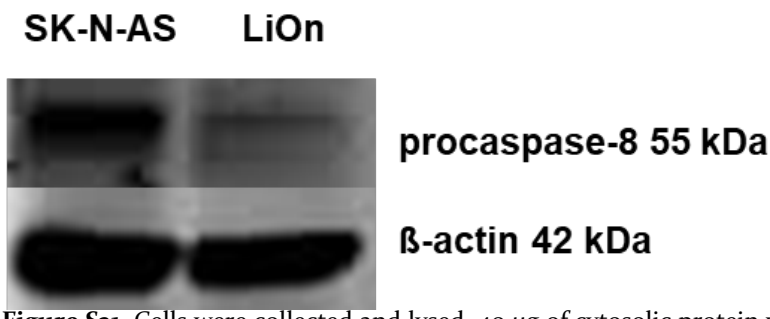

Figure S21. Cells were collected and lysed. 40 µg of cytosolic protein were separated by sodium SDS-PAGE and subjected to western blot analysis. Immunoblot developed with anticaspase-8 is shown. The position of the 55 kDa active procaspase-8 is indicated. Equal loading and blotting were verified by detection of ß-actin (42 kDa).

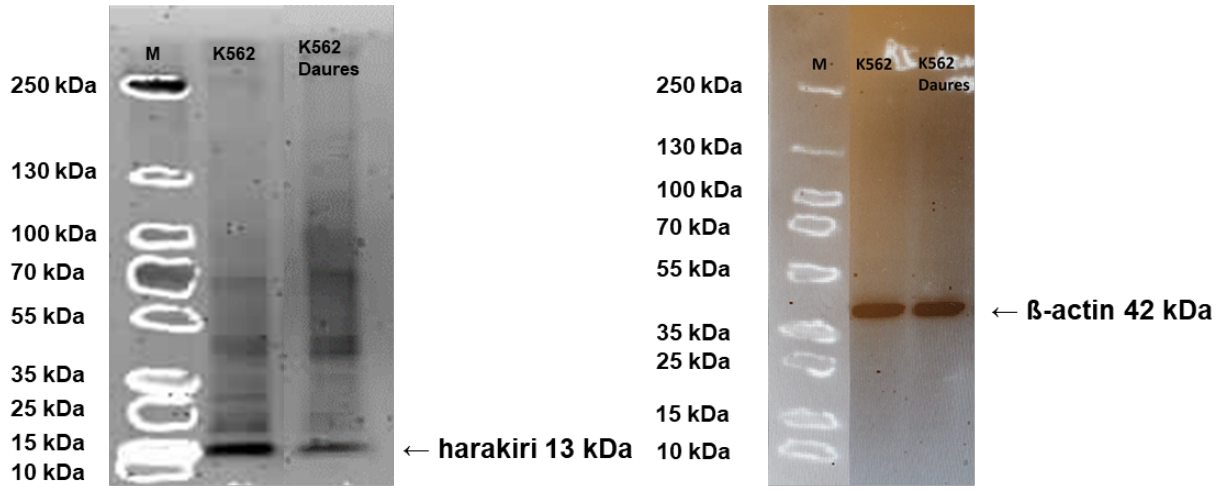

Figure S22. K562 and NiWi-. (K562 Daures) cells were collected and lysed. 30 µg of cytosolic protein were separated by sodium SDS-PAGE and subjected to western blot analysis. Immunoblot developed with anti-harakiri is shown. The position of the 13 kDa harakiri band is indicated. Equal loading and blotting were verified by detection of ß-actin (42 kDa). The prestained protein ladder respectively MW marker (M) is used to monitor the progress of SDS-polyacrylamide gel electrophoresis to assess the efficacy of the transfer to the membrane.

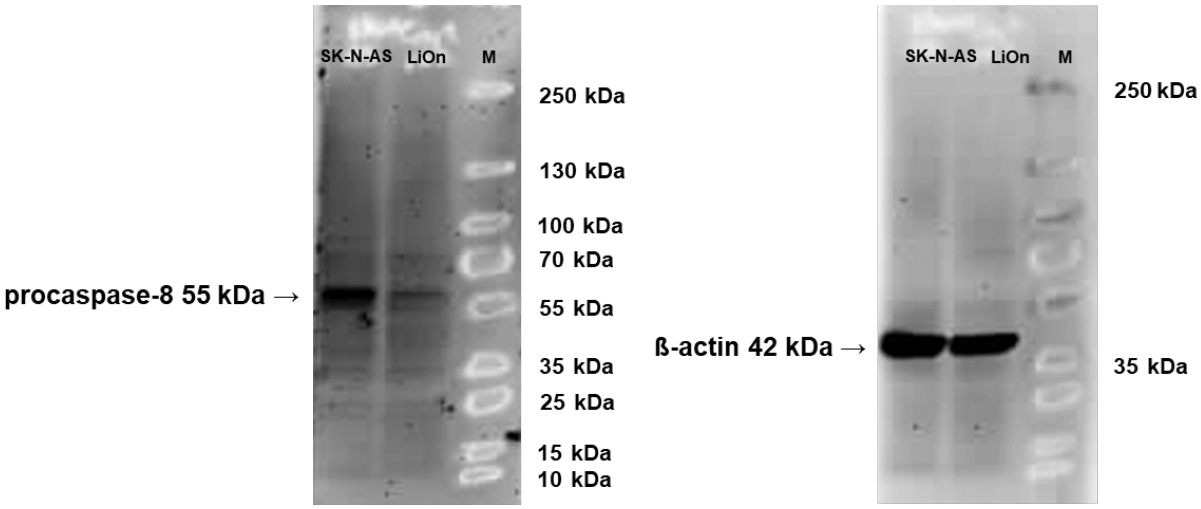

Figure S23. SK-N-AS and LiOn cells were collected and lysed. 40 µg of cytosolic protein were separated by sodium SDS-PAGE and subjected to western blot analysis. Immunoblot developed with anticaspase-8 is shown. The position of the 55 kDa active procaspase-8 is indicated. Equal loading and blotting were verified by detection of ß-actin (42 kDa). The prestained protein ladder respectively MW marker (M) is used to monitor the progress of SDS-polyacrylamide gel electrophoresis to assess the efficacy of the transfer to the membrane.

Determination of the Antiproliferative Activity – MTT Assay

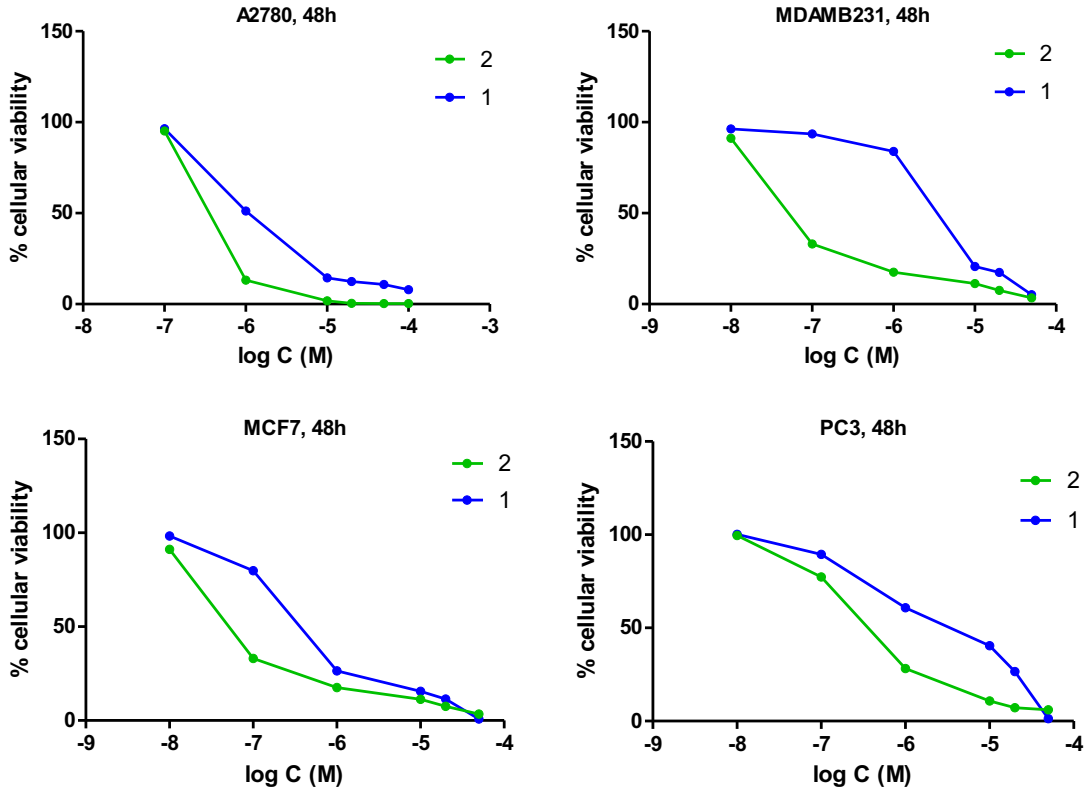

Figure S24. Dose-response curves for calculation of the IC_{50} values of **1** and **2**, using the GraphPad Prism software (vs. 5.0)

Annexin-V/Propidium Iodide Double Staining

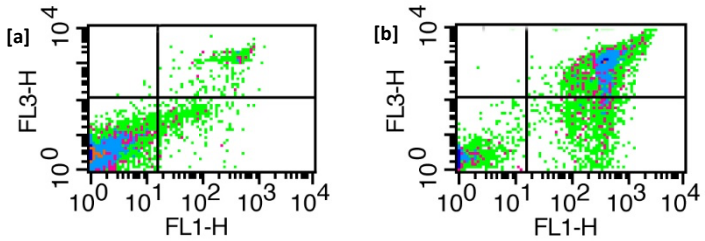

Quad	Events	% Total
UL	8	0.08
UR	362	3.62
LL	9118	91.18
LR	512	5.12

Quad	Events	% Total
UL	3	0.03
UR	3608	36.08
LL	1491	14.91
LR	4898	48.98

Figure S25. Plots for evaluation of flow cytometric measurement of annexin-V/Propidium Iodide double staining of control ([a]) and sample ([b]); X-axis (FL1-H): annexin-V fluorescence, Y-axis (FL3-H): Propidium Iodide fluorescence; quadrants: UL: upper left, UR: upper right, LL: lower left, LR: lower right

Measurement of DNA Fragmentation

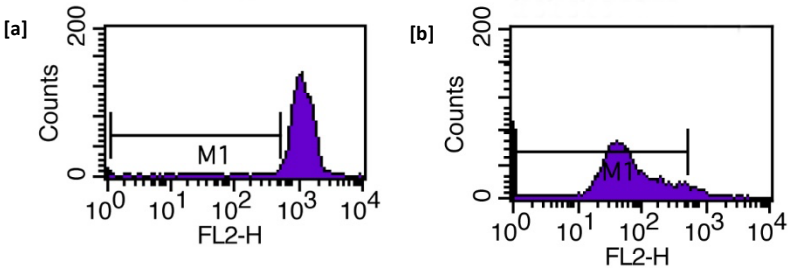

Marker	Events	% Total
All	10000	100.00
M1	333	3.33

Marker	Events	% Total
All	10000	100.00
M1	9587	95.87

Figure S26. Histogram plots and statistics for evaluation of flow cytometric measurement of DNA fragmentation of control ([a]) and sample ([b]); X-axis (FL2-H): PI fluorescence, Y-axis (Counts): cell count, M1: marker for quantification of hypoploid cells.

Inhibition of NaIm-6 Cell Proliferation

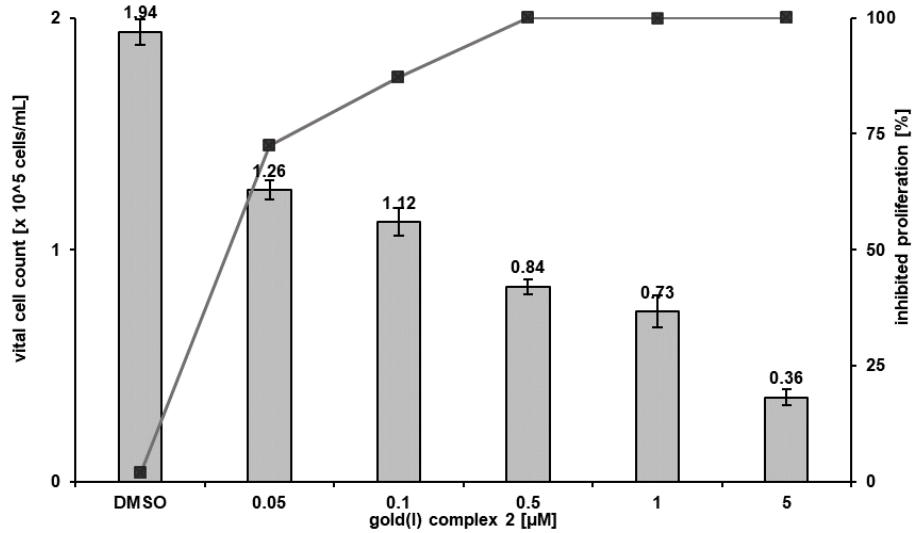

Figure S27. After 24 h of incubation of Nalm-6 cells with different concentrations of **2** the number of cells was determined using CASY cell counter system. The number of solvent treated cells (DMSO) served as control and was set as 0% growth inhibition. Values are given as percentage of inhibition of cell proliferation and as mean values ± SD (n=3).

Overcoming of Daunorubicin Resistance

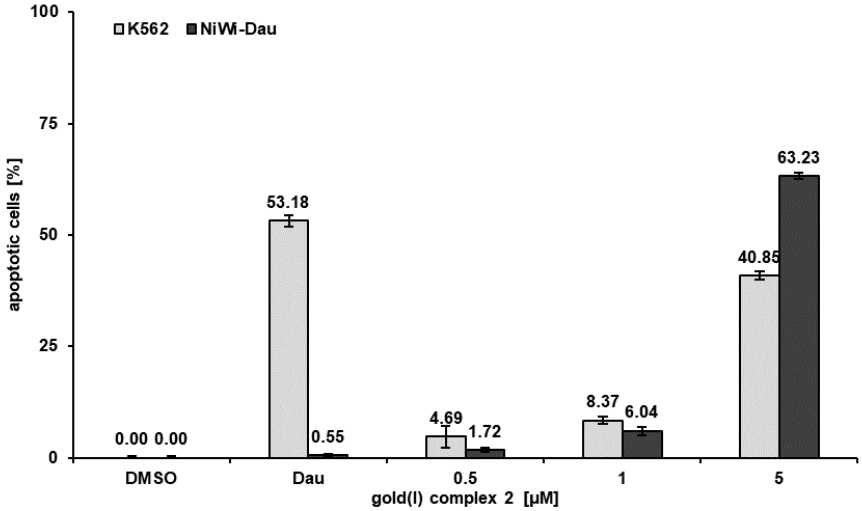

Figure S28. K562 and NiWi-Dau cells were treated with 0.5 µM, 1 µM and 5 µM of **2**. Solvent treated cells (DMSO) served as control. 2.3 µM daunorubicin (Dau) was used as positive control to prove the resistance. After 72 h of incubation, DNA fragmentation was measured by flow cytometric analysis. Values are given in percentage of apoptotic cells as mean values ± SD (n=3).

Thioredoxin (TrxR) Activity Assay

To determine the inhibition of TrxR by the gold complexes, a Thioredoxin Reductase Assay Kit (Sigma-Aldrich) was used with minor modifications for a 96-well plate format assay. 200 µL of reaction mixture contained 2 µL of TrxR solution, 11 µL of assay buffer (phosphate buffer pH 7.0 containing 50 mM EDTA), 180 µL of working buffer (phosphate buffer containing 0.25 mM NADPH) and 1 µL of the complexes' solutions. The enzymatic reaction was started with the addition of 6 µL DTNB (0.1 M in DMSO). A blank sample (without enzyme) and a positive control (without compounds) were included in the assays. After proper shaking for 30 min, the formation of TNB was monitored at 412 nm with a plate spectrophotometer.

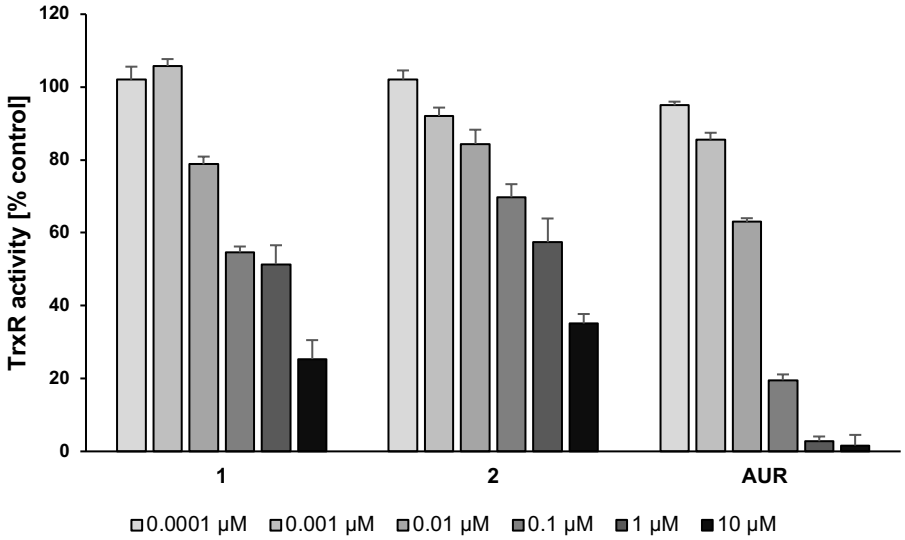

Figure S29. Inhibition of TrxR by **1**, **2** and auranofin (AUR). Data are mean±SD of two independent experiments done with four replicates for each condition.

Selectivity of 1 for Malignant Cells

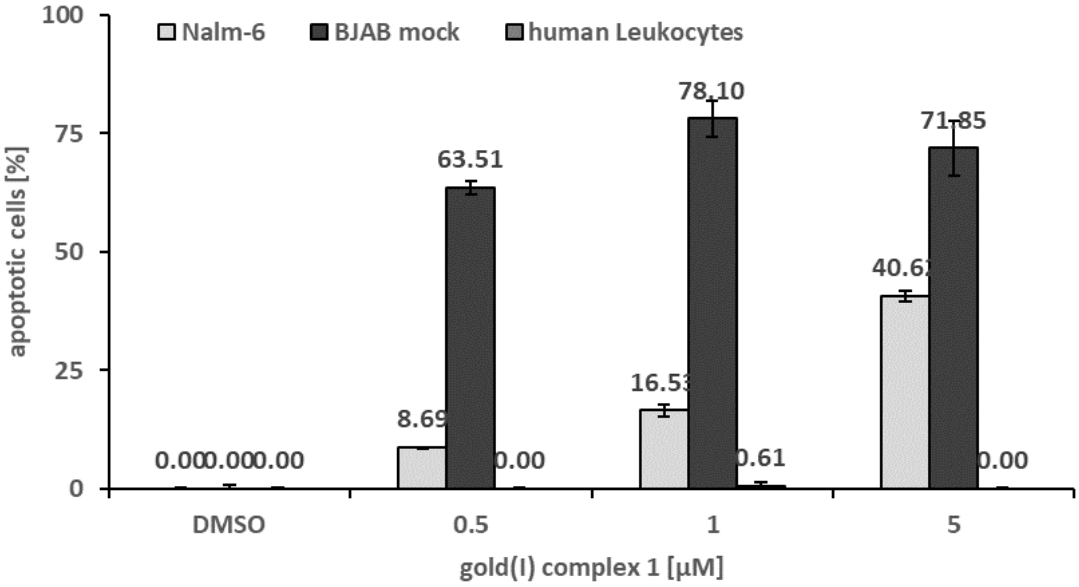

Figure S30. Nalm-6 cells, BJAB mock cells and human leukocytes were treated with different concentrations of **1**. Solvent treated cells (DMSO) served as control. All cells were incubated for 72 h. Then, induction of apoptosis was measured by flow cytometric analysis of cellular content. Values are given as percentage of cells with hypodiploid DNA as mean values ± SD (n=3).

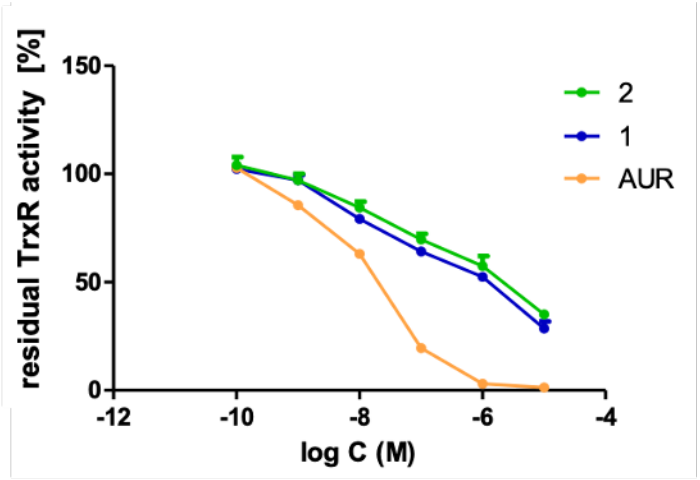

Figure S31. The inhibitory effect of **1**, **2** and auranofin (AUR) on thioredoxin reductase. TrxR activity was assayed by measuring NADPH- dependent reduction of DTNB at 412 nm.

Octanol-Water Partition Coefficients

The lipophilicity of the complexes 1 and 2 was determined by the shake-flask method.[1] Before the experiments, n-octanol and distilled water were mixed vigorously for 24 h at 25 °C, to promote solvent saturation of both phases. The phases were separated, and the two compounds were dissolved in the n-octanol phase (5.7 x 10-4 M and 1.6 x 10-4 M, for **1** and **2** respectively). The solutions were equilibrated with water for 4h in a mechanical shaker, with a phase ratio of 2 mL/2 mL (water/n-octanol). The aqueous and octanol layers were then carefully separated (by centrifugation at 5000 rpm for 10 min), and UV–vis absorption spectra of the compounds were registered in the n-octanol phase. The concentration for each sample was determined using the n-octanol calibration curve. The experiments have been performed in triplicate for each complex and the averages were calculated. The partition coefficients were calculated using the equation:

$$\log P_{oct/water} = \log\left(\frac{[complex]_{oct}}{[complex]_{water}}\right)$$

In the development of new drugs, it is very important to consider lipophilicity/ hydrophobicity of the compounds, since it affects their cytotoxicity, tissue permeability, absorption, drug-receptor interaction, etc.[2] The n-octanol/water partition coefficient was determined by the shake-flask method, at room temperature. Compounds 1 and 2 are lipophilic, with log P values of 0.264 ± 0.002 and 1.592 ± 0.030 for complexes, respectively. As expected, complex 2, with mesityl groups, is more lipophilic than complex **1.**

Analytical HPLC

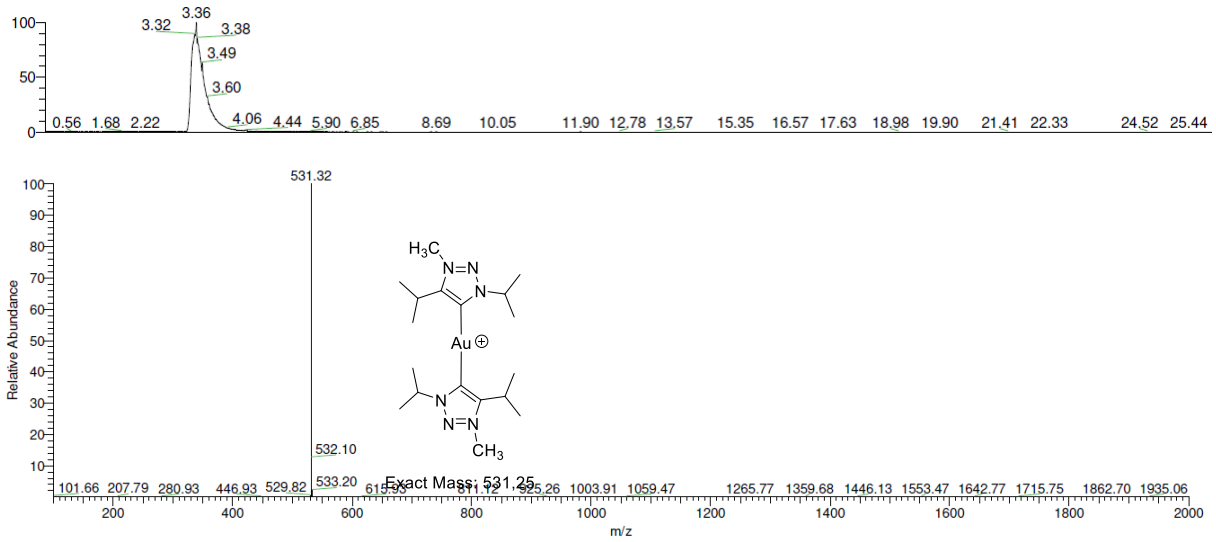

Figure S32. Analytical RP-HPLC (50-100% MeCN/H_2O with 0.1% formic acid, 20 min) and HESI-MS spectra of **1**. m/z calculated for: $C_{18}H_{34}AuN_6^+$(**1**-PF_6^-), 531.25 found: 531.32 $[M]^+$.

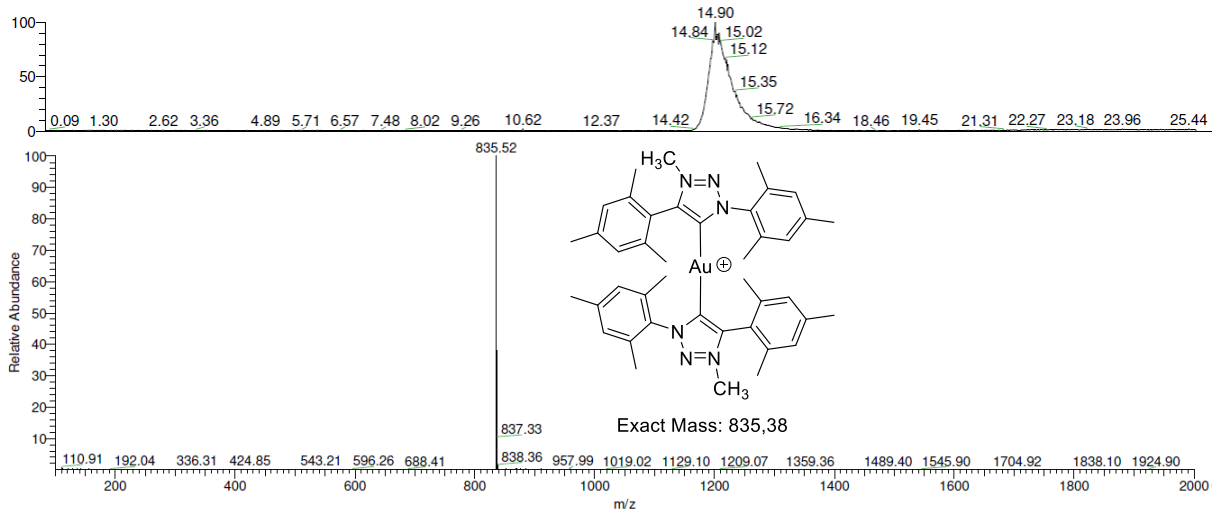

Figure S33. Analytical RP-HPLC (50-100% MeCN/H_2O with 0.1% formic acid, 20 min) and HESI-MS spectra of 2. m/z calculated for: $C_{42}H_{50}AuN_6^+$ (**2**-PF_6), 835.38 found: 835.52$[M]^+$.

References

1. Berthod, A.; Carda-Broch, S., Determination of Liquid–Liquid Partition Coefficients by Separation Methods. *J. Chromatogr. A* **2004,** *1037* (1), 3-14.
2. Hollósy, F.; Lóránd, T.; Örfi, L.; Erös, D.; Kéri, G.; Idei, M., Relationship between Lipophilicity and Antitumor activity of Molecule Library of Mannich Ketones determined by High-Performance Liquid Chromatography, clogP Calculation and Cytotoxicity Test. *J. Chromatogr. B* **2002,** *768* (2), 361-368.